1997_157

TÜBİTAK

TÜRKİYE BİLİMSEL VE
TEKNİK ARAŞTIRMA KURUMU

THE SCIENTIFIC AND TECHNICAL
RESEARCH COUNCIL OF TURKEY

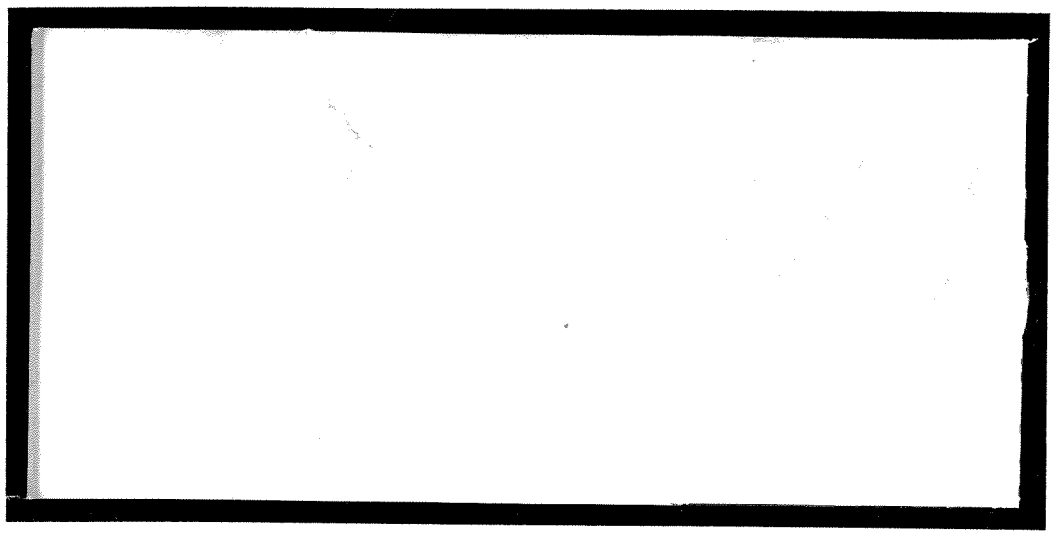

Temel Bilimler Araştırma Grubu

Basic Sciences Research Grant Committee

MAKROGÖZENEKLİ POLİMERİK JEL SENTEZLERİ

PROJE NO : TBAG-1561

Prof. Dr. Oğuz OKAY (İstanbul Teknik Üniversitesi)
Prof. Dr. A. Altan ERARSLAN (Kocaeli Üniversitesi)
Prof. Dr. Hikmet AĞIRBAŞ (Kocaeli Üniversitesi)
Yrd. Doç.Dr. Sibel ZOR (Kocaeli Üniversitesi)
Yük. Kimyager Selda DURMAZ (MAM Başkanlığı)

Haziran 1999
İSTANBUL

İÇİNDEKİLER

ÖNSÖZ

Bu proje 1997 - 1999 yılları arasında TÜBİTAK Temel Bilimler Araştırma Grubunun katkıları ile gerçekleşmiştir. Projenin deneysel kısmını büyük bir özveri ile gerçekleştiren Kocaeli Üniversitesi Kimya Bölümü Yüksek Lisans öğrencileri Ufuk AKKAN, Nurgül Kalyoncu BALIMTAŞ, Muzaffer KESKİNEL, Safiye Bozkurt SARIŞIK, ve Erol ERBAYa, cıvalı porozimetre ölçümlerinin yapılmasına olanak sağlayan PETKİM AŞye, projenin aksamadan ilerlemesinde yardımlarını esirgemeyen Kocaeli Üniversitesi Kimya Bölümü elemanlarının tümüne teşekkürlerimizi belirtmek isteriz.

ÖZ

Makrogözenekli stiren - divinilbenzen kopolimer kürecikleri suspansiyon polimerizasyonu yöntemi ile sentezlendi ve karakterize edildi. Cıvalı porozimetre ile yapılan ölçümler yardımı ile polimerik jellerin sentez şartlarına bağlı olarak gözenek yapılarındaki değişmeler incelendi. Gözenek yapılarındaki dayanıklı ve dayanıksız gözeneklerin oluşma şartları aydınlatıldı. Sentez şartlarının uygun bir şekilde seçimi ile tersinir gözenekli polimerlerin sentezlenebileceği gösterildi. Termodinamik ve kinetik açıdan gözenekli yapı oluşumu incelenerek kopolimer sentez şartları ile kopolimerin gözenek yapısı arası bağıntıyı veren teorik bir model geliştirildi ve bu model stiren-divinilbenzen sistemine uygulandı. Diğer yandan poliakrilamid esaslı iyonik jeller sentez sonrası iyi çözücü-kötü çözücü karışımları ile muamele edilerek heterojen hale dönüştürüldü.

2-Akrilamido-2-metilpropan sulfonik asit (AMPS) esaslı kuvvetli elektrolit hidrojeller sentezlendi ve bu jellerin su ve tuzlu sulardaki şişme oranları belirlendi. 1 mL si 2,5 litreye kadar su emebilen AMPS esaslı jellerin sentezleri gerçekleştirildi. Deneysel şişme değerlerinin açıklanabilmesi için Flory-Rehner teorisi ile ideal Donnan dengesi göz önüne alındı. Ağ yapının çapraz bağ yoğunluğu veya iyonik grup sayısı bir ayarlama parametresi olarak alındığında teori ile deney arasında uyum sağlandı ve bulguların sodyum akrilat esaslı zayıf elektrolit jeller için de geçerli olduğu gösterildi.

Anahtar Kelimeler: Polimerik jel, makrogözenekli polimer ağ yapılar, gözenek yapılar, hidrojeller, şişme

ABSTRACT

Macroporous styrene-divinylbenzene copolymer beads were synthesized by the suspension polymerization technique. The variation of the pore structure of the copolymer beads depending on the synthesis parameters was studied by the mercury porosimetric technique . The formation conditions of the stable and unstable pores in the copolymers were determined. It was shown that a porous copolymer network with a reversible pore structure can be synthesized by adjusting the synthesis parameters. A model taking into account both the thermodynamic and kinetic aspects of the porosity formation was developed and applied to the styrene-divinylbenzene copolymerization system. Moreover, polyacrylamide gels were converted into heterogeneous ones by treatment with solvent-nonsolvent mixtures.

2-Acrylamido-2-methylpropane sulfonic acid (AMPS) based strong polyelectrolyte hydrogels were synthesized and their swelling capacities in water as well as in aqueous salt solutions were determined. AMPS based hydrogels with swelling capacities up to 2.5 liter of water per mL of dry gel were prepared. Experimental swelling data were compared with the predictions of the Flory-Rehner theory including the ideal Donnan equilibria. It was shown that the theory correctly predicts the swelling behavior of the hydrogels if the network crosslink density or the network charge density is used as an adjustable parameter in the calculations. Similar results were also obtained with sodium acrylate based weak polyelectrolyte hydrogels.

Key words: Polymeric gels, macroporous polymer networks, porous structures, hydrogels, swelling.

ŞEKİLLER LİSTESİ

1. GİRİŞ

1.1 POLİMERİK JELLER

Polimerler insan yaşamında çok önemli yer tutan malzemelerdir. 2000 yılında kişi başına materyal tüketiminin senede 287 litreye ulaşacağı ve bunun yaklaşık %80 lik kısmının polimerik malzemeler olacağı belirtilmektedir (Richardson 1989). Günümüzde kullanılan polimerik malzemelerin yarıya yakın bir kısmı serbest-radikal mekanizma ile üretilmektedir. Serbest-radikal mekanizma ile üretilen polimerik malzemelerin önemli bir bölümü ise çapraz bağlı yapıdadır (Andreis 1989). Bu nedenle serbest-radikal mekanizma ile çapraz bağlı polimerlerin yani "polimerik ağ yapıların" oluşum mekanizmaları, sentez şartları - yapıları - özellikleri arası ilişkiler geçtiğimiz 60 sene boyunca yoğun araştırmalara konu olmuştur.

Polimerik jeller, polimer ağ yapısı ile ağ yapı içindeki çözücüden ibaret iki (sürekli) fazlı bir sistem olarak tanımlanabilir. Polimer ağ yapı, çözücünün jelin dışına akmasını engellerken çözücü de ağ yapının çökmemesini sağlar. Şekil 1 de şematik olarak bir polimer jeli görülüyor.

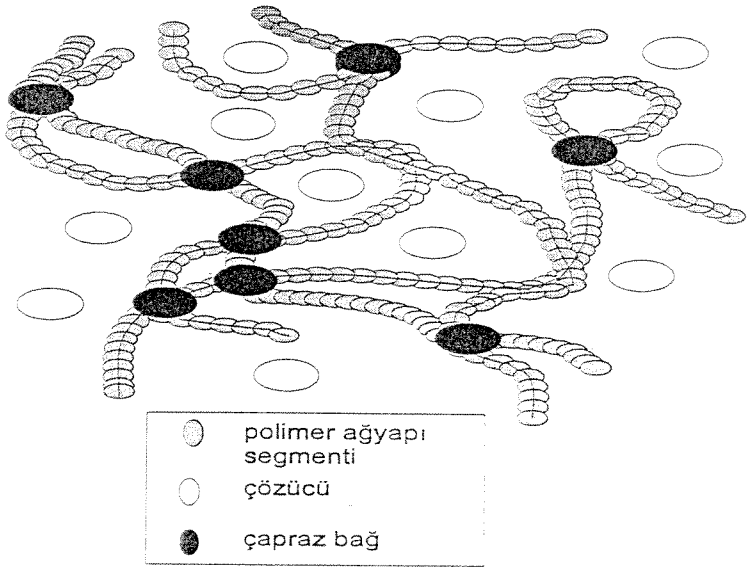

Şekil 1. polimerik jel.

Polimerik jeller konusunda teorik ve deneysel çalışmalar yoğun olarak devam etmekte olup bu konuda onbinlerce çalışma yapılmıştır. Bilim elemanlarının polimer ağ yapı - solvent (jel) sistemlerine olan yoğun ilgisi böyle sistemlerin yüksek çözücü absorplama yetenekleri ve jel halinde her türlü kimyasal reaksiyona girebilmeleri nedeniyledir. Polimerik jellerin bu gibi üstün özellikleri sonucu *süperabsorban, iyon-değiştirici reçine, selektif reçine, GPC kolon dolgu maddesi, fotorezist, katalizör, dişçilik malzemesi, kontakt lens, kontrollu salınım sistemi, enzim ve hücrelerin immobilizasyonunda taşıyıcı, yapay organlar, yapay kar, zirai uygulamalarda su tutucu, kayaları parçalayıcı v.b.* olarak çok geniş uygulama alanları ortaya çıkmıştır. Diğer yandan çıplak gözle takip edilemeyen düz zincirli polimerlerin boyutlarında dış etkenlere bağlı değişimler polimer jellerinin makroskopik hacım değişimlerinde görülebilmektedir. Bu durum teorik fizikçi ve kimyacıların da jeller üzerinde yoğun çalışmalarına yol açmıştır.

İlk olarak 1935 yılında Chemische Berichte dergisinde çıkan Hermann Staudinger'in bir yazısında serbest-radikal mekanizma ile çapraz bağlı polistiren oluşumunun kaydına rastlıyoruz (Staudinger 1935). Staudinger stiren ile divinilbenzen karışımının ısıtılması ile hiçbir solventte çözünmeyen ama solventlerde şişebilen bilinmeyen bir maddenin oluştuğunu belirtiyordu. Takip eden yıllarda deneysel çalışmalar yoğun olarak devam etmiş ve 1940'lı yıllarda Flory ile Stockmayer polimerik ağ yapı oluşumlarının teorik temellerini atarak jelleşme prosesinin istatistiksel teorisini geliştirmişlerdir (Flory 1941, Stockmayer 1943, Stockmayer 1944). Serbest radikal mekanizma ile polimer ağ yapı oluşumu için geliştirilen istatistiksel teoriler şu varsayımlara dayanırlar (Flory 1953, Dusek 1982, Dotson 1992):

a) eşit vinil grubu reaktifliği,

b) sadece molekül arası reaksiyonların varlığı (halka oluşum reaksiyonları gözardı ediliyor), ve

c) rastgele polimerizasyon ve çapraz bağlanma reaksiyonları.

1945 yılında Walling metil metakrilat (MMA) ile etilen glikol dimetakrilatın (EGDM) polimerleşmesi ile ağ yapı oluşumunu incelemiş ve deneysel olarak gözlemlediği jelleşme noktalarının Flory - Stockmayer teorisinin öngördüğü değerlerden büyük

sapmalar verdiğini saptamıştır (Walling 1945). Walling'i takip eden yıllarda yapılan deney sonuçları istatistiksel teorilerin varsayımlarının serbest-radikal mekanizma ile ağ yapı oluşumunda geçerli olmadığını göstermiştir (Dusek 1982, Okay 1990, Okay 1995). Bulgular, jel oluşumu prosesinde vinil grup reaktifliklerinin farklı olduğunu, asılı vinil gruplarının reaktifliğinin dönüşüme bağlı azaldığını göstermiş ve halka oluşum reaksiyonlarının varlığı kanıtlanmıştır (Okay 1995). Ayrıca deneysel bulgular polimerik jellerde birden çok camsı geçiş sıcaklığının olabildiğini, jel oluşumu sırasında hapis olmuş radikallerin varlığını ve ortamdaki vinil gruplarının tamemen dönüşemediğini göstermiştir.

Yukarıda belirtilen bulgular polimerik jellerde çapraz bağ yoğunluğunun homojen olmadığını ortaya koymuştur. Serbest radikal mekanizma ile jel oluşumunda, jelleşme noktasından önce, büyüyen radikaller divinil monomerin (DVM) daha reaktif olması nedeniyle DVM ünitelerince zengindir. Diğer yandan bu zincirler reaksiyona girmemiş monomer ve solvent nedeniyle seyreltik bir çözelti halinde bulunduklarından halka oluşum reaksiyonlarına öncelikle girerler. Bunun sonucu olarak büyüyen zincirler molekül içi çapraz bağlanırlar ve yapıları bir mikrojel yapısını andırır (Funke 1998). Burada ağ yapı oluşum prosesi sırasında mikrojel oluşumunu klasik jelleşme teorilerindeki primer molekül oluşumuna benzetebiliriz. Polimerizasyonun ilerlemesi ile mikrojeller birbirleri ile reaksiyona girerek aglomeratlar ve nihayet bir makrojel verirler. Gerçek ağ yapı oluşumunu açıklamak amacı ile son yıllarda kinetik teoriler geliştirilmiştir (Dusek 1982, Fukuda 1985, Mikos 1986, Tobita 1989, Okay 1994a,b,c). Bu teoriler istatistiksel teorilere göre daha gerçek sonuçlar iletmektedir. Ancak polimerik ağ yapıların özellikleri ile sentez şartları arasında ki ilişkiler halen tam olarak aydınlatılamamıştır.

1.2 HİDROJELLER

Hidrofilik jellerin diğer bir adıyla hidrojellerin su veya tuz çözeltileri içerisinde şişme davranışları üzerine araştırmalar da son 40 senedir süregelmektedir. Bu çalışmalarda çoğunlukla karboksilik asit gibi zayıf iyonik gruplar içeren hidrojeller kullanılmıştır

(Katchalsky 1955, Hasa 1975, Oppermann 1985, Konak 1989). Bu jellerin şişme davranışları pH ya bağlı olarak değişme göstermektedir. Ancak, kuvvetli elektrolit içeren hidrojeller tüm pH aralığında dissosiye olurlar ve pH ya bağımsız bir şişme davranışı gösterirler. Sulfonik asit grupları içeren hidrojeller yüksek derecede iyonizasyon gösteren kuvvetli polielektrolit jellere örnek olarak gösterilebilir. 2-Akrilamido-2-metilpropansulfonik asit (AMPS) monomerinden elde edilen linear polimerler sulu çözeltiler içinde sarmal boyutlarında çok büyük genişleme göstermektedir (Fisher 1977); 5M NaCl çözeltisi içinde bile, iyonik grupların birbirlerini itmeleri sonucu, polimer sarmalı genleşmiş durumdadır. AMPS ve N,N-dimetilakrilamid (DMAA) monomerlerinden elde edilen hidrojellerin şişme davranışları su ve NaCl çözeltileri içinde incelenmiş olup ve bu jellerin aşırı oranda şiştiklerini gözlenmiştir (Liu 1995). Bazı kuvvetli polielektrolit akrilamid esaslı katyonik ve amfolitik hidrojellerin şişmeleri incelenmiş ve deneysel sonuçlar Flory-Huggins teorisi ile karşılaştırılmıştır (Hooper 1990, Baker 1994).

1970 li yıllarda hidrojellerde birinci dereceden faz geçişlerinin deneysel olarak gözlenmesi ile hidrojeller üzerine yapılan araştımalar daha da yoğunluk kazanmıştır (Tanaka 1978, Tanaka 1981). Yapılan çalışmalar daha çok iyonik jellerde çözücü bileşimine, sıcaklığa, pH'ya v.b. gibi dış etmenlere bağlı faz geçişlerinin deneysel olarak gözlenmesi ve sonuçların ortalama alan teorisi ile açıklanmasına yöneliktir (Katayama 1984, Zhang 1992, Hirokawa 1984, Ishidao 1993).

1.3 MAKROGÖZENEKLİ JELLER

Polimerik ağ yapıların özelliklerini yapılarındaki çapraz bağların sayısı belirler. Örneğin düşük çapraz bağ yoğunluğunda bir ağ yapı (Şekil 2a) çok şişer, dolayısıyla kimyasal reaksiyonlara kolaylıkla girer; ancak mekanik dayanıklılığı düşük ve çok yumuşak olduğundan kullanıma uygun değildir. Buna karşılık yüksek çapraz bağ yoğunluğundaki ağ yapılar sert ve dayanıklıdır; ancak solventlerde çok az şiştiklerinden tepkimelere sadece yüzeyleri ile katılırlar (Şekil 2b). Hem dayanıklılığı yüksek hemde kolaylıkla reaksiyonlara girebilen bir ağ yapı dizaynı Şekil 2c de

görülüyor; Yüksek çapraz bağ yoğunluğu ağ yapıyı sert ve dayanıklı kılmakta, ağ yapı içinde oluşturulan gözenekler ise yüzey alanını arttırmakta ve reaksiyonlara girmesini kolaylaştırmaktadır.

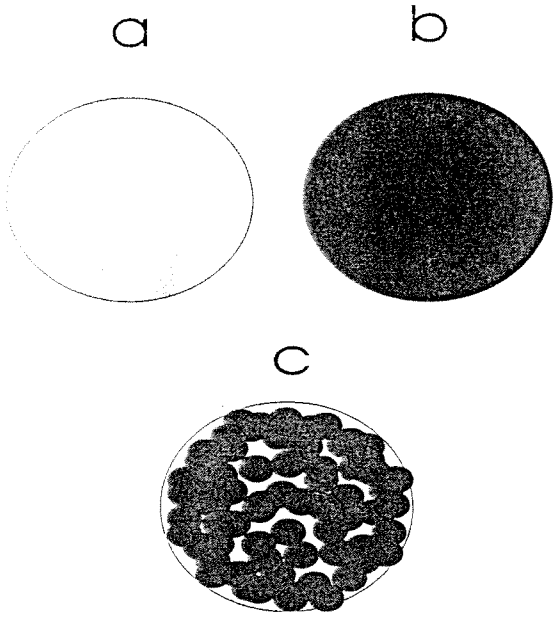

Şekil 2. Az çapraz bağlı (a), çok çapraz bağlı (b) ve gözenekli (c) ağ yapıların şematik olarak görünüşü.

Makrogözenekli polimer ağ yapı sentezleri dünyada ilk olarak 1960 lı yıllarda gerçekleştirilmiştir (Seidl 1967). Makrogözenekli polimerik jeller günümüzde iyon değiştirici reçine, selektif reçine ve absorban olarak geniş oranda kullanılmaktadır. Ağ yapı oluşumu sırasında ortamda uygun bir seyrelticinin (inert bir çözücü veya polimer) bulunması bir faz ayrımına ve bu da gözenekli yapı oluşumuna yol açmaktadır. Ağ yapıların sentez şartları ile gözenek özellikleri arası ilişkiler yoğun olarak incelenmektedir (Dusek 1982, Okay 1985, Okay 1986, Okay 1988). Gözenekli polimer ağ yapı sentezinde kullanılan seyreltici cinsinin, seyreltici ve çapraz bağlayıcı monomer konsantrasyonlarının gözenek yapıyı belirlediği artık bilinmektedir (Okay 1992, Kücük 1995). Seyreltici olarak iyi bir çözücü kullanıldığında küçük gözenekler içeren ve dolayısıyla yüzey alanı büyük olan polimer kürecikleri oluşmakta, buna karşılık kötü bir çözücü veya polimerik seyrelticiler kullanıldığında ise büyük gözenekler oluşmaktadır. Diğer yandan gözenekli polimer jellerinin çeşitli çözücülerle muamelesi ile gözenek yapılarda

değişimlere yol açılabildiği gözlenmiştir (Okay 1986). Ancak bugüne kadar makrogözenekli polimer ağyapıların sentez şartları ile gözenek yapıları arasında kantitatif bir ilişki kurulamamıştır.

1.4. PROJENİN KONUSU VE AMACI

Projenin konusunu ileri teknoloji malzemesi olarak insan yaşamında geniş bir yer tutan ve uygulama alanları giderek genişleyen polimerik jeller oluşturmaktadır. Projenin amacı, makrogözenekli (heterojen) ve homojen polimerik jellerin kürecikler ve parça halinde çeşitli monovinil ve divinil monomer (çapraz bağlayıcı) sistemlerinden yola çıkılarak serbest radikal mekanizma ile sentezleri, jel sentezlerinin bilgisayarda simulasyonu için kinetik + termodinamik bir modelin geliştirilmesi, jel özelliklerinin geliştirilmesi ve bunların biyoteknolojik uygulamaları konularında araştırmalar yapmaktır.

Proje önerisinde jel sentezlerinde kullanılmak üzere yeni monomerlerin örneğin vinilkaprolaktam türevlerinin sentezlenmesi ve elde edilen jellerin enzim ve hücre immobilizasyonunda kullanımları üzerinde araştırmaların da yapılması planlanmıştı. Ancak, yukarıda belirtilen çalışmaların başarı ile yürümesi ve tamamlanmaları için çok sayıda ilave denemelerin yapılması sonucu bu belirtilen konularda planlanan çalışmalar yapılamamış ve bu çalışmaların projeyi takiben yapılması planlanmıştır.

2. MAKROGÖZENEKLİ STİREN-DİVİNİLBENZEN KOPOLİMER KÜRECİKLERİ

2.1. DAYANIKLI GÖZENEKLERİN OLUŞUM ŞARTLARI

Makrogözenekli stiren-divinilbenzen (S-DVB) kopolimer küreciklerinin dayanıklı ve dayanıksız (çökebilen, kaybolabilen) gözeneklerden oluştuğu önceki yıllarda grubumuzda yapılan çalışmalarla bulunmuştu (Okay 1986, Okay 1992). Bu yapılan çalışmalar iyi bir çözücüde örneğin toluende şişmiş durumdaki bir S-DVB kopolimer

ağ yapının kurutulması sırasında bazı gözeneklerin kaybolduğunu ortaya koymuştur. Aynı kopolimer kötü bir çözücüde örneğin metanolde büzülmüş durumda kurutulduğunda ise gözenek yapısı tamamen korunabilmekteydi (Okay 1988). Gözenek yapısında çözücüye bağlı olarak ortaya çıkan bu değişimin polimerin inhomojenliğinden yani çapraz bağ yoğunluğunun polimerin her bölgesinde aynı olmamasından ileri geldiği tarafımızdan öne sürülmüştü (Okay 1986). Ancak, bu dayanıklı ve dayanıksız gözeneklerin polimerizasyon reaksiyonunun hangi safhalarında ortaya çıktığı ve gözenek boyutları bilinmemekteydi. Bu bölümdeki çalışmalar bu konuyu aydınlatmak üzere yapılmıştır.

Stiren-divinilbenzen (S-DVB) kopolimer küreciklerinin gözenek yapılarının polimerizasyon süresine bağlı olarak değişimlerini incelemek amacı ile molce % 10 DVB içeren makrogözenekli S-DVB kopolimer kürecikleri seyreltici olarak siklohekzanol içeren ortamda ve suspansiyon polimerizasyonu tekniği ile sentezlenmiştir. Çeşitli reaksiyon sürelerinde reaktörden alınan küreciklerin gözenek yapıları cıvalı porozimetrede ölçülmüştür. Polimer küreciklerinin sentezi ve karakterizasyonu ile ilgili ayrıntılı bilgiler ekte bu çalışmadan çıkan makalede verilmiştir (Erbay 1999). Şekil 3 de küreciklerin gözenek çap dağılımlarının polimerizasyon süresi ile değişimi görülmektedir.

Toluenden kurutulan küreciklerde sadece dayanıklı olan gözenekler kalmakta olup metanolden kurutulan küreciklerde ise tüm gözenekler değişmeden kalabilmektedir (Okay 1986). Şekil 3 den dayanıklı gözeneklerin kopolimerizasyonun hemen başlarında yani jelleşme noktası civarında oluştuğu görülmektedir. Dolayısıyla ilk olarak faz ayrımına uğrayan ve çapraz bağ yoğunluğu yüksek olan bölgelerdeki gözenekler kurutma işlemi ile çökmemekte ve gözenekli yapının kararlı kısmını oluşturmaktadır. Kararlı gözeneklerin sayısı polimerizasyon sırasında değişmemektedir.

Polimerizasyon reaksiyonunun sonlarına doğru oluşan gözenekler ise kararlı olmayıp kurutma işlemi sırasında çökmektedir. Bu durum reaksiyon sonlarına doğru oluşan

bölgelerin düşük çapraz bağlı olması nedeniyledir. Yapılan çalışma ile ilgili ayrıntılı bilgiler ekteki yayında verilmiştir (Erbay 1998).

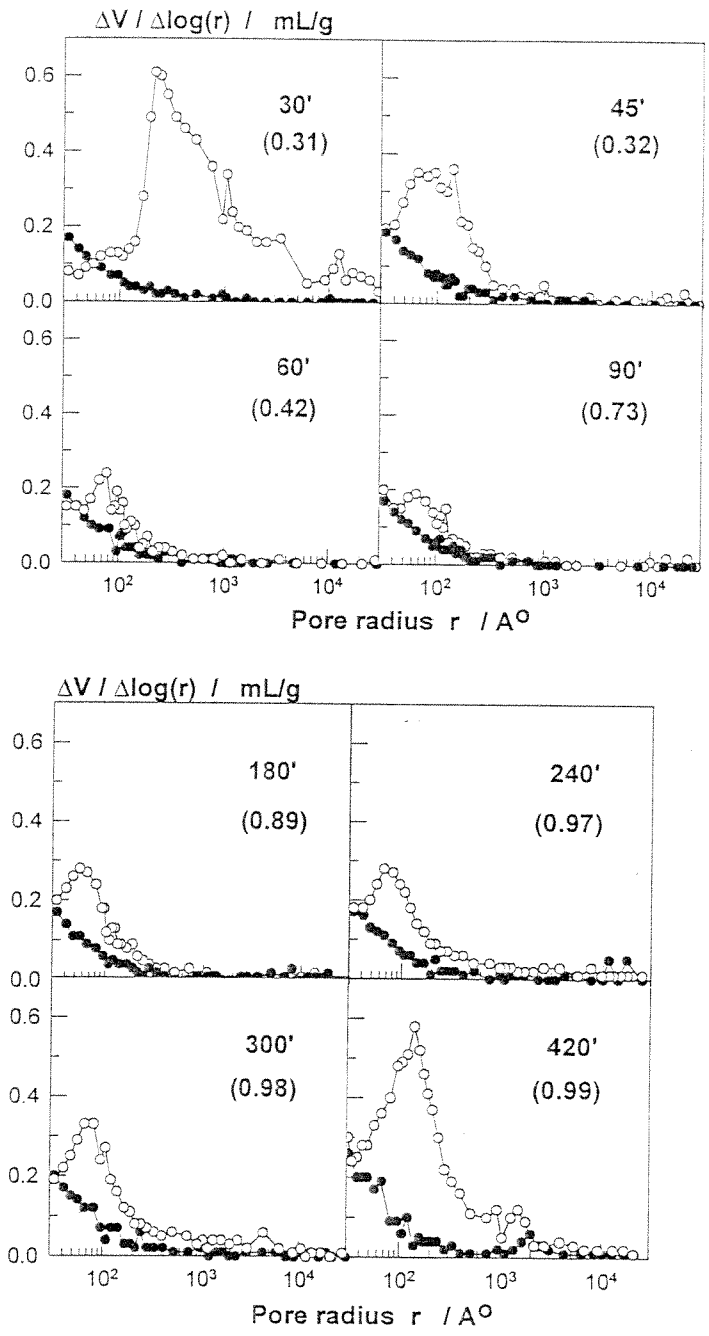

Şekil 3. Toluenden (içi dolu semboller) ve metanolden (içi boş semboller) kurutulan S-DVB kopolimerlerinin diferensiyal gözenek çap dağılımları. DVB = % 10. Organik fazdaki monomer konsantrasyonu = % 50 (v/v), Seyreltici = siklohekzanol. Reaksiyon süreleri ve monomer dönüşümleri (parentez içinde) şekilde verilmiştir. Toluenden kurutma ile dayanıklı gözenekler, metanolden kurutma ile ise dayanıklı+dayanıksız gözenekler ölçülebilmektedir.

2.2. GÖZENEKLERİN HAFIZASI

Bu bölümde yapılan çalışmalarda S-DVB kopolimer küreciklerinin gözenek yapısının gerek reaksiyon şartlarına ve gerekse polimerizasyondan sonra jellerin çeşitli solventler ile muamelesine bağlı değişimleri incelenmiştir. Makrogözenekli kürecikler farklı DVB oranlarında ve çeşitli toluen-siklohekzanol karışımlarında sentezlenmiştir. Şekil 4 den görüldüğü gibi çapraz bağlayıcı DVB konsantrasyonunun artışı veya seyreltici kalitesinin düşmesi ile (yani seyreltici ile kopolimer çözünürlük parametreleri farkı $\delta_1 - \delta_2$ nin artması ile) küreciklerin gözenekliliği artmaktadır.

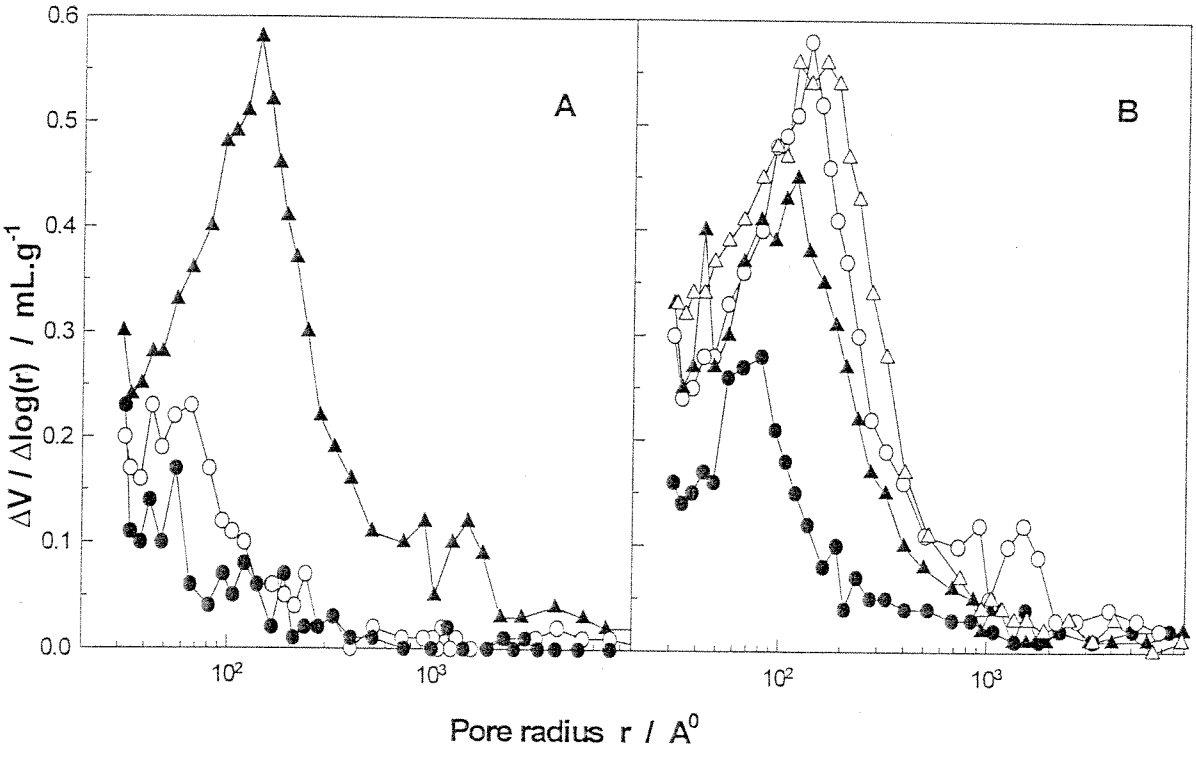

Şekil 4. Seyreltici kalitesinin (A) ve DVB konsantrasyonunun (B) makrogözenekli S-DVB kopolimerlerinin gözenek çap dağılımına etkisi. Organik fazdaki monomer (S+DVB) konsantrasyonu = %50. (A): DVB = % 10. Seyreltici = toluen (●), siklohekzanol/toluen (75/25 v/v) (○), ve siklohekzanol (▲). (B): Seyreltici = siklohekzanol. % DVB = 5 (●), 10 (○), 17.5 (▲), and 24 (△).

Şekil 5 de toluenden ve metanolden kurutulan bir S-DVB kopolimer küreciğinin gözenek çap dağılımı verilmiştir. 10^1 nm çapında olan gözenekler toluenden kurutma işlemi sonrası kaybolmaktadır. Bu kaybolan gözenekler aynı kopolimerin metanolden kurutulması sırasında tekrar ortaya çıkmaktadır.

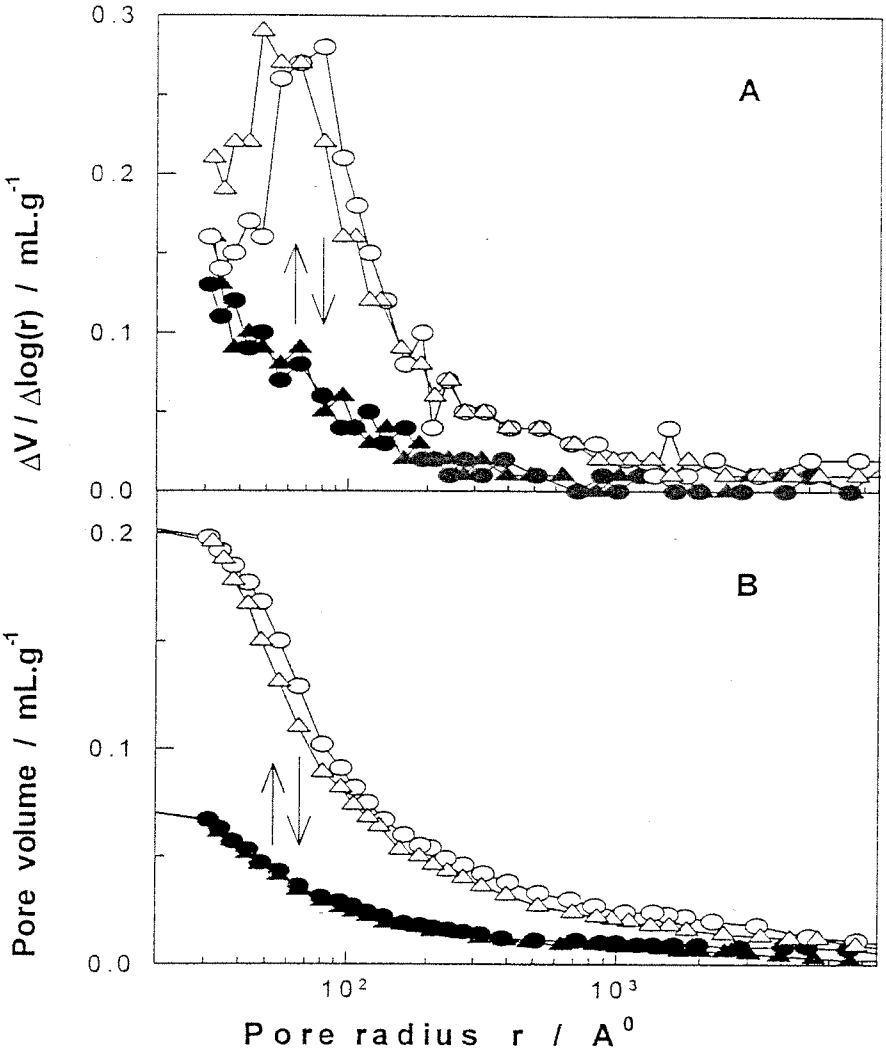

Şekil 5. Makrogözenekli bir S-DVB kopolimerin diferensiyal (A) ve integral (B) modlarda gözenek çap dağılımları. İçi dolu semboller toluenden kurutulan, içi boş semboller ise metanolden kurutulan küreciklere aittir. DVB = 10 %. Seyreltici = Siklohekzanol. Organik faz içindeki monomerin konsantrasyonu = % 50.

10^1 nm çapında olan gözeneklerin kaybolması ve tekrar ortaya çıkmasının tamamen tersinir olduğu tespit edilmiştir. Gözenek yapıdaki bu değişimlerin tersinir olması polimerizasyon sırasında oluşan gerçek gözenek yapının jelin "hafızasında" kaldığını ortaya koymaktadır.

Yapılan deneysel çalışmalar ile polimer - seyreltici etkileşim parametresinin ve çapraz bağlayıcı DVB miktarının gözenek kararlılığında önemli rol oynadığı ortaya konmuştur.

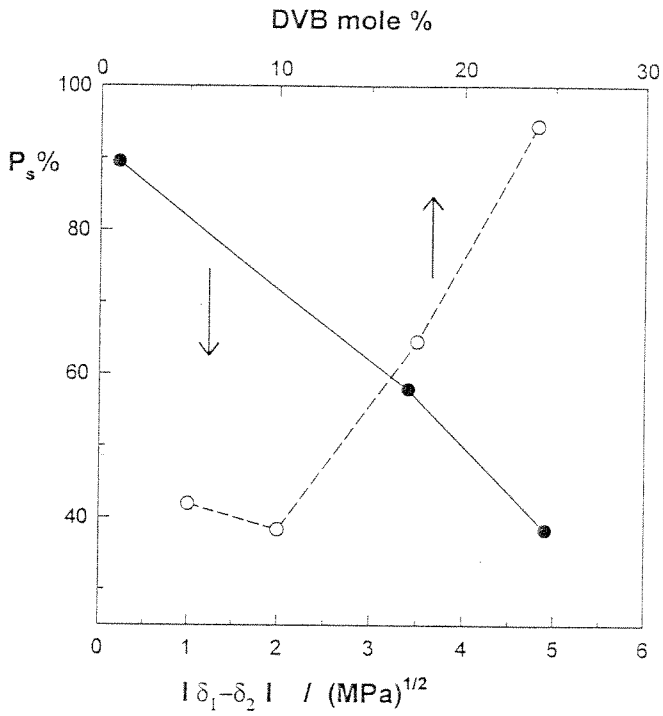

Şekil 6. S - DVB kopolimerlerinde kararlı gözeneklerin hacım yüzdesinin (P_s %) seyreltıcinin solvatasyon gücü $(\delta_1 - \delta_2)$ ve DVB konsantrasyonu ile değişimi. Organik fazdaki monomer konsantrasyonu = % 50. % DVB = 10 (●). Seyreltici = siklohekzanol (○).

Şekil 6 da kararlı gözenek fraksiyonunun (kararlı gözeneklerin hacmi / toplam gözenek hacmi) DVB konsantrasyonu ve seyreltici kalitesi ile değişimi verilmiştir.

Seyreltici kalitesinin düşmesi (χ parametresinin yani $\delta_1 - \delta_2$ nin artması) veya DVB konsantrasyonunun azalması ile gözenekler dayanıksız hale geçmekte ve Şekil 5 de görülen gözenek yapıdaki değişimin boyutları artmaktadır. Yapılan çalışma ile ilgili detaylı bilgiler bir makale olarak yayınlanmış olup ekte verilmiştir (Erbay 1999). Bu makalenin yayınlanmasını takiben "Advanced Coating and Surface Technology Alert" (John Wiley) dergisinin 15 Ocak 1999 tarihli sayısında çalışmayı tanıtıcı bir yazı derginin editörü tarafından yayınlanmıştır (Ekte verilmektedir). Bu tanıtıcı yazıda çözücü ile muamele suretiyle gözenek yapıda tersinir değişiklik yaratmanın uygulamadaki önemi vurgulanmıştır. Bu yöntemle tek bir reçine -kullanım alanına bağlı olarak - gözenek yapısı kullanıcı tarafından değiştirilerek uygulanabilecektir.

3. HETEROJEN POLİAKRİLAMİD JELLERİ ELDESİ

Yapılan çalışmalar ile bir seri iyonik ve iyonik olmayan poliakrilamid (PAAm) jeli N,N-metilenbisakrilamid çapraz bağlayıcısı ve amonyum persulfat / N,N,N,N-tetrametiletilen diamin başlatıcı sistemi yardımı ile % 5 başlangıç monomer konsantrasyonunda elde edilmiştir. İyonik komonomer olarak farklı oranlarda sodyum akrilat kullanılmıştır. Her bir jel örneği sentez sonrası üç kısma ayrılmıştır:

- Birinci kısım herhangi bir işleme tabi tutulmamıştır (sentez sonrası durumdaki jel),
- İkinci kısım vakumda ve oda ısısında tamamen kurutulmuştur (kuru jel),
- Üçüncü kısım ise saf su içinde denge konumuna kadar şişirilmiştir.

Jel örnekleri daha sonra farklı bileşimlerdeki su - kötü solvent (aseton, n-butanol, etanol, veya metanol) karışımlarına daldırılmış ve denge konumuna gelmeleri 6 aya kadar beklenmiştir. Termodinamik denge konumuna ulaşılması halinde jelin her üç kısmınında aynı oranda şişmeleri gerekmektedir. Ancak Şekil 7 den de görüleceği gibi, önceden suda şişirilmiş olan iyonik PAAm jelleri yüksek oranlarda aseton içeren su-aseton karışımlarında denge konumuna kadar büzülememektedir ve jel içinde bir miktar su hapsolmaktadır. Yapılan denemeler ile yüksek oranlarda kötü solvent içeren kötü solvent-su karışımlarına daldırılan ve iyonik grup taşıyan

poliakrilamid jellerinde heterojen yapıların oluştuğu ortaya konmuştur. Jelin başlangıçtaki şişme oranının artışı yani çapraz bağ yoğunluğunun azalması veya kötü solventin polaritesinin azalması ile heterojenlikte artma olduğu gözlenmiştir. Deneysel çalışmalar, kötü solvent-su karışımında bulunan jelde çökmüş (collapsed) bölgelerin ortaya çıktığı ve bu bölgelerin jelin tüm olarak çevre ile termodinamik olarak denge konumuna gelmesini kinetik olarak önlediğini göstermiştir. Yapılan çalışma ile ilgili detaylı bilgiler yayınlanan makalede yazılmış olup ekte verilmektedir (Okay 1998).

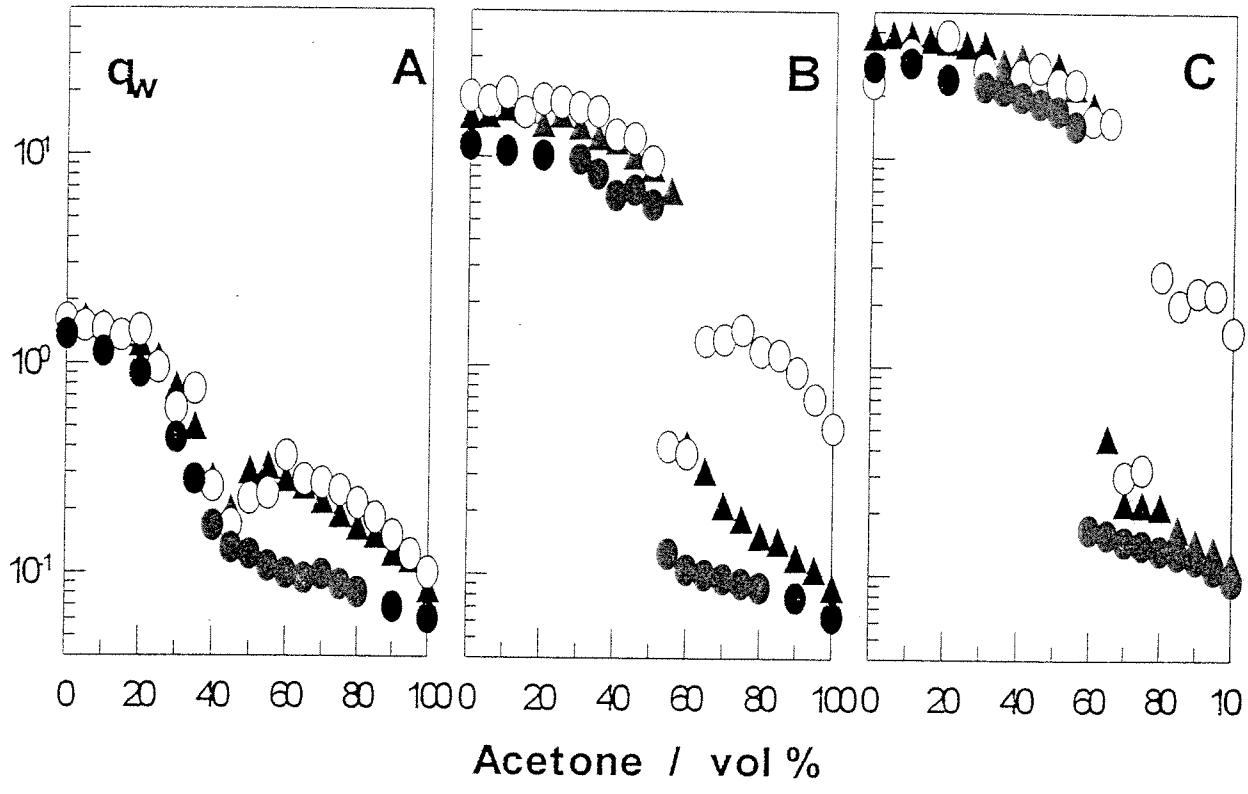

Şekil 7. Poliakrilamid jellerinin şişme oranı q_w nin (dengedeki şişmiş ağırlık / sentez sonrası ağırlık) aseton-su karışımındaki aseton yüzdesi ile değişimi. Jellerin başlangıç durumları: kuru (●), önceden suda şişirilmiş (○), sentez sonrası (Δ). N,N,-metilenbisakrilamid = % 1, sodium akrilat = % 0 (A), % 4.6 (B), ve % 28 (C)

4. MAKROGÖZENEKLİ KOPOLİMERLERİN OLUŞUM TEORİSİ

Makrogözenekli jellerin sentezi ile ilgili literaturde çok sayıda deneysel çalışma olmasına karşılık teorik bir çalışma yoktur. Proje kapsamında makrogözenekli polimerlerin sentez şartları ile yapıları arası bağıntıyı veren bir teori geliştirilmiştir. Serbest radikal mekanizma ile gözenekli polimer ağyapı oluşumu kinetiği ve termodinamiğinin detaylı olarak incelendiği teorik modelde reaksiyon şartlarından gözenekli polimer özelliklerini verebilmektedir. Makrogözenekli bir yapıda jel eldesi için jel oluşumu sırasında bir faz ayrımının gerçekleşmesi gerekmektedir (Dusek 1967). Şekil 8 de faz ayrımı öncesi ve sonrası polimerizasyon sistemi şematik olarak görülüyor. Faz ayrımı sonrası reaksiyon sistemindeki seyreltici, reaksiyona girmemiş monomer ve sol polimerler her iki faz arasında dağılırlar. İki faz arası termodinamik denge durumunda difüzlenebilen bileşenlerin (monomerler, seyreltici ve sol molekülleri) her iki fazdaki kimyasal potansiyellerinin birbirine eşit olması gerekir.

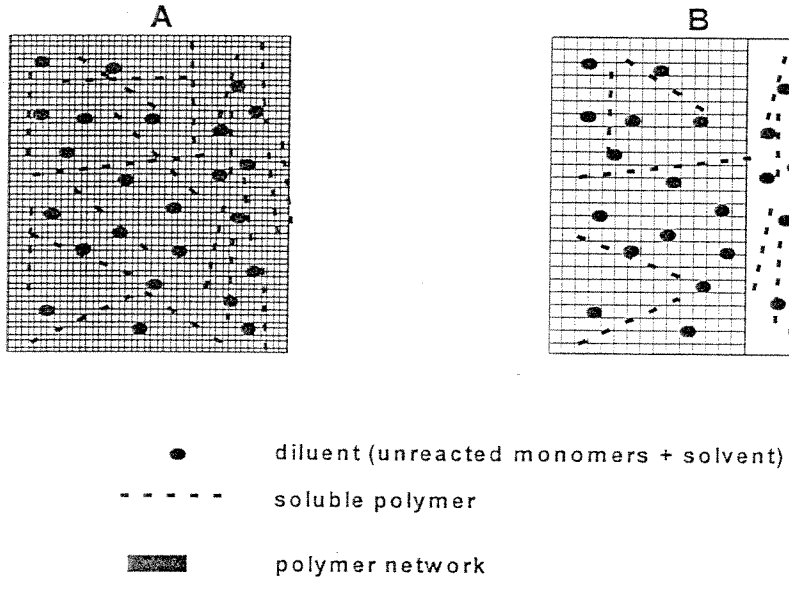

Şekil 8. Serbest radikal mekanizma ile jel oluşumunda reaksiyon sisteminin faz ayrımı öncesi (A) ve sonrası (B) şematik görünüşü.

Geliştirilen modelde, Flory-Huggins teorisi yardımı ile vinil-divinil monomer kopolimerizasyonunda jel fazı ile ayrılan faz arasındaki faz dengelerini tarif eden termodinamik denklemler türetilmiştir. Bu denklemlerin çözümü için reaksiyon süresine (veya monomer dönüşümüne) bağlı olarak değişen sol ve jel özelliklerinin bilinmesi gerekmektedir. Bu bilgiler ise ağyapı oluşumunu simüle eden kinetik denklemler yardımı ile hesaplanmıştır. Geliştirilen kinetik-termodinamik model ile ilgili detaylı bilgiler ve denklemler yayınlanan makalelerde ve ekte verilmiştir (Okay 1999).

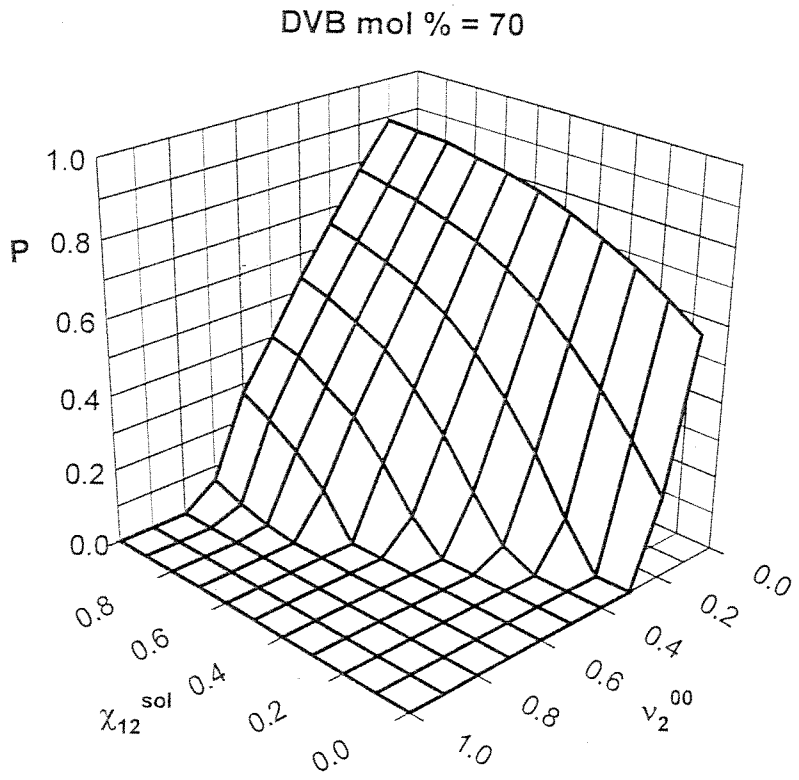

Şekil 9. S-DVB kopolimerlerinin gözenekliliğinin P başlangıç monomer konsantrasyonu ve polimer - seyreltici etkileşim parametresi ile değişimi.

Geliştirilen modelin stiren-divinilbenzen kopolimerizasyon sistemine uygulanması ile elde edilen sonuçlar Şekil 9 ve 10 da görülüyor. Şekillerde P toplam gözenek fraksiyonunu (gözeneklerin toplam hacmi / polimerin hacmi), v_2^{00} organik fazdaki monomerin reaksiyon başlangıcındaki hacim fraksiyonunu, ve χ_{12}^{sol} polimer -

seyreltici + reaksiyona girmemiş monomer arasındaki Flory etkileşim parametresini göstermektedir. Sabit bir çapraz bağlayıcı konsantrasyonu için (% 70 DVB, Şekil 9) polimerik ağ yapının gözenekli olması için monomer konsantrasyonunun (ν_2^{00}) kritik bir değerin altında veya χ_{12}^{sol} un kritik bir değerinin üzerinde bulunması gerekmektedir. Monomer konsantrasyonunun azalması veya polimer - çözücü etkileşim parametresinin artması ile ürünün gözenekliliği de artmaktadır.

Diğer yandan, sabit bir χ_{12}^{sol} değeri için, yani belli bir seyreltici sistemi için DVB konsantrasyonunun artması veya monomer konsantrasyonunun azalması ile kopolimer gözenekliliği artmaktadır (Şekil 10). Hesap sonuçları deneysel sonuçlar ile tamamen uyum halindedir. Teori ile deneysel sonuçların ayrıntılı bir karşılaştırması bu çalışmadan çıkan makalede yayınlanmış olup ekte sunulmuştur (Okay 1999).

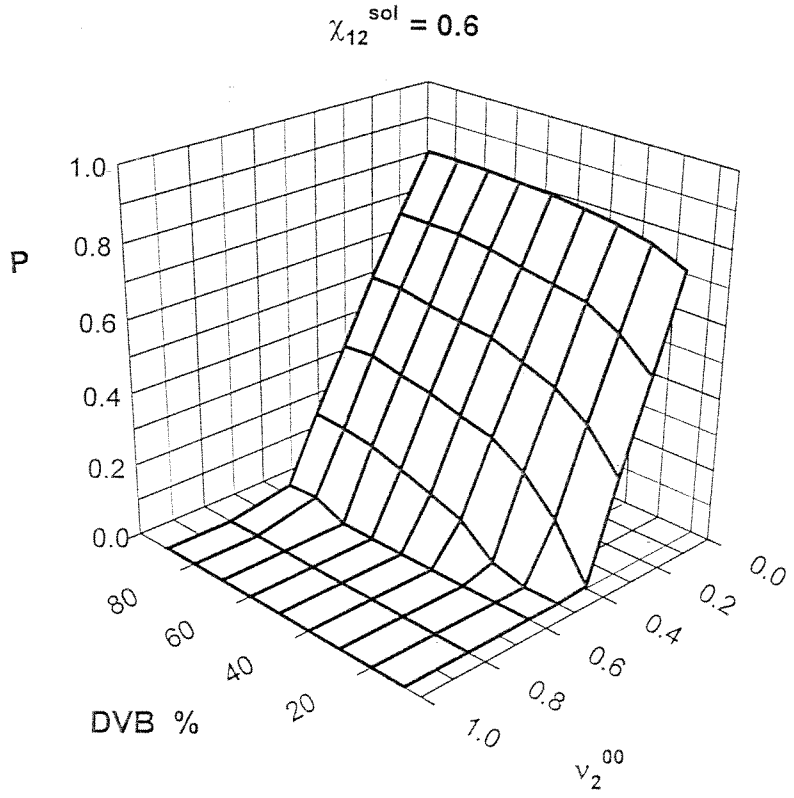

Şekil 10. S-DVB kopolimerlerinin gözenekliliğinin P sentez sırasında kullanılan DVB konsantrasyonu ve başlangıç monomer konsantrasyonu ile değişimi.

5. HALKA OLUŞUMU VE ELEKTROSTATİK ETKİLEŞMELERİN JEL OLUŞUMUNA ETKİSİ

Serbest radikal mekanizma ile jel oluşumu sırasında halka oluşumu, çok katlı çapraz bağlanma, difüzyon kontrollu sonlanma reaksiyonlarının ve büyüyen polimer zincirleri üzerindeki iyonik grupların jel oluşumu prosesine etkilerini incelemek için aşağıda yazılı monovinil-divinil monomer sistemlerinde jel oluşum reaksiyonları dilatometrik ve gravimetrik tekniklerle takip edilmiştir.

- Metil metakrilat (MMA) - Etilenglikoldimetakrilat (EGDM)
- Akrilamid (AAm) - N,N-metilenbisakrilamid (BAAm) - iyonik komonomer (sodyum akrilat NaAc veya 2-akrilamido-2-metilpropan sulfonik asit sodyum tuzu AMPS).

Deneysel çalışmalarla ilgili ayrıntılı bilgiler ekteki yayında verilmiştir (Okay 1998). Şekil 11 de farklı çapraz bağlayıcı (A) ve iyonik komonomer (B) konsantrasyonlarında jel oluşumu prosesi sırasında zaman-dönüşüm grafikleri verilmiştir. Çapraz bağlayıcı konsantrasyonunun artışı ile dönüşüm hızı önce artmakta sonra ise azalmaktadır. İyonik komonomer katkısı ise reaksiyon hızını azaltmaktadır. Zaman-dönüşüm grafiklerinden jelleşme prosesinde büyüyen radikallerin relatif sonlanma hızlarının hesaplanması mümkündür (Okay 1995). Reaksiyon başındaki (t = 0 anındaki yani ilk polimer radikallerinin oluştuğu andaki) relatif sonlanma hız sabiti $k_{t0,rel}$; çapraz bağlayıcı içeren ortamdaki sonlanma hız sabitinin çapraz bağlayıcı içermeyen ortamdaki hız sabitine oranı olarak tanımlanırsa, $k_{t0,rel}$ in çapraz bağlayıcı ve iyonik grup konsantrasyonlarına bağlı değişimi Şekil 12 de verilmiştir. Reaksiyon ortamındaki eser miktarlarda ki çapraz bağlayıcı $k_{t0,rel}$ i arttırmaktadır, yani radikaller çapraz bağlayıcı içeren ortamda daha büyük bir hızla sonlanmaktadır. Daha sonra çapraz bağlayıcı konsantrasyondaki artış $k_{t0,rel}$ i düşürmektedir. İyonik komonomer içeren ortamlarda ise $k_{t0,rel}$ sürekli olarak azalmaktadır, yani zincirler üzerine iyonik grupların takılması ile zincir daha yavaş sonlanmaktadır.

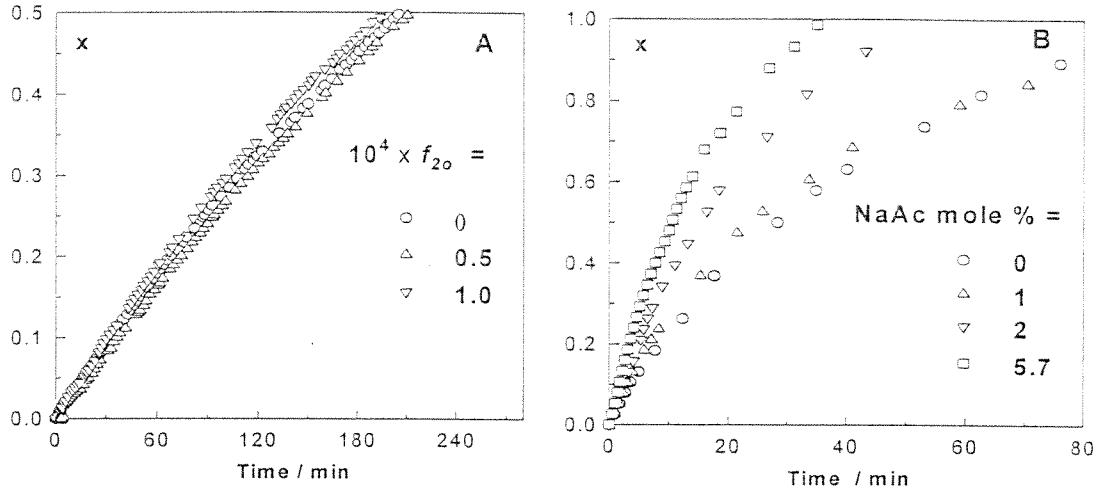

Şekil 11. Çapraz bağlayıcı (A) ve iyonik komonomer konsantrasyonu (B) ile zaman-dönüşüm eğrilerinin değişimi. (A) MMA/EGDM sistemi. Başlatıcı (AIBN) konsantrasyonu = 0.02 M. (B) AAm/BAAm systemi. Monomer karışımı içindeki çapraz bağlayıcının mol fraksiyonu $f_{2o} = 5x10^{-4}$.

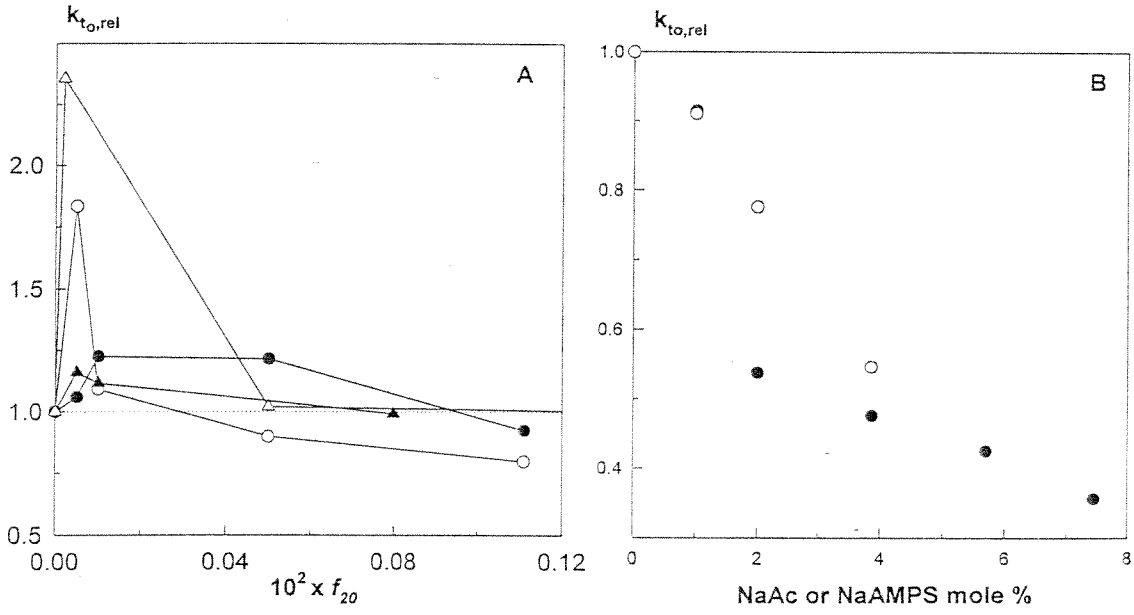

Şekil 12. Relatif sonlanma hız sabiti $k_{t0,rel}$ in çapraz bağlayıcı (f_{2o}) ve iyonik komonomer (NaAc veya AMPS) konsantrasyonu ile değişimi. (A) MMA/EGDM sistemi. $[I]_0 = 0.1$ (●), 0.02 (○), and $3.75x10^{-3}$ M (▲). AAm/BAAm sistemi: (△). (B) AAm/BAAm sistemi: $f_{2o} = 5x10^{-4}$, İyonik komonomer = NaAc (●), AMPS (○).

Deneysel bulgular serbest radikal mekanizma ile jel oluşumu prosesinde etkin olan iki zıt dışlanmış hacım etkisi ile açıklanmıştır:

- Termodinamik dışlanmış hacım etkisi,
- Sterik dışlanmış hacım etkisi.

Şekil 13 de aynı kinetik zincir uzunluklarına sahip iki polimer zinciri şematik olarak görülüyor. A zinciri genleşmiş, B zinciri ise büzülmüş konformasyondadır. Serbest radikal mekanizma ile jel oluşumu prosesinde ortamda az miktarda çapraz bağlayıcı bulunduğunda halka oluşumu reaksiyonları sonucu zincir boyutları küçülmekte ve makroradikal zinciri A konformasyonundan B ye geçmektedir. Küçülen zincir sarmalının difüzyon hızı ve bunun sonucu olarak ta $k_{t0,rel}$ artmaktadır (Şekil 12). Ancak çapraz bağlayıcı konsantrasyonundaki artışın devamı sterik nedenlerle B konformasyonundaki zincirin sonlanmasını zorlaştırmaktadır (sterik dışlanmış hacım etkisi).

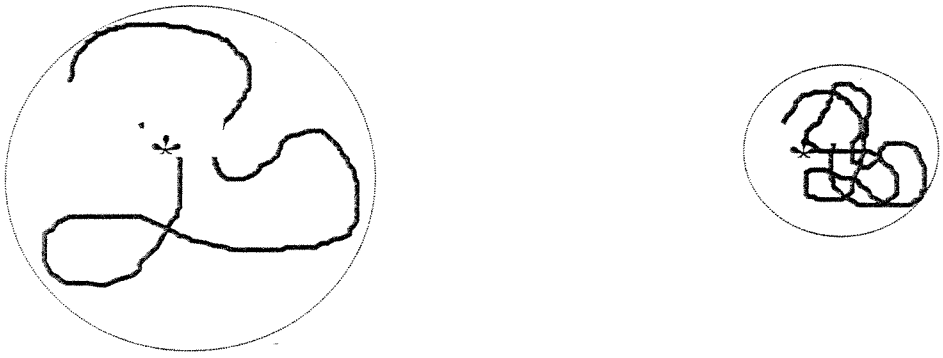

Şekil 13. Aynı kinetik zincir uzunluklarında genleşmiş (A) ve büzülmüş konformasyonda (B) iki makroradikal sarmalı. A ve B sarmallarının segmental difüzyonlarında sırası ile termodinamik ve sterik dışlanmış hacım etkileri belirgin bir rol oynamaktadır.

Diğer yandan zincir üzerine iyonik grupların takılması elektrostatik etkileşmeler ve karşı iyonların ozmotik basıncı sonucu zinciri B konformasyonundan A ya çevirmekte ve büyüyen zincir boyutları sonucu olarak zincir radikalinin sonlanması daha yavaş olmaktadır (termodinamik dışlanmış hacım etkisi). Serbest radikal mekanizma ile jel oluşumunda her iki dışlanmış hacım etkisinin teorik modelleme çalışmalarında hesaba alınması gereklidir.

6. İYONİK POLİAKRİLAMİD JELLERİNİN SU VE TUZLU ÇÖZELTİLERDE ŞİŞME DAVRANIŞLARI

Su içindeki bir hidrojelin denge anındaki şişme oranı ağ yapının çapraz bağ yoğunluğuna, ağ yapının taşıdığı iyonik grup sayısına, polimer-su etkileşim parametresine ve sentez sonrası hidrojeldeki polimer konsantrasyonuna bağlı olarak değişmektedir (Flory 1953). Flory-Rehner teorisine ideal Donnan dengesi eklenerek elde edilen teorik bağıntı jellerin dengedeki hacımca şişme oranları (q_v) ile jel özellikleri arası bağıntıyı vermektedir. Şekil 14 de Flory-Rehner teorisi + ideal Donnan dengesi yardımı ile hesaplanan jelin hacımca şişme oranı q_v değerlerinin aşağıdaki parametreler ile değişimi verilmiştir:

1. Jelin çapraz bağ yoğunluğu N^{-1} (N ardışık iki çapraz bağ noktası arası ünite sayısıdır),
2. Jeldeki iyonik grup sayısı f (f polimer ağ yapıdaki ozmotik olarak etkin iyonik grup fraksiyonudur.),
3. Sentez sonrası jeldeki polimer ağyapının hacım fraksiyonu v_2^0.

Şekil 14 e göre 1 gramı 1 litre veya daha fazla su emebilen süperabsorban hidrojellerin sentezi için düşük çapraz bağlayıcı ve yüksek iyonik komonomer konsantrasyonlarında, ve düşük toplam monomer konsantrasyonlarında çalışılması gerekmektedir. Ancak Şekil 14 te verilen teorik öngörümler serbest radikal mekanizma ile sentezlenen jellerde deneysel olarak sadece kalitatif olarak

Bu bölümde yapılan çalışmalarda:

- farklı sentez şartlarında kuvvetli ve zayıf elektrolit jeller hazırlanmış ve onların su ve tuzlu sulardaki şişme oranları ölçülmüştür,
- deneysel bulgular Flory-Rehner teorisi + ideal Donnan dengesinin öngörümleri ile karşılaştırılmış ve aradaki sapmaların nedenleri açıklanmıştır.

6.1 AKRİLAMİD / 2-AKRİLAMİDO-2-METİLPROPAN SULFONİK ASİT ESASLI HİDROJELLER

Sulfonik asit içeren hidrojeller yüksek iyonizasyon dereceleri ile kuvvetli elektrolit jeller sınıfına girerler. Yapılan çalışmalarda akrilamid monomeri 2-akrilamido-2-metilpropan sulfonik asit (AMPS) iyonik komonomeri ile % 5 monomer konsantrasyonunda N,N-metilenbisakrilamid (BAAm) çapraz bağlayıcısı ile polimerleştirilmiştir.

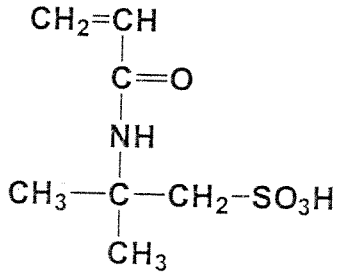

2-akrilamido-2-metilpropan sulfonik asit (AMPS)

AMPS monomeri polimerizasyondan önce NaOH ile nötralize edilmiştir. Yapılan denemelerde çapraz bağlayıcı oranı (BAAm/monomer mol oranı) 1/81 olarak sabit tutulmuş monomer karışımındaki AMPS yüzdesi ise 0 ile 80 arasında değiştirilerek bir seri jel sentezlenmiştir. Jellerin sentezi ve karakterisayonu ile ilgili ayrıntılı bilgiler yayınlanan makalede ve ekte verilmiştir (Okay 1999). Şekil 15 de monomer karışımındaki AMPS mol fraksiyonu f_e ye bağlı olarak jellerin saf su ve farklı konsantrasyonlardaki NaCl çözeltilerindeki dengedeki hacımca şişme oranları q_v

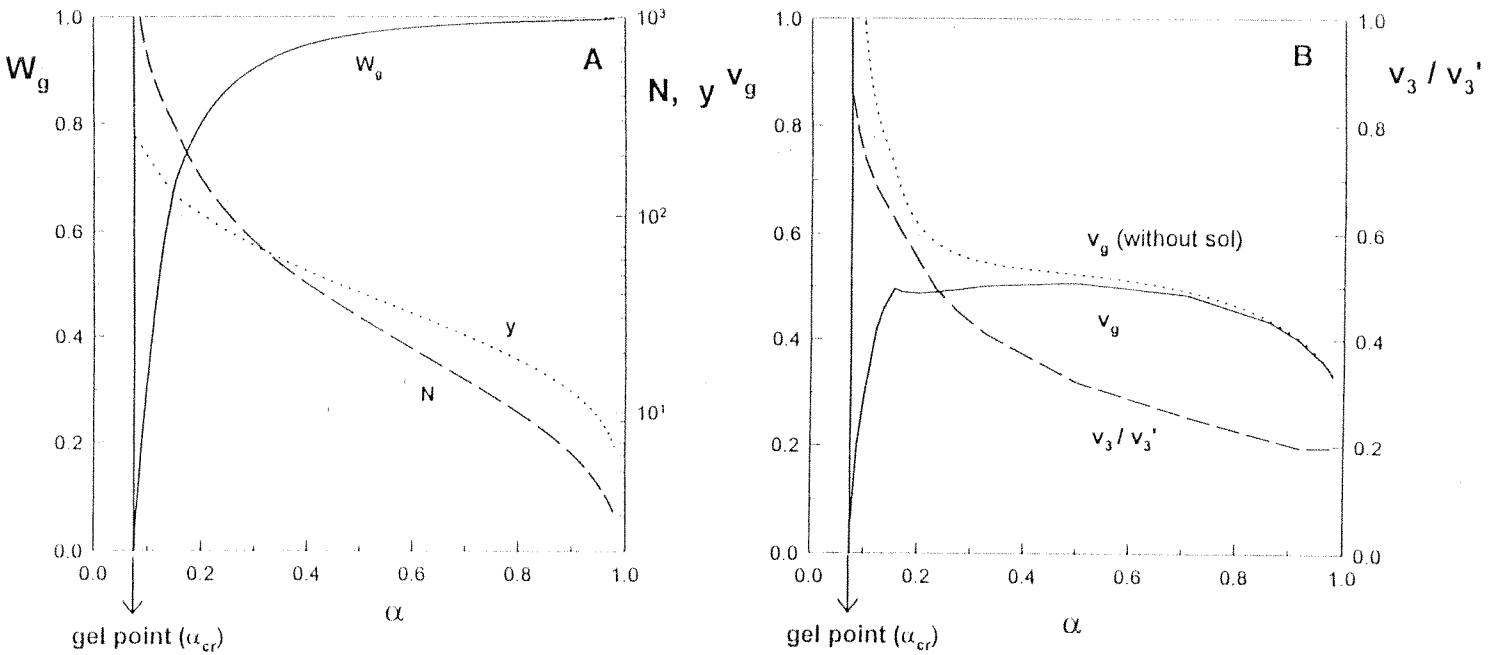

Fig. 2. (A) The weight fraction of gel W_g the number-average degree of polymerization of sol polymers *y and* the number of segments in the network chains *N* shown as a function of the volume conversion α in *Sim*-DVB copolymerization with AIBN as an initiator. The calculations were for 67 mol% *m*-DVB in the initial monomer mixture and for $v_2^{00} = 0.20$. The solid vertical line represents the location of the kinetic gel point. (B): The volume fraction of the network phase v_g and the distribution of the soluble polymers between the gel and separated phases v_3/v_3' shown as a function of the monomer conversion α. Calculations were for $\chi_1 = 0.46$. The solid curve represents the v_g values calculated using the present model, whereas the dotted curve is the result of v_g calculations with neglected sol fraction.

doğrulanabilmektedir. Üç sentez parametresi ile jelin şişme oranı arasında kantitatif bir bağıntı bugüne kadar geliştirilememiştir.

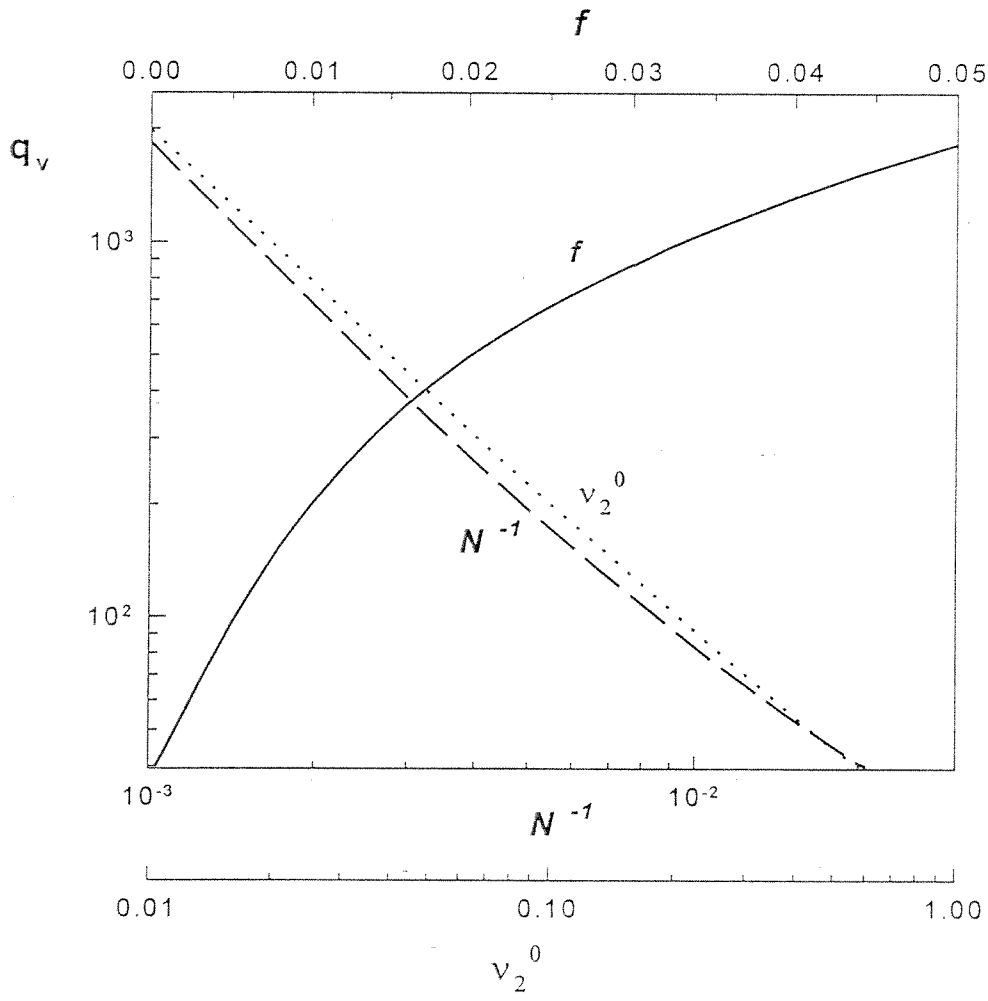

Şekil 14. Flory-Rehner teorisine göre bir jelin hacımca şişme oranı q_v nin N^{-1}, f, ve ν_2^0 a bağlı olarak değişimi. Hesaplamalar için polimer-çözücü etkileşim parametresi 0.48, çözücünün molar hacmi 18 mL/mol olarak alınmıştır.

Kesiksiz eğri: $N^{-1} = 10^{-3}$, $\nu_2^0 = 0.04$

Kesikli eğri: $f = 0.05$, $\nu_2^0 = 0.04$

Noktalı eğri: $N^{-1} = 10^{-3}$, $f = 0.02$.

görülüyor. Monomer karışımındaki AMPS miktarının % 0 dan %5 e çıkması ile jelin şişme oranı 50 den 750 e çıkmakta daha sonra % 20 ye kadar artan AMPS miktarı ile q_v değişmemektedir. AMPS nin daha da arttırılması ile jelin şişme oranı sürekli olarak artmaktadır. Molce % 80 AMPS içeren jelin 1 mL si 2500 mL yani 2,5 litre suyu emebilmektedir. Bu değer bugüne kadar rapor edilmiş şişme oranları arasında bir rekor oluşturmaktadır. Jelin tuz çözeltileri içinde şişme oranı daha az olup artan tuz konsantrasyonu ile şişme oranı azalmaktadır. Bu durum, artan tuz konsantrasyonu ile jelin içi ile dışı arasındaki haraketli iyon (Na^+) konsantrasyonu farkının azalması nedeniyledir.

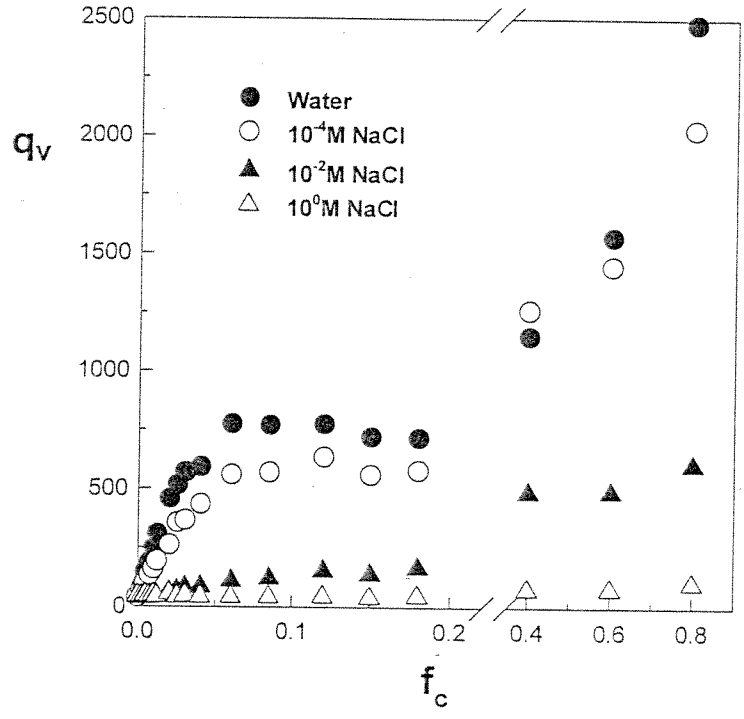

Şekil 15. Monomer karışımındaki AMPS mol fraksiyonu f_c ye bağlı olarak jellerin saf su ve farklı konsantrasyonlardaki NaCl çözeltilerindeki dengedeki hacımca şişme oranları q_v.

Şekil 15 deki deneysel sonuçları Flory-Rehner teorisi açıklayamamaktadır. Teoriye göre q_v nin artan f_c ile sürekli olarak ve çok büyük bir hızla artması gerekmektedir.

Yapılan teorik çalışmalarda Flory-Rehner teorisi + ideal Donnan dengesinin deneysel olarak gözlenen şişme değerlerini verebilmesi için jelin çapraz bağ yoğunluğunun (N^{-1}) veya ozmotik olarak etkin iyonik grup sayısının (f) f_c ile nasıl değişmesi gerektiği incelendi yani N ve f birer ayarlama parametresi olarak hesaplamalarda kullanıldı.

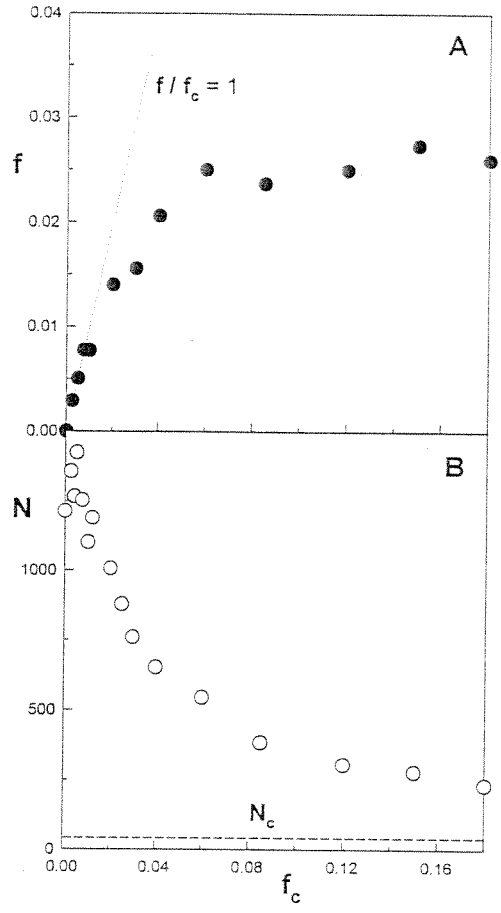

Şekil 16. Hidrojel sentezinde kullanılan AMPS mol fraksiyonu f_c ye bağlı olarak ağ yapı parametreleri N ve f nin değişimleri.

Şekil 16A da f ayarlama parametresi olarak alındığında f nin f_c ile değişimi görülüyor. Flory-Rehner denklemi ile hesaplanan etkin iyon sayısı f, % 1-2 AMPS oranına kadar kimyasal olarak polimerik yapıya sokulan iyon sayısı f_c e eşittir. Artan AMPS miktarı ile sapma ortaya çıkmakta ve etkin iyon sayısı kimyasal iyon sayısının altında kalmaktadır. Bu durum karşı-iyonların kondenzasyonu ve/veya zincirlerin sınırlı olan

uzayabilirliğinden ileri gelebilir. Şekil 16 B de ise N ayarlama parametresi olarak alındığında N nin f_c ile değişimi veriliyor. Jel sentezinde kullanılan çapraz bağlayıcı oranından hesaplanan N değeri N_c olarak şekilde görülüyor. Sentez sırasında kullanılan BAAm çapraz bağlayıcısının tümünün jel içinde elastik olarak etkin çapraz bağlar oluşturduğu varsayılsa Flory-Rehner denkleminden N = 41 olarak bulunması gerekliydi. Halbuki deneysel şişme değerlerinin Flory-Rehner denklemine uygulanması ile iyonik olmayan PAAm jelleri için N 1200 civarında bulunmuştur. Bu sonuç kullanılan çapraz bağlayıcının % 80 oranında elastik olarak etkin olmayan halka ve çok katlı çapraz bağlanma reaksiyonlarına harcandığını ortaya koymaktadır.

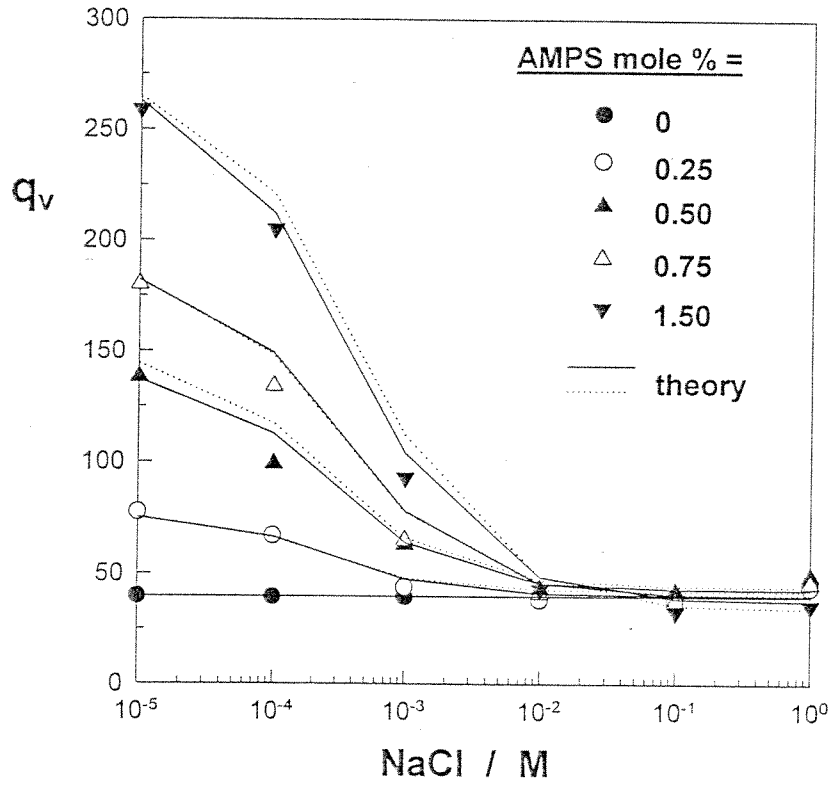

Şekil 17. % 0 ile 1,5 mol oranları arasında değişen miktarlarda AMPS içeren hidrojellerin hacımca şişme oranlarının tuz konsantrasyonu ile değişimi.

Şekil 17 ve 18 de farklı AMPS oranlarında sentezlenen hidrojellerin 10^{-5}M ile 1M arası değişen konsantrasyonlardaki NaCl çözeltilerinde şişme oranları verilmiştir. Şekillerdeki eğriler Flory-Rehner teorisi + ideal Donnan dengesi yardımı ile hesaplanmıştır. Kesiksiz eğriler için f, kesikli eğriler için ise N ayarlama parametresi olarak hesaplamalarda kullanılmıştır. Görüldüğü gibi jelin çapraz bağ yoğunluğunun bir ölçüsü olan N veya etkin iyonik grup sayısı f teorik hesaplamalarda ayarlama parametresi olarak alınırsa teori deneysel bulguları verebilmektedir. Gerek Flory-Rehner teorisinin ve gerekse ideal Donnan dengesinin bazı varsayımları çok fazla şişen jellerde geçerli olmayıp aradaki farklar ayarlama paametreleri N veya f ile telafi edilebilmektedir. Bu bölümde yapılan çalışmalarla ilgili ayrıntılı bilgiler ekteki ilgili yayında verilmiştir (Okay 1998, Okay 1999).

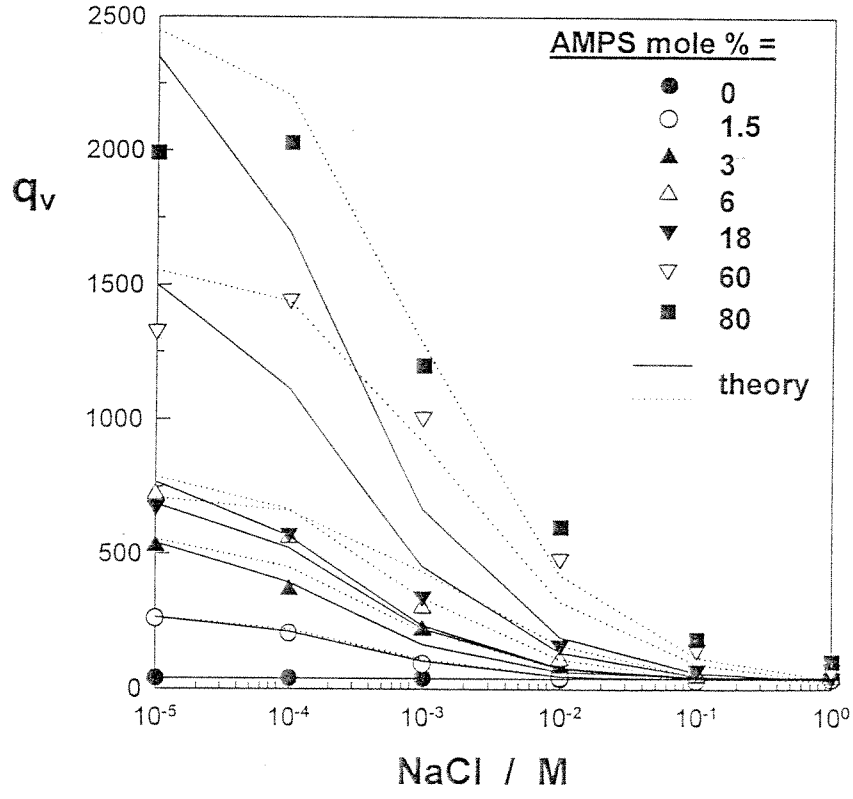

Şekil 18. % 0 ile 80 mol oranları arasında değişen miktarlarda AMPS içeren hidrojellerin hacımca şişme oranlarının tuz konsantrasyonu ile değişimi.

6.2 AKRİLAMİD / SODYUM AKRİLAT ESASLI HİDROJELLER

Kuvvetli elektrolit AMPS esaslı hidrojellerin deneysel olarak ölçülen şişme oranlarından Flory-Rehner teorisi yardımı ile hesaplanan ağ yapı parametrelerinin diğer tip jellere aktarılabilirliği bu bölümde incelenmiştir. Deneysel çalışmalar zayıf elektrolit AAm / sodyum akrilat (NaAc) hidrojelleri ile yapılmıştır. Jellerin sentezi ve karakterizasyonu ile ilgili detaylar ekteki ilgili yayında verilmiştir. (Okay 1999). Şekil 19 ve 20 de AAm/NaAc jellerinin su ve tuz çözeltilerindeki dengedeki şişme oranlarının jel sentezinde kullanılan NaAc mol fraksiyonu f_c ve tuz konsantrasyonu ile değişimi görülüyor.

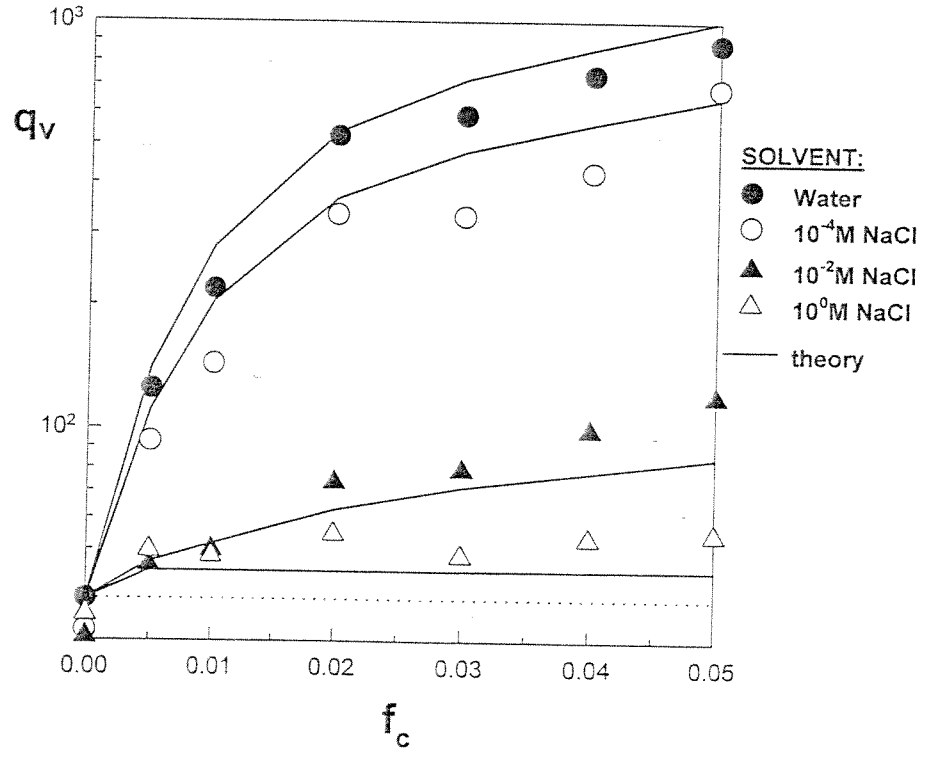

Şekil 19. AAm/NaAc jellerinin hacımca şişme oranlarının NaAc ın mol fraksiyonu f_c ile değişimi.

Eğriler teorik olarak hesaplanmış olup f parametresi için bir önceki bölümde bulunan değerler kullanılmıştır. Şekillerden teori ile deney arasında iyi bir uyum olduğu yani tek bir ayarlama parametresi ile tüm hidrojellerin şişme davranışlarının Flory-Rehner teorisinin ideal Donnan dengesi ile birleştirilmesi suretiyle açıklanabileceği görülüyor. İlginç bir gözlem ise yüksek tuz konsantrasyonlarında iyonik jellerin şişme davranışlarıdır; bu bölgede beklenenin aksine artan tuz konsantrasyonu ile jelin şişme oranı tekrar artmaktadır. (Şekil 20 de ki küçük kare). Bu durumun poliakrilamid segmanları ile NaCl arasındaki spesifik etkileşmelerden ileri geldiği düşünülmektedir.

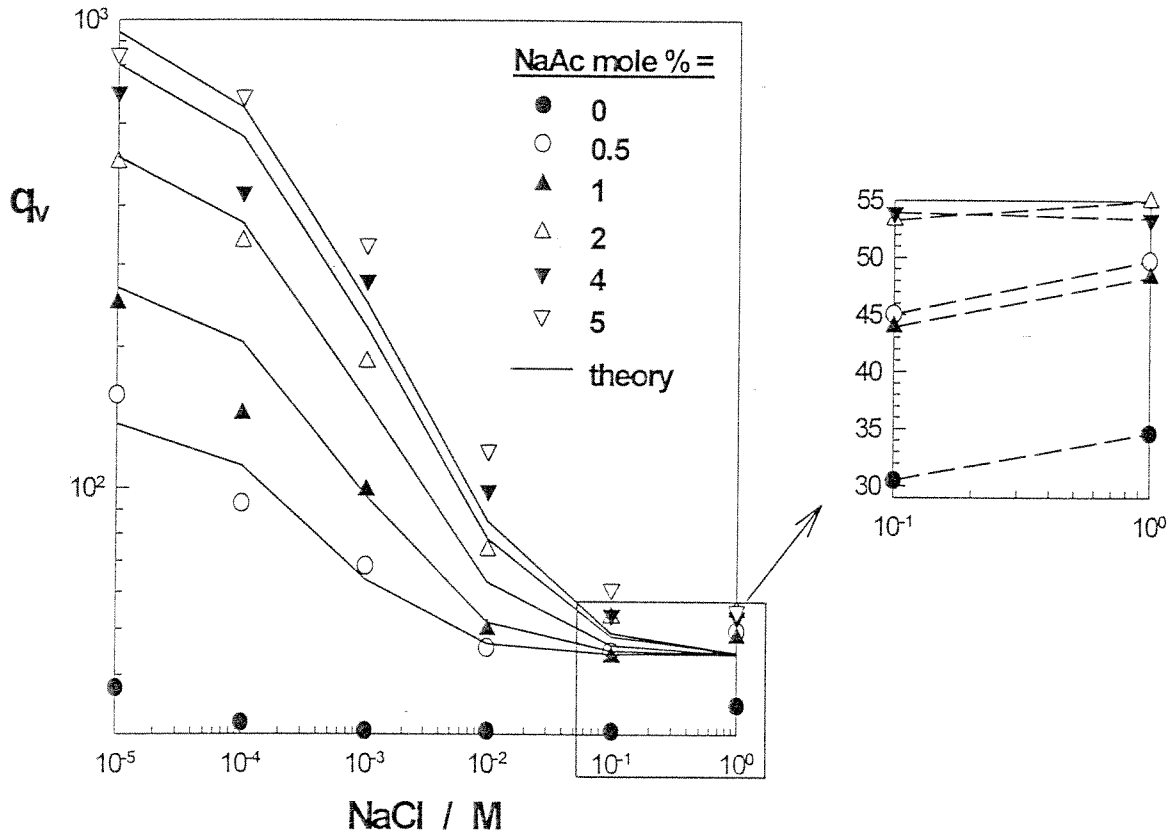

Şekil 20. AAm/NaAc jellerinin hacımca şişme oranlarının tuz konsantrasyonu ile değişimi.

7. SONUÇLAR

- Makrogözenekli stiren-divinilbenzen kopolimer küreciklerinin sentez şartları ile gözenek yapıları arası bağıntıyı veren bir model geliştirilmiştir. Makrogözenekli polimer oluşumu prosesinde fazlar arası termodinamik dengeleri ve her bir fazdaki bileşenlerin konsantrasyonlarındaki zamana bağlı değişimleri gözönüne alan model öngörümleri deneysel bulgular ile uyum halindedir.
- Makrogözenekli stiren-divinilbenzen kopolimer küreciklerinde dayanıklı (kararlı) gözeneklerin jelleşme prosesinin hemen başlarında ortaya çıktığı saptanmıştır. Çapraz bağ yoğunluğu yüksek olan jel bölgelerinin içindeki boşluklara karşılık gelen dayanıklı gözeneklere oranla dayanıksız gözenekler reaksiyon sonlarında oluşmaktadır.
- Tersinir gözenekli stiren-divinilbenzen kürecikleri sentezlenmiş ve en uygun sentez şartları belirlenmiştir.
- Gözenekli poliakrilamid jelleri homojen jellerin sentez sonrası solventlerle muamelesi sonucu elde edilmiştir.
- Serbest radikal mekanizma ile jel oluşumu prosesinde termodinamik ve sterik dışlanmış hacım etkileri kavramı ortaya atılmıştır.
- Kuvvetli ve zayıf elektrolit hidrojeller sentezlenmiş ve bu jellerin su ve tuzlu sulardaki dengedeki şişme oranları ölçülmüştür. 1 mL si 2,5 litreye kadar su emebilen süperabsorban hidrojeller sentezlenmiştir. Deneysel sonuçları açıklayamayan klasik Flory-Rehner teorisi ideal Donnan dengesi ile birleştirilmiş ve deneysel sonuçların teoriye bir ayarlama parametresi ile uyumu sağlanmıştır.

8. KAYNAKLAR

Andreis, M, Konig, JL, Adv. Polym. Sci. 1989, 89, 69

Baker, J.P., Blanch, H.W., Prausnitz, J.M., Polymer 1995, 36, 1061

Baker, J.P., Hong, L.H., Blanch, H.W., Prausnitz, J.M., Macromolecules 1994, 27, 1446

Dotson, N. A. Macromolecules 1992, 25, 308.

Dusek, K, Developments in Polymerization - 3, ed. R. N. Haward, Applied Science, London, 1982, p 1436

Dusek, K, J. Polym. Sci. C. 16, 1289 (1967).

Fisher, L.W., Sochor, A.R., Tan, J.S., Macromolecules 1977, 10, 949

Flory, P. J. J. Am. Chem. Soc. 1941, 63, 3083.

Flory, P. J. Principles of Polymer Chemistry; Cornell University Press: Ithaca, NY, 1953.

Fukuda, T.; Ma, Y-D.; Inagaki, H. Macromolecules 1985, 18, 17.

Funke, W.; Okay, O, Joos-Muller, Adv. Polym. Sci. 126,126 (1998)

Hasa, J., Ilavsky, M., J. Polym. Sci. Polym. Phys. Ed. 1975, 13, 263

Hirokawa, Y., Tanaka, T., J. Chem.Phys. 1984, 81, 6379.

Hooper, H.H., Baker, J.P., Blanch, H.W., Prausnitz, J.M. Macromolecules 1990, 23, 1096

Ishidao, T., Akagi, M., Sugimoto, H., Iwai, Y., Arai, Y., Macromolecules 1993, 26, 7361

Katayama, S., Hirokawa, Y., Tanaka, T., Macromolecules 1984, 17, 2641.

Katchalsky, A., Michaeli, I., J. Polym. Sci. 1955, 15, 69

Konak,C., Bansil, R., Polymer 1989, 30, 677

Küçük, I., Kuyulu, A. and Okay, O., Polymer Bulletin 35, 511-516 (1995)

Liu, X., Tong, Z., Hu, O., Macromolecules 1995, 28, 3813

Mikos, A. G.; Takoudis, C. G.; Peppas, N. A. Macromolecules 1986, 19, 2174.

Naghash, H.J., Okay, O., and Yýldýrým H, J. Appl. Polym. Sci. 56, 477 - 483 (1995)

Okay, O. , Makromol. Chem., Theory and Simul. 3, 417 - 427 (1994)

Okay, O., J. Appl. Polym. Sci. 32, 5533-5542 (1986).

Okay, O., Makromol. Chem. 189, 2201-2217 (1988).

Okay, O., Polymer 35, 2608 (1994)

Okay, O., Polymer 35, 796 (1994)

Okay, O., and Naghash, H.J., Polymer Bulletin 33, 665 - 672 (1994)

Okay, O., Angew. Makromol. Chem. 143, 209-214 (1986).

Okay, O., Angew. Makromol. Chem. 153, 125-134 (1987).

Okay, O., Angew. Makromol. Chem. 157, 1-13 (1988).

Okay, O., Angew. Makromol. Chem. 157, 15-21 (1988).

Okay, O., Balkas, T.I., J. Appl. Polym. Sci. 31, 1785-1795 (1986).

Okay, O., Funke, W., Macromolecules 23, 2623-2628 (1990).

Okay, O., Funke, W., Makromol. Chem. 191, 1565-1573 (1990).

Okay, O., Funke, W., Makromol. Chem., Rapid Commun. 11, 583-587 (1990).

Okay, O., Gürün, Ç., J. Appl. Polym. Sci. 46, 401-410 (1992)

Okay, O., Gürün, Ç., J. Appl. Polym. Sci. 46, 421-434 (1992)

Okay, O., J. Appl. Polym. Sci. 34, 307-317 (1987).

Okay, O., Kurz, M., Lutz, K., and Funke, W., Macromolecules 28, 2728 (1995)

Okay, O., Naghash, H. J. and Pekcan, Ö, Macromol. Theory & Simul. 4, 967(1995)

Okay, O., Naghash, H.J. and Capek, I, Polymer 36, 2413-2419 (1995)

Okay, O., Soner, E., Gungor, A., Balkas, T.I., J. Appl. Polym. Sci. 30, 2065-2074 (1985).

Oppermann, W., Rose, S., Rehage, G., Br. Polym. J. 1985, 17, 175

Richardson, T. L., Industrial Plastics: Theory and Applications, 2nd ed, Delmar Publ. Inc, NY, 1989

Seidl, J., Malinsky, J., Dusek, K., Heitz, W. Adv. Polym. Sci. 1967, 5, 113

Staudinger, H., Husemann, E. Ber. 1935, 68, 1618.

Stockmayer, W. H. J. Chem. Phys. 1943, 11, 45.

Stockmayer, W. H. J. Chem. Phys. 1944, 12, 125.

Tanaka, T., Phys. Rev. Lett., 1978, 40, 820.

Tanaka, T., Polymer 1979, 20, 1404.

Tanaka, T., Sci. Am. 1981, 244, 124

Tobita, H.; Hamielec, A. E. Macromolecules 1989, 22, 3098.

Tobita, H.; Hamielec, A. E. Makromol. Chem. Macromol. Symp. 1988, 20/21, 501.

Tong, Z., Liu, X., Macromolecules 1994, 27, 844

Walling, C. J. Am. Chem. Soc. 1945, 67, 441.

Zhang, Y.Q., Tanaka, T., Shibayama, M., Nature 1992, 360, 142.

9. EK - TBAG 1561 KAPSAMINDA YAPILAN BİLİMSEL YAYINLAR

1. Okay, O., "Phase Separation in Free-Radical Crosslinking Copolymerization: Formation of Heterogeneous Polymer Networks"
Polymer 40, 4117-2129 (1999)

2. Erbay, E. and Okay, O., "Pore-memory of Macroporous Styrene -Divinylbenzene Copolymer Beads"
J. Appl. Polym. Sci. 71, 1055-1062 (1999)

3. Erbay, E. and Okay, O., "Macroporous Styrene - Divinylbenzene Copolymers: Formation of Stable Porous Structures during the Copolymerization"
Polymer Bulletin 41, 379-385 (1998)

4. Okay, O., Sarıışık, S. B., Zor, D.S., "Swelling Behavior of Anionic Acrylamide-based Hydrogels in Aqueous Salt Solutions: Comparison of Experiment with Theory"
J. Appl. Polym. Sci. 70, 567-575 (1998)

5. Keskinel, M. and Okay, O., "Effects of Cyclization and Electrostatic Interactions on the Termination Rate of Macroradicals in Free-Radical Crosslinking Copolymerization"
Polymer Bulletin 40, 491- 498 (1998)

6. Okay, O. and Akkan, U., "Heterogeneities in polyacrylamide gels immersed in acetone- water mixtures"
Polymer Bulletin 41, 363-370 (1998)

7. Okay, O., and Sarıışık, S. B., "Swelling Behavior of Poly(acrylamide-co-sodium acrylate) Hydrogels in Aqueous Salt Solutions: Theory versus Experiments"
Eur. Polymer J. (1999)

8. Okay, O., "Formation of Heterogeneous Styrene - Divinylbenzene Copolymer Networks: Theory versus Experiments"
J. Appl. Polym. Sci. (1999)

ELSEVIER

Polymer 40 (1999) 4117–4129

polymer

Phase separation in free-radical crosslinking copolymerization: formation of heterogeneous polymer networks

Oğuz Okay

Department of Chemistry, Istanbul Technical University, 80626 Maslak, Istanbul, Turkey

Received 17 December 1997; accepted 18 August 1998

bstract

A model combining both the thermodynamic and kinetic aspects of free-radical crosslinking copolymerization (FCC) is presented to redict the formation conditions and the properties of heterogeneous (porous) networks. The model involves thermodynamic equations escribing the phase equilibria between the network and separated phases during FCC of vinyl/divinyl monomers and kinetic equations ving the concentration of reacting species and the polymer properties as a function of the monomer conversion. Calculation results are esented for styrene/*m*-divinylbenzene (S/*m*-DVB) copolymerization system in the presence of inert diluents. S/*m*-DVB copolymerization stem at a high *m*-DVB concentration, or, at a low monomer concentration phase separates at the gel point and results in the formation of a icrogel solution. The calculation results also show that the heterogeneity in S/*m*-DVB copolymer networks increases on increasing DVB or luent concentration, or, on decreasing the solvating power of the diluent, in accord with the experimental data published previously. The odel also predicts correctly the equilibrium volume swelling ratio of heterogeneous networks in solvents. © 1999 Elsevier Science Ltd. All ghts reserved.

ywords: Phase separation; Heterogeneous networks; Kinetic–thermodynamic modeling

Introduction

Heterogeneous (porous) polymer networks are widely ed as starting materials for ion exchangers and as specific rbents, and, therefore, have been the subject of a large mber of studies [1–3]. These materials are prepared ainly by free-radical crosslinking copolymerization enceforth referred to as FCC) of vinyl/divinyl monomers. g. styrene/divinylbenzene or acrylamide/*N*,*N*′-methylene isacrylamide), in the presence of an inert diluent. The uent, which is a solvent, a nonsolvent, or a linear polyer, is included in the FCC system as a pore forming agent. d plays an important role in the design of the pore struce of crosslinked materials [2].

If the diluent remains in the gel throughout the copolyrization, an expanded network structure is obtained. The panded networks thus formed collapse during the removal the diluent after their synthesis and therefore, they are nporous in the glassy state. Heterogeneities in the work structure appear if the diluent separates out of the phase during polymerization. The incipient phase paration during FCC may occur before the onset of crogelation; this results in the formation of a polymer persion in the liquid phase. Otherwise, if the system ase separates beyond the gel point, the gel shrinks and results in a dispersion of the expelled liquid droplets in the network phase. In both cases, after complete conversion of the monomers a heterogeneous network consisting of network and diluent phases is obtained. Removing of the diluent from the network creates voids (pores) of sizes 10 Å up to 1 μm in the glassy state.

Relationships between the synthesis conditions and the structure of heterogeneous networks have been the subject of intensive studies during the last four decades [4–21]. Experiments showed that a phase separation during FCC is promoted, i.e. the pore volume of the final network increases as the concentration of the divinyl monomer or that of the diluent increases, or as the solvating power of the diluent decreases. It was also shown that good solvents as a diluent create small pores and therefore, a large specific surface area, whereas bad solvents or linear polymers produce materials with irregularly shaped large pores.

Although many experimental studies have dealt with the porosity formation in FCC in the presence of several diluents, only a few were concerned with the theory of formation of heterogeneities in such systems. Dusek was the first who treated the phase separation during the network formation process under the assumption of thermodynamic equilibrium between the network and separated phases [22–24]. By using Flory's theory of swelling equilibrium and the

2-3861/99/$ - see front matter
S0032-3861(98)00640-5

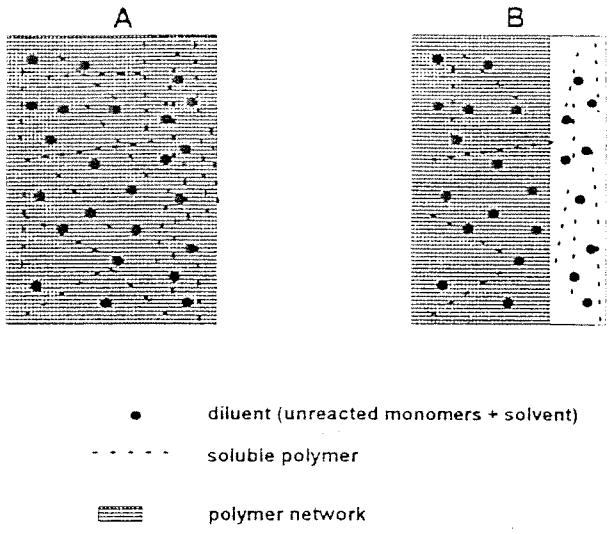

Fig. 1. Schematic representation of FCC system (A) before and (B) after phase separation.

theory of rubber elasticity, he derived relations between the volume of the network phase and the monomer conversion. Similar thermodynamic relations were also reported by Boots et al. to predict the onset of phase separation in crosslinking copolymerization of divinyl monomers [25]. An important assumption involved in the derivation of Dusek's and Boots equations is that all polymer molecules beyond the gel point belong to the gel. Thus, in these models, the existence of sol molecules in the reaction system is simply ignored. However, the gel fraction W_g, i.e. the weight fraction of polymer chains that belong to the gel, is known to be zero at the gel point and it increases as the polymerization proceeds, but never attains unity at a monomer conversion less than 100%. Therefore, a realistic thermodynamic model that describes the phase equilibria in FCC system should take into account the distribution of soluble polymers between the gel and the separated diluent phases. Moreover, in Dusek's and Boots models, the kinetics of FCC was not taken into account. For example, different vinyl group reactivities in FCC system as well as the variation of the gel crosslink density depending on the reaction condition are neglected.

In this paper, we combine thermodynamic and kinetic aspects of FCC system to predict the condition of phase separation and the volume of the separated phase as a function of the system parameters. In the present model, we take into account the kinetic features of FCC of vinyl/divinyl monomers. The effect of soluble polymers on the phase equilibria between the network and separated phases is also considered. In the following sections, we first consider the thermodynamic condition for a phase separation in FCC system consisting of a network, unreacted monomers, a diluent and soluble polymers (sol). Equations describing the thermodynamic equilibria between the network and separated phases for a given monomer conversion will be derived here. The solution of thermodynamic equations requires conversion-dependent network and polymer properties, which will be obtained from the kinetic treatment of FCC system examined later. In the last section, the kinetic–thermodynamic model is applied to the FCC of styrene/*m*-divinylbenzene in the presence of diluents. Finally, the simulation results are compared with the experimental data available in the literature.

In the treatment that follows, the main assumptions made are as follows: (1) thermodynamic equilibrium in every step of the reactions, (2) limitations of the Flory–Huggins theory, the theory of rubber elasticity and the kinetic theories of gel formation, (3) polymerization and crosslinking reactions in the network and separated phases are identical, (4) from the thermodynamic point of view, the soluble polymers beyond the gel point are monodisperse at any monomer conversion and, the number of segments on each chain is equal to the number-average degree of polymerization. Further, in the interest of simplicity, we assumed that (5) the diluent has the same thermodynamic characteristics as the monomer, and (6) the onset of phase separation occurs beyond the gel point. Although the last assumption can easily be removed from the model, the composite network structure formed in such polymerization systems cannot be studied within the framework of the Flory's theory of swelling.

2. Thermodynamics

2.1. Swelling of polymer network in free-radical crosslinking copolymerization

In the FCC of vinyl/divinyl monomers, the reaction system beyond the gel point involves the unreacted monomers, solvent, soluble polymers and a polymer network. For the following analysis, we will call the mixture of the unreacted monomers and the solvent as the diluent. The FCC system at a given degree of monomer conversion can thus be considered as a ternary system consisting of the diluent, network, and the soluble polymer (Fig. 1(A)). For this ternary system where components 1, 2 and 3 are the diluent, network, and soluble polymer, respectively, all concentrations and properties of the components are functions of the monomer conversion. Consider now the reaction system at a volume conversion of the monomers α, which is above the critical conversion for the onset of a phase separation. At this conversion, the diluent and soluble polymers will distribute between the network and separated phases, whereas the network will only exist in the network phase (Fig. 1B). We can thus analyze the system as a network immersed in polymer solution. Swelling of a polymer network in such a system is governed by at least three free energy terms [26,27], i.e., the changes in the free-energy of mixing ΔG_m, in the free energy of elastic deformation ΔG_{el} and in the free energy of electrostatic

nteractions ΔG_i

$$G = \Delta G_m + \Delta G_{el} + \Delta G_i. \quad (1)$$

According to the Flory–Huggins theory [28], ΔG_m is iven by

$$G_m = RT\left(\sum_i n_i \ln v_i + \sum_{i<j} n_i v_j \chi_{ij}\right) \quad (1a)$$

here n_i is the moles of the species i ($i = 1, 2$, and 3), v_i its olume fraction, χ_{ij} the interaction parameter between the ecies i and j, R the gas constant and T the temperature. For e free energy of elastic deformation ΔG_{el}, although several eories are available in the literature, the simplest affine twork model will be used here to describe qualitatively e behavior of polymer gels [28],

$$G_{el} = (3/2)(RT/NV_s)\left(\left(v_2^0/v_2\right)^{2/3} - 1 - \ln\left(v_2^0/v_2\right)^{1/3}\right) \quad (1b)$$

here N is the average number of segments in the network ains v_2^0 is the volume fraction of polymer network in the twork phase at a given degree of conversion, and V_s is the olar volume of solvent. Note that the validity of Eq. (1b) any similar equation for gels containing dissolved poly- er is unknown. Interchain entanglements between the twork and polymers should be mentioned as the possible urce of error with the use of Eq. (1b) for the present stem. However, previous experimental works showed at the Flory–Rehner theory represented by Eq. (1) orks satisfactorily if the equilibrium swelling degrees of gels are calculated instead of energies [29,30]. This is, as inted out by De Gennes and Brochard, owing to the favor- le cancellation of two opposite approximations of the ory [31,32]. Another important point with the use of . (1b) for the present system is that, after phase separa- n, the volume of the gel phase changes continuously, so t the gel growth occurs at different degrees of dilution, resented by v_2^0. This means that the configuration of the work chains is determined by the history of the network mation process. In order to account for this effect, Dusek d the two network hypothesis proposed by Andrews and ry [23]. However, if one prepares a homogeneous work by FCC in the absence of any added diluent, the growth also occurs at different dilution degrees. (Here, unreacted monomers whose concentration changes ntinuously act as a diluent.) Since the Flory–Rehner ory is well applicable to the swelling behavior of gels pared by FCC, it is plausible to neglect this effect at this ge of the model development and include it into the ond assumption mentioned in the introduction.

For weakly charged ionic gels, the free energy of electro- ic interactions ΔG_i may be written as follows [28]:

$$_i = RT\frac{N_i}{N}\frac{v_2}{v_1} n_1 \ln(N_i v_2/N) \quad (1c)$$

where N_i is the average number of ionic units in a network chain.

Substitution of Eqs. (1a)–(1c) into Eq. (1) and differentiating with respect to the number of moles of the diluent n_1 and the soluble polymer n_3 yield the following equations for the excess chemical potentials μ of the components 1 and 3 in both network and separated phases:

$$\frac{\Delta\mu_1}{RT} = N^{-1}\left(v_2^{1/3} v_2^{02/3} - v_2/2\right) + \ln v_1 + (1 - v_1) - v_3/y + (\chi_{12} v_2 + \chi_{13} v_3)(1 - v_1) - \chi_{23} v_2 v_3 - v_2 N_i/N, \quad (2a)$$

$$\frac{\Delta\mu_1'}{RT} = \ln v_1' + v_3'(1 - 1/y) + \chi_{13} v_3'^2, \quad (2b)$$

$$\frac{\Delta\mu_3}{yRT} = N^{-1}\left(v_2^{1/3} v_2^{02/3} - v_2/2\right) + (1/y)\ln v_3 + (1/y)(1 - v_3) - v_1 + (\chi_{13} v_1 + \chi_{23} v_2)(1 - v_3) - \chi_{12} v_1 v_2 - v_2 N_i/N, \quad (3a)$$

$$\frac{\Delta\mu_3'}{yRT} = (1/y)\ln v_3' - v_1'\left(1 - y^{-1}\right) + \chi_{13} v_1'^2 \quad (3b)$$

where y is the number of segments in the soluble polymer. Note that the symbols with a superscript prime ($'$) relate to the separated phase, whereas those without this superscript relate to the network phase.

2.2. Conversion-dependent phase equilibria in FCC system

The reaction mixture of FCC remains homogeneous as long as the growing polymer network is able to absorb all the available monomers and the diluent. As the copolymerization and crosslinking reactions proceed, that is as the crosslink density of the network increases, a critical point is passed, at which the equilibrium degree of swelling of the network in the diluent becomes equal to its degree of dilution. At this point, since the dilution of a homogeneous network cannot be greater than its equilibrium degree of swelling, the reaction system will separate into two phases: network and separated phases. Thus, the condition for incipient phase separation during FCC is given by:

$$v_2 = v_2^0 \quad (4)$$

After phase separation, both v_2 and v_2^0 will change with further copolymerization and crosslinking reactions, but the equality given by Eq. (4) still holds for the network phase. The state of equilibrium between the network and separated phases in FCC is obtained when the diluent and the soluble polymers inside the network phase are in thermodynamic equilibrium with those in the separated phase. This equilibrium state is described by the equality of the chemical

Table 1
Kinetic constants and parameters for S/*m*-DVB copolymerization at 60°C using AIBN as an initiator ($[I]_0 = 0.1$ M)

Constants	Ref.
$k_d = 0.85 \times 10^{-5}$ (s^{-1})	[33]
$k_{p/1} = 145$ (l mol^{-1} s^{-1})	[33][a]
$k_{p/2} = 165$ (l mol^{-1} s^{-1})	[34]
$k_{p/3} = 19$ (l mol^{-1} s^{-1})	[35]
$k_{tcij} = 2.9 \times 10^7$ (l mol^{-1} s^{-1})	[33]
$k_{tdij} = 0$	[33]
$f = 0.45$	[34]
$d_M = 0.91$ (g ml^{-1})	
$d_P = 1.08$ (g ml^{-1})	
$\alpha_i = 0$	
$\bar{V}_1 = 114.2$ ml mol^{-1})	
$\bar{V}_2 = 142.9$ ml mol^{-1})	

[a] Rate constant for the homopolymerization of styrene.

potential of these components in both phases. Thus, at swelling equilibrium, we have:

$$\Delta\mu_1 - \Delta\mu_1' = 0 \tag{5}$$

$$\Delta\mu_3 - \Delta\mu_3' = 0 \tag{6}$$

Substitution of Eqs. (2a), (2b) and (3a), (3b) into Eqs. (5) and (6) and using the phase separation condition given by Eq. (4), we obtain the following system of equations describing the equilibrium condition between the network and separated phases during FCC:

$$N^{-1}v_2^0(0.5 - N_i) + \ln\left(\frac{v_1}{v_1'}\right) + (1 - v_1 - v_3') - (v_3 - v_3')/y + \chi_{12}v_2^{02} + \chi_{13}(v_3^2 - v_3'^2) + (\chi_{12} + \chi_{13} - \chi_{23})v_2^0 v_3 = 0, \tag{7}$$

$$-\ln\left(\frac{v_1}{v_1'}\right) + (1/y)\ln(v_3/v_3') + 2\chi_{13}(v_3' - v_3) + (\chi_{23} - \chi_{12} - \chi_{13})v_2^0 = 0. \tag{8}$$

Application of material balance to each phases gives the following two additional equations:

$$v_1 + v_2^0 + v_3 = 1, \tag{9}$$

$$v_1' + v_3' = 1. \tag{10}$$

At the start of the polymerization, the reaction mixture only contains the monomers and the solvent with volume fractions v_2^{00} and $1 - v_2^{00}$, respectively. Let W_g be the weight fraction of polymer chains that belong to the gel and v_g be the volume fraction of the network phase in the reaction system at volume conversion α, from the material balance, we have the following equalities:

$$v_2^0 = \bar{v}_p W_g / v_g, \tag{11}$$

$$\bar{v}_p(1 - W_g) = v_3 v_g + v_3'(1 - v_g) \tag{12}$$

where $\bar{v}_p$ is the volume fraction of sol + gel polymer in the whole reaction system (network + separated phases), i.e.

$$\bar{v}_p = \frac{\alpha v_2^{00}(1 - \varepsilon)}{(1 - \alpha v_2^{00}\varepsilon)} \tag{13}$$

ε is the contraction factor defined by $\varepsilon = 1 - d_M/d_P$, d_M and d_P being the densities of the monomers and the polymer respectively (we assume equal densities for the monomers used).

The system of the six equations, Eqs. (7)–(12), contains 16 parameters. Five of these parameters (v_2^{00}, χ_{12}, χ_{13}, χ_{23} and ε) are system specific and therefore, they are fixed by the experimental conditions. However, four parameters (W_g, N, y, N_i) change continuously with the monomer conversion. These four conversion-dependent parameters are the output of the kinetic model of FCC given in the Appendix. Thus, knowing these 9 parameters and taking α as the independent variable, Eqs. (7)–(12) can be solved numerically for the six remaining unknowns: v_g, v_1, v_2^0, v_3, v_1' and v_3'.

3. Results and discussion

The kinetic–thermodynamic model was solved for the crosslinking copolymerization of styrene (S) and *m*-divinylbenzene (*m*-DVB) at 60°C using 2,2′-azobisisobutyronitrile (AIBN) as an initiator. The values of the kinetic constants and the parameters used in the calculation of the conversion-dependent gel and sol properties are presented in Table 1. For the present simulation, we neglected cyclization and multiple crosslinking reactions ($k_{cyc} = k_{mc} = 0$) and the gel effect during the reactions. We first calculated the gel point conversion α_{cr} and the values of W_g, y, and N using the kinetic rate equations as a function of the volume conversion α. Then, these data were used for the solution of the thermodynamic Eqs. (7)–(12) to predict the critical conversion for the onset of a phase separation in FCC, the volume fraction of the gel phase v_g, as well as the distribution of soluble polymers between the gel and separated phases v_3/v_3'.

The most common methods to produce heterogeneous S/DVB copolymers are to work at a high DVB concentration (v-induced syneresis), or to use a poor solvent as the inert diluent [3] (χ-induced syneresis). Here, theoretical results are presented showing the effect of these parameters on the development of the heterogeneity in S/*m*-DVB copolymers. All calculations were performed up to a volume conversion of $\alpha = 0.98$. Since the sol molecules and the gel have the same chemical composition, it was assumed that $\chi_{23} = 0$ and $\chi_{12} = \chi_{13}$.

In Fig. 2A, the dependencies of the weight fraction of gel

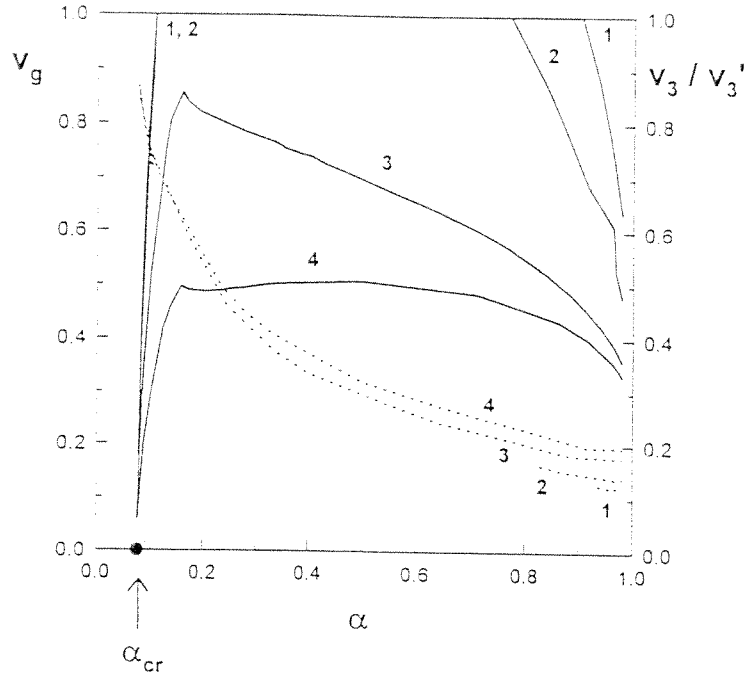

Fig. 3. Variations of v_g (solid curves) and v_3/v_3' (dotted curves) with the monomer conversion α in S/*m*-DVB copolymerization. *m*-DVB = 67 mol%. $v_2^{00} = 0.20$. $\chi_{23} = 0$. $\chi_{12} = \chi_{13} = 0$ (1), 0.20 (2), 0.40 (3) and 0.46 (4).

W_g, the number-average degree of polymerization of sol polymers y, and the number of segments in the network chains N are shown as a function of the volume conversion α. The calculations were for 67 mol% *m*-DVB in the initial monomer mixture and for $v_2^{00} = 0.20$ (volume fraction of the monomers in the initial reaction mixture). The solid vertical line represents the location of the gel point, at which the second moment of the polymer distribution goes to infinity. This critical point corresponds to $\alpha_{cr} = 0.075$. Beyond the gel point, the amount of the network W_g increases and the number of segments between successive crosslinks N decreases as the polymerization and crosslinking reactions proceed. At the same time, the size of soluble polymers, represented by y, rapidly decreased because of the predominant crosslinking reactions between the sol molecules of larger sizes and the gel. Fig. 2A also shows that, even at high monomer conversions, soluble polymers with y of the order of 10^1 are present in the reaction mixture. Previous experimental works carried out on the same system also support this prediction and provided good agreement with the kinetic calculations [36].

For the same copolymerization system (67 mol% *m*-DVB, $v_2^{00} = 0.20$), variations of the volume fraction of the network phase v_g and the distribution of the soluble polymers between the gel and separated phases v_3/v_3' are shown Fig. 2b as a function of the monomer conversion α. Calculations were for $\chi_{12} = 0.46$, the value reported for S/DVB–toluene system [37]. The solid curve in the figure represents the v_g values calculated using the present model, which takes into account the effect of soluble polymers on the phase equilibria in FCC system. The dotted curve is the result of v_g calculations with neglected sol fraction ($v_3 = v_3' = 0$, i.e. $W_g = 0$), as was done by Dusek [23]. It is seen that the calculation results with neglected sol fraction become a reasonable approximation only if $\alpha \cong 1$. At high conversions, since both the amount and the size of soluble polymers are small (Fig. 2A), the effect of sol polymers on phase equilibria becomes insignificant so that both approaches match each other. However, significant deviations appear at low conversions ($\alpha = \alpha_{cr} - 0.6$) on account of the existence of a large number of soluble chains in the reaction system.

One of the remarkable results of the present simulation method is that the volume of the gel is not equal to the reaction volume at the gel point predicted by the kinetic theory. It is seen that, at a high crosslinker content, a phase separation sets in at the gel point, even in the presence of a good solvent as a diluent. This is because of the fact that the crosslink density of the first formed network (N^{-1}) increases much more rapidly than its amount in the reaction mixture ($\alpha v_2^{00} W_g$). As a result, the "infinite network" cannot absorb the whole unreacted monomers and the diluent, i.e. it cannot occupy the whole available volume, and becomes a micronetwork. Thus, the kinetic gel point corresponds to the microgelation rather than the macrogelation point and results in the formation of a microgel solution in monomer + diluent mixture. The volume fraction of the gel phase v_g, which is zero at the gel point, rapidly increases with increasing conversion up to $\alpha = 0.15$ as a result of the

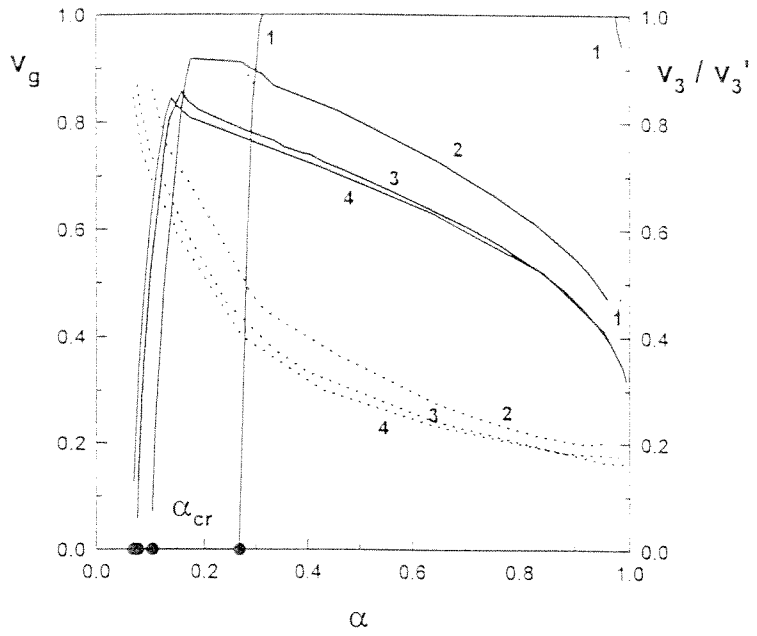

g. 4. Variations of v_g (solid curves) and v_3/v_3' (dotted curves) with the monomer conversion α in S/*m*-DVB copolymerization. $\chi_{12} = \chi_{13} = 0.40$, $\chi_{23} = 0$. $_2^0 = 0.20$. *m*-DVB = 10 (1), 37.5 (2), 67 (3) and 90 mol% (4).

multaneous increase of the amount of the network W_g (Fig. A). The rate of change of W_g decreases after $\alpha = 0.15$, as en in Fig. 2A, which is reflected in the cessation of the owth of the gel phase in the reaction system. At high nversions, the rate of change of W_g becomes negligible it the crosslink density of the gel (N^{-1}) continues to crease owing to the intermolecular reactions of pendant nyl groups, which results in a decrease in the gel volume . After polymerization, 67% of the volume of the hetero- neous network consists of the separated pure diluent ıase.

In Fig. 2B, the dashed curve shows the variation of v_3/v_3' tio with the monomer conversion α. v_3/v_3' represents the tio of the volume fraction of sol polymers in the network ase (v_3) to that in the separated diluent phase (v_3'); thus $/v_3' = 1$ means that the sol polymer concentration inside e network is equal to that in the separated phase, whereas $/v_3' = 0$ means that the network excludes al the sol mole- les. Fig. 2B indicates that a large amount of sol polymers n penetrate into the gel phase at conversions close to the crogel point α_{cr}. This is as a result of the loosely cross- ked structure of the gel phase (microgels) in the vicinity the gel point so that the soluble chains can easily enter in e gel without an essential loss in their conformational tropy. As polymerization proceeds, the v_3/v_3' ratio creases monotonically, i.e., the gel phase becomes less cessible for the soluble chains because of the increased osslink density N^{-1} of the gel. The concentration differ- ce of soluble chains between the inside and outside the gel ase creates an additional osmotic pressure compressing e network. This additional osmotic pressure is responsible the different results of calculations of v_g with and without neglecting sol fraction at low conversions (dotted and solid curves).

For the same reaction conditions (67 mol% *m*-DVB, $v_2^{(0)} = 0.20$), effect of the solvating power of the diluent on the volume of the gel phase v_g and on the sol polymer distribution v_3/v_3' is shown in Fig. 3. Here, the solvating power of the diluent is represented by χ_{12} which is varied between 0 and 0.46. It is seen that, even for athermal interactions between the network segments and diluent molecules ($\chi_{12} = 0$), the reaction system becomes heterogeneous at the kinetic gel point owing to the high crosslinker and diluent concentrations, which limit the swellability of the network. For $\chi_{12} \leq 0.2$, polymerization-induced heterogeneities at the gel point disappear again within a few conversion intervals as a result of the high growth rate of the network; but at high monomer conversions, the reaction system again phase separates owing to the presence of a large amount of diluent. As the solvating power of the diluent decreases, i.e. as χ_{12} increases, the volume of the gel phase decreases, indicating increasing heterogeneity (porosity) in the final network. Another feature shown in Fig. 3 is that, for a given monomer conversion, v_3/v_3' ratio decreases as the solvating power of the diluent increases. Since the separated diluent phase becomes a better solvent for the soluble polymers with decreasing χ_{12} their concentration in the separated phase v_3' increases, which shifts the v_3/v_3' ratio toward smaller values.

Effects of the *m*-DVB concentration and the initial degree of dilution of the monomers ($v_2^{(0)}$) on v_g and v_3/v_3' versus α dependencies are shown in Figs. 4 and 5, respectively. The kinetic gel points, shown in the figures as filled circles, shift

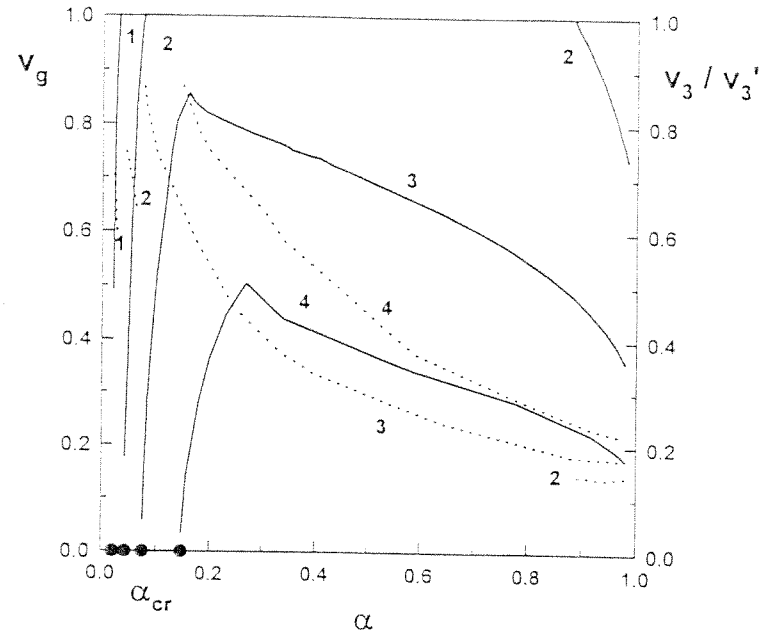

Fig. 5. Variations of v_g (solid curves) and v_3/v_3' (dotted curves) with the monomer conversion α in S/*m*-DVB copolymerization. $\chi_{12} = \chi_{13} = 0.40$. $\chi_{23} = 0$. *m*-DVB = 67 mol% $v_2^{00} = 1.00$ (1), 0.40 (2), 0.20 (3) and 0.10 (4).

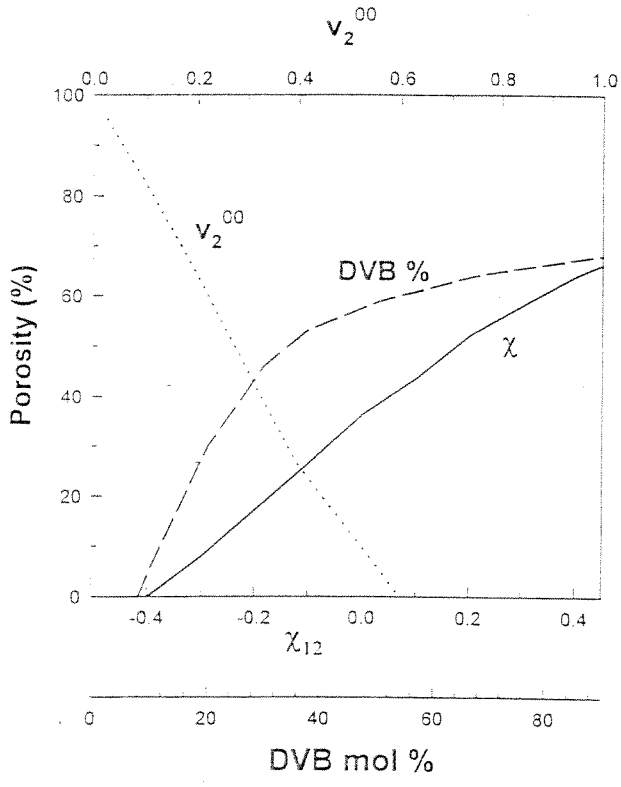

Fig. 6. The total porosity of S/*m*-DVB copolymer networks shown as a function of the *m*-DVB concentration, initial degree of dilution of the monomer(v_2^{00}) and χ_{12} parameter. Solid curve: *m*-DVB mol% = 67, $v_2^{00} = 0.20$. Dashed curve: $\chi_{12} = 0.40$, $v_2^{00} = 0.20$. Dotted curve: *m*-DVB mol% = 67, $\chi_{12} = 0.40$.

toward higher monomer conversions as the crosslinker or total monomer concentration decreases. Under the selected reaction conditions, the reaction mixture always phase separates at the kinetic gel point because of the high degree of initial dilution (20 v/v% initial monomer concentration, Fig. 4), or owing to the high crosslinker concentration (67 mol % *m*-DVB, Fig. 5). Even under bulk polymerization condition ($v_2^{00} = 1$, curve 1 in Fig. 5), the system separates into two phases at the gel point but it rehomogenize immediately and remains homogeneous during the course of the reaction. The appearance of a turbidity in highly crosslinked FCC systems even in a bulk state is an experimental fact and indicates the scattering of light from the spatial inhomogeneities of the system refractive index [38,39]. As was reported by Horie et al. [39], bulk methyl methacrylate–ethylene glycol dimethacrylate (EGDM) copolymerization with >20% EGDM content leads to the formation of opaque polymers in the first stage of the reaction. But as the reaction proceeds, these microgels are connected with one another and the opaque polymer turns to a polymer which is transparent and homogeneous in appearance [39]. Thus, the simulation results are in accord with the experiments. At a given monomer conversion, the volume of the gel phase decreases as the DVB concentrations increase or the initial monomer concentration decreases. The higher the *m*-DVB concentration, the higher the crosslink density of the gel at a given monomer conversion, which implies that the volume of the gel phase decreases on rising the *m*-DVB concentration, as shown in Fig. 4. Further, at a given *m*-DVB concentration, the lower the monomer concentration represented by v_2^{00}, the higher the volume of the diluent, which results that the volume of the separated diluent phase increases on

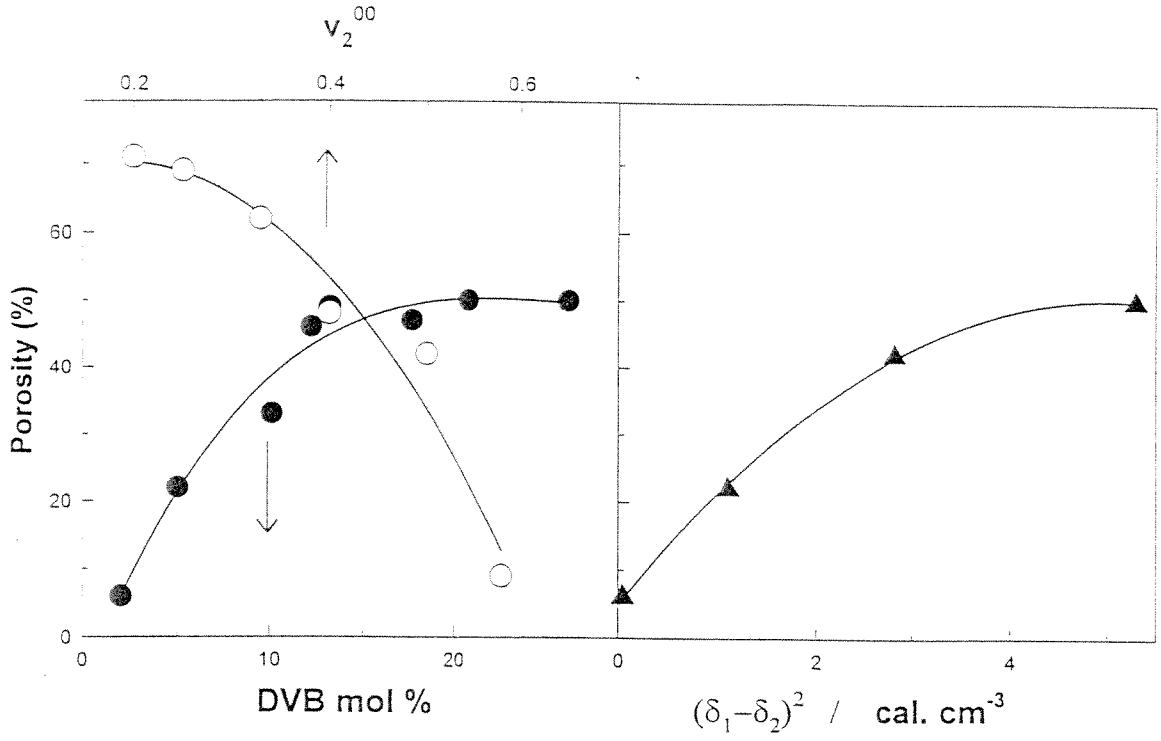

g. 7. The total porosity of S/commercial DVB copolymer networks shown as a function of the DVB concentration, initial degree of dilution of the monomers $^{0})$ and the diluent quality $(\delta_1 - \delta_2)^2$. Experimental data points are from Okay [13,15]. The curves only show the trend of the data. Experiments were for ious DVB concentrations at $v_2^{00} = 0.50$ with cyclohexanol as a diluent (filled circles), for various initial monomer concentrations (v_2^{00}) at 17 mol% DVB h cyclohexanol/toluene mixture (75/25 v/v) as a diluent (empty circles) and for various types of diluent at 20 mol% DVB and $v_2^{00} = 0.50$ (filled triangles). e diluent quality is represented by $(\delta_1 - \delta_2)^2$ where δ_1 and δ_2 are the solubility parameters of the diluent and the polymer, respectively [15].

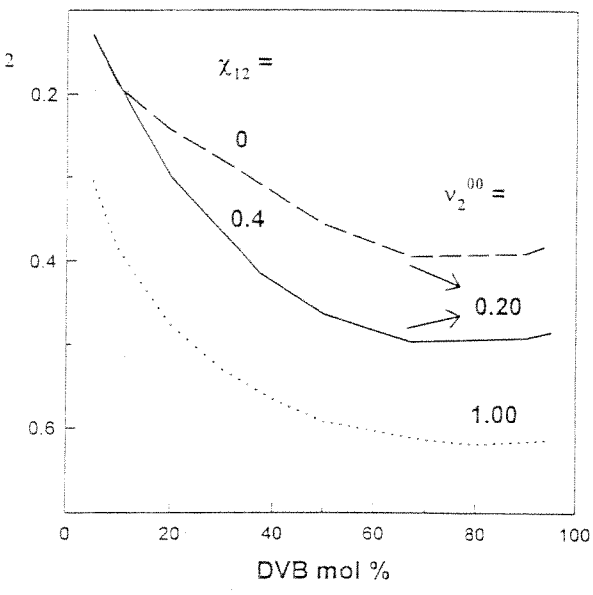

8. The equilibrium swelling ratio of S/*m*-DVB copolymer networks, in ns of v_2, shown as a function of the *m*-DVB concentration. $\chi = 0.46$. culations were for $v_2^{00} = 1.00$ (dotted curve), $v_2^{00} = 0.20$; $\chi_{12} = 0$ hed curve) and $v_2^{00} = 0.20$; $\chi_{12} = 0.40$ (solid curve).

increasing dilution of the monomers. Figs. 4 and 5 also show that the concentration of sol polymers inside the gel phase decrease on increasing *m*-DVB or total monomer concentration. Since the crosslink density of the gel phase increase on rising DVB or monomer concentration, it becomes less accessible for the soluble chains.

After complete conversion of the monomers, the heterogeneous network formed consists of a gel phase of volume fraction v_g with the rest being the separated diluent phase. Removing of the diluent from the network creates pores of various sizes. Although the present model does not yield the size distribution of the separated diluent droplets, it predicts the volume of the whole diluent phase using the equation:

$$p\% = (1 - v_g) \times 100 \qquad (14)$$

where $p\%$ is the total porosity of the final material. The calculated porosities of S/*m*-DVB copolymers are shown in Fig. 6 as a function of the χ_{12} parameter, initial *m*-DVB and total monomer concentrations. It is seen that, a porous structure in the copolymer starts to appear after crossing a critical *m*-DVB or diluent concentration, or after a critical value of χ_{12}. The porosity increases first abruptly but then slightly on rising *m*-DVB concentration. Increasing initial dilution of the monomers or, decreasing solvating power of the diluent also increases the porosity m S/*m*-DVB copolymers. These model predictions are in good agreement with

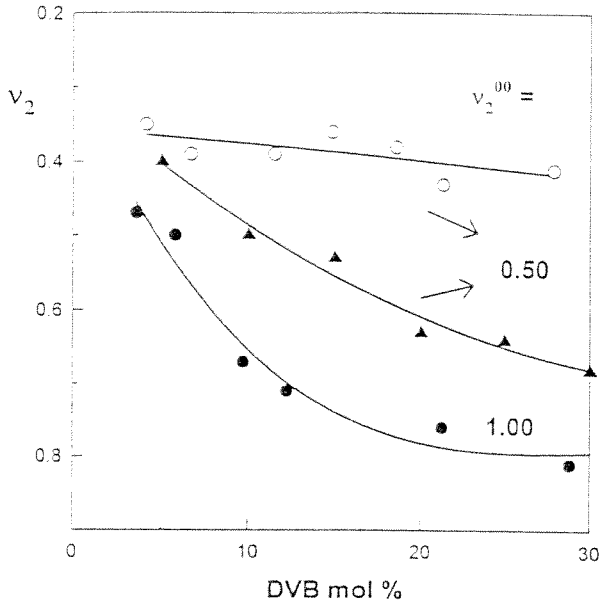

Fig. 9. The equilibrium swelling ratio of S/commercial DVB copolymer networks in toluene, in terms of ν_2, shown as a function of the DVB concentration. Experimental data are from Okay [13,15]. The curves only show the trend of the data. $\nu_2^{00} = 1.00$ (●); $\nu_2^{00} = 0.50$, diluent = toluene (○) and $\nu_2^{00} = 0.50$, diluent = toluene/cyclohexanol (50/50 v/v) mixture (▲).

the experimental data reported in the literature [3]. For comparison, some of the reported porosity data of S/commercial DVB copolymers [13,15] are collected in Fig. 7 as a function of the reaction conditions. Experiments were for various DVB concentrations at $\nu_2^{00} = 0.50$ with cyclohexanol as a diluent (filled circles), for various initial monomer concentrations at 17 mol% DVB with cyclohexanol/toluene mixture (75/25 v/v) as a diluent (empty circles), and for various types of diluent at 20 mol% DVB and $\nu_2^{00} = 0.50$ (filled triangles). The diluent quality is represented by $(\delta_1 - \delta_2)^2$ where δ_1 and δ_2 are the solubility parameters of the diluent and the polymer, respectively [15]. Comparison of Figs. 6 and 7 shows that the model correctly predicts all the trends observed by experiments.

One of the characteristics of heterogeneous networks is their volume swelling ratio in solvents. According to the Flory's swelling equation, the equilibrium volume swelling ratio of a polymer network q_v is related to its crosslink density through the following equation [28]:

$$\ln(1 - \nu_2) + \nu_2 + \chi\nu_2^2 + N^{-1}\left(\nu_2^{1/3}\nu_2^{02/3} - \nu_2/2\right) = 0 \qquad (15)$$

where $\nu_2 = 1/q_v$ and χ is the interaction parameter between the polymer network and the swelling agent. Using the N and ν_2^0 values, calculated using the present model at $\alpha = 0.98$, and for $\chi = 0.46$, the equilibrium ν_2 values of S/*m*-DVB networks were calculated using Eq. (15). Calculation results are presented in Fig. 8. Here, the dotted curve represents $\nu_2$versus DVB mol% dependence for S/*m*-DVB copolymer networks prepared without using a diluent ($\nu_2^{00} = 1.00$), which we call thereafter standard networks. The dashed and solid curves were calculated for networks prepared in the presence of a diluent ($\nu_2^{00} = 0.20$) with $\chi_{12} = 0$ and 0.4, respectively. One can see that the network prepared in the presence of a good solvent as a diluent ($\chi_{12} = 0$) swells much more than the corresponding standard network. As the solvating power of the diluent decreases ($\chi_{12} = 0.4$), the swelling capacity of the network decreases and it approaches to that of the standard network. According to the model calculations, the heterogeneity in the network structure appears as a result of the separation of the diluent out of the gel phase during the reactions. Therefore, the distribution of the diluent between the gel and the separated phases determines the heterogeneity as well as the volume swelling ratio of the networks. The diluent separated out of the gel phase act as a pore forming agent, whereas the other part remains in the network structure and increases its volume swelling ratio, i.e., decreases its ν_2 value. According to Fig. 8, the good solvent present during the network formation process mostly remains in the network throughout the copolymerization and thus, increases its volume swelling ratio, i.e. decreases the ν_2 value of the final network. As the diluent quality decreases, i.e. as χ_{12} increases, increasing amount of the diluent separates out of the gel phase and therefore, it mainly acts as a pore forming agent and so the volume swelling ratio decreases. In Fig. 9, experimental ν_2 versus DVB mol% dependencies are shown for S-commercial DVB copolymers swollen in toluene. Experimental data were taken from the literature [13,15]. It is seen that the networks prepared in the presence of toluene as a diluent remain in the swollen state, whereas those prepared with cyclohexanol as a diluent deswell on rising DVB concentration and their swelling ratio approaches to that of the standard networks. Thus, the present model fully describes the behavior of heterogeneous networks.

4. Conclusions

A new kinetic–thermodynamic model for the heterogeneous network formation in FCC was presented. The model can predict the formation conditions of heterogeneities during the FCC of vinyl/divinyl monomers and the properties of the resulting heterogeneous networks. The model takes into account all the kinetic features of FCC system and uses conversion-dependent sol and gel properties (the weight fraction and the crosslink density of the gel, the molecular weight of soluble chains) as input data for the solution of thermodynamic equations. Thermodynamic equations describe the phase equilibria between the gel and the separated phases and predict the volume of the gel phase as well as the distribution of soluble chains between the phases as a function of the monomer conversion. Calculation results were presented for S/*m*-DVB

polymerization system in the presence of diluents. S-*m*-VB copolymerization system at a high *m*-DVB concentration, or, at a low monomer concentration phase separates at e gel point and results in the formation of a microgel lution. The calculation results also show that the terogeneity in S/*m*-DVB copolymer networks increases increasing DVB or diluent concentration, or, on decreasg the solvating power of the diluent, in accord with the perimental data published previously. The model also rrectly predicts the equilibrium swelling ratio of heteroneous networks.

It must be pointed out that in real systems, the equilibrium ndition during the course of FCC process may not be filled. For example, if the relaxation rate of the network ains is slower than the rate of copolymerization and crossking reactions, kinetically frozen structures may appear d they become fixed with further polymerization. Moreer, the volume of the separated diluent phase may not cessarily correspond to the pore volume in the final mate-l because of the collapse of the network structure on ying or on post-treatment [13]. However, the present odel gives at least qualitative informations regarding the enomena occurring during the FCC of vinyl/divinyl nomers in dilute solutions.

knowledgements

This work was supported by the Scientific and Technical search Council of Turkey (TUBITAK) under grant nber TBAG-1561.

pendix. Kinetics of free-radical crosslinking olymerization (FCC)

/inyl-group conversions: FCC of vinyl/divinyl monos involves three types of vinyl groups: those on monoyl monomer MVM (M_1), on divinyl monomer DVM), and on polymer chains, i.e. pendant vinyls (M_3). olymerization of these three types of vinyl groups ılts in the formation of three types of growing radicals, ending on the location of the radical center, namely, se with MVM unit at the end (M_1*), DVM unit with unreacted vinyl (pendant vinyl) at the end (M_2*), and M unit with both reacted vinyls at the end (M_3*). In order implify the kinetic treatment of the reaction system, the antaneous rate constants for propagation, crosslinking, termination reactions are defined as follows [35]:

$$= \sum_{j=1}^{3} k_{pji} x_j \qquad (i = 1, 2, 3), \tag{A1a}$$

$$= \sum_{i=1}^{3} \sum_{j=1}^{3} k_{tcij} x_i x_j, \tag{A1b}$$

$$k_{td} = \sum_{i=1}^{3} \sum_{j=1}^{3} k_{tdij} x_i x_j, \tag{A1c}$$

$$k_t = k_{tc} + k_{td}. \tag{A1d}$$

Here, k_{pji} is the propagation rate constant between radicals M_j* and vinyls M_i, k_{tcij} and k_{tdij} are the termination rate constants between radicals of types M_i* and M_j* by coupling (c) and by disproportionation (d) respectively, x_j is the instantaneous mole fraction of the radical M_j*, i.e. $x_j = [M_j^*]/[R^*]$, where $[R^*]$ is the total radical concentration defined by $[R^*] \equiv \sum_{j=1}^{3} [M_j^*]$.

Applying Eqs. (A1a)–(A1d) and neglecting chain transfer reactions, one may derive the rate equations for the concentration of the initiator I, vinyl groups M_i, crosslinks μ and the nth moment of the primary molecules Q_n' defined as $Q_n' \equiv \sum_{r=1}^{\infty} r^n [P_r']$, where P_r' represents the primary molecules of chain length r, as follows [35]:

$$r_I = -k_d[I], \tag{A2}$$

$$r_{M_1} = -k_{p1}[R^*][M_1], \tag{A3}$$

$$r_{M_2} = -2k_{p2}[R^*][M_2], \tag{A4}$$

$$r_{m_1} = -r_{M_1}, \tag{A5}$$

$$r_{m_2} = -0.5 r_{M_2}, \tag{A6}$$

$$r_\mu = k_{p3}[R^*][M_3], \tag{A7}$$

$$r_{M_3} = (1 - k_{cyc}) r_{m_2} - (1 + k_{mc}) r_\mu, \tag{A8}$$

$$r_{Q_n'} = \left(k_{td} + \frac{n+1}{2} k_{tc}\right) Y_0' Y_n' \qquad (n = 0, 1, 2, \ldots) \tag{A9}$$

where

$$Y_0' = [R^*] = (2fk_d[I]/k_t)^{0.5}, \tag{A10}$$

$$Y_1' = \left(k_{p1}[M_1] + k_{p2}[M_2]\right)/k_t, \tag{A11}$$

$$Y_n' = n!(Y_1'/Y_0')^n Y_0' \tag{A12}$$

f is the initiator efficiency, k_d is the decomposition rate constant of the initiator, m_1 and m_2 are the structural units formed from MVM and DVM respectively, k_{cyc} is the fraction of DVM units consumed by cyclization reactions, and k_{mc} is the number of multiple crosslinks formed per intermolecular link. Note that (A1a–A1d; A2–A12) hold during the course of the whole polymerization process.

Gel point: up to the gel point all molecules present in the reaction system are finite. At the incipient formation of infinite structures, which is called the gel point, the second moment of the branched polymer distribution Q_2 goes to

infinity:

$$\lim_{t \to t_g} (Q_2)^{-1} = 0 \tag{A13}$$

where Q_2 is defined as $Q_2 \equiv \sum_{r=1}^{\infty} r^2[P_r]$ and P_r represents the branched polymer molecules of chain length r. Application of the method of moments to the kinetic model of the reactions given in Ref. [35] yields the rate equation for Q_2 as follows:

$$r_{Q_2} = (2k_t + k_{tc})\left\{Y_1^{\cdot} + \left(k_{p3}[M_3]/k_t\right)\left(Q_2/Q_1^{\cdot}\right)\right\}^2. \tag{A14}$$

Eqs. (A13) and (A14) together with the previous equations predict the gel point at which the system changes from liquid to solid-like state.

Post-gelation period: Beyond the gel point, both an infinite network (gel) and finite molecules (sol) coexist in the polymerization system. Henceforth, the superscripts (s) and (g) will be used to denote the species in the sol and in the gel, respectively, whereas those without any primes refer to species in the whole polymerization system. The kinetic treatment of the post-gelation period assumes a steady state concentration for the radical concentration in the sol and in the whole reaction system. For instance, invoking the steady state approximation for the radical concentration in the sol, i.e.

$$\frac{d[R^{s*}]}{dt} = 2fk_d[I] - \left(k_t[R^*] + k_{p3}[M_3^g]\right)[R^{s*}] \cong 0, \tag{A15}$$

one obtains the fraction of radicals belonging to the sol fraction (ϕ_s) as:

$$\phi_s = \left(1 + \frac{k_{p3}[M_3^g]}{k_t[R^*]}\right)^{-1} \tag{A16}$$

Using this approach, the moment equations for sol molecules were derived previously [40]. The equations needed for the present simulations are:

$$W_s = 1 - W_g = \phi_s^2\left[1 - \frac{k_{tc}}{k_t}(1 - \phi_s)\right]. \tag{A17}$$

$$y = \left\{(\phi_s Q_1^{\cdot}/Q_0^{\cdot})^{-1} - \mu W_s/Q_1^{\cdot}\right\}^{-1}. \tag{A18}$$

$$N = \left\{\frac{2\mu}{Q_1^{\cdot}}(1 + W_s) - \frac{2Q_1^{\cdot}}{Q_2^{\cdot}}\right\}^{-1} \tag{A19}$$

where W_s is the weight fraction of sol. If MVM has an ionic substituent with a degree of ionization α_i (ratio of ionic groups to the total number of MVM units), the concentration of ions per network chain N_i is obtained as:

$$N_i = \alpha_i N \frac{m_1}{Q_1^{\cdot}} \tag{A20}$$

In order to solve the equations given above, one needs to know the concentrations of pendant vinyl groups in the gel M_3^g. The rate equations for the formation of pendant vinyl groups on the gel molecule is given as [40]:

$$r_{M_3^g} = \left(1 - k_{cyc}\right) \times \left(k_{p2}[R^*][M_2]\right)_0 + \left\{k_{p2}[M_2] - (1 + k_{mc})k_{p3}[M_3^g]\right\} \times [R^*](1 - \phi_s)$$

$(t < 2t_g)$, (A21a)

$$r_{M_3^g} = k_{p2}[R^*][M_2] - (1 + k_{mc})k_{p3}[M_3^g][R^*](1 - \phi_s)$$

$(t > 2t_g)$ (A21b)

where the subscript 0 denotes the initial concentrations.

Calculations: The kinetic model is solved for a batch isothermal copolymerization of vinyl/divinyl monomers. Owing to the differences in the densities of the monomer and the polymer the reaction volume V will change during the polymerization. If S represents the concentration of species I, M_i, m_i, Q_n and μ, a mass balance requires:

$$r_S = \frac{d(VS)}{V dt} = \frac{dS}{dt} + \frac{S}{V}\frac{dV}{dt}. \tag{A22}$$

where dV/dt is the rate of volume change, which, assuming ideal solutions, is given by:

$$\frac{dV}{dt} = -\varepsilon V \sum_{i=1}^{2} r_{m_i} \bar{V}_i. \tag{A23}$$

where $\bar{V}_i$ is the molar volume of the monomer with vinyl group of type i.

The mass-balance equations of the kinetic model represented by Eq. (A22) can be solved numerically to predict the vinyl group conversions, gel points, chain length averages and the gel crosslink density as a function of the reaction time. The independent variable reaction time t can be replaced with the mole conversion x or the volume conversion α of the monomers using the equations:

$$x = \frac{Q_1^{\cdot} V}{M_0 V_0}. \tag{A24}$$

$$\alpha = 1 - \left(\frac{1 - f_2 \Delta\bar{V}/\bar{V}_1}{1 - f_{20}\Delta\bar{V}/\bar{V}_1}\right)(1 - x) \tag{A25}$$

where V_0 is the initial volume, M_0 is the initial monomer concentration, $\Delta\bar{V} = \bar{V}_2 - \bar{V}_1$, f_2 and f_{20} are the mole fractions of DVM at conversion x and at zero conversion, respectively.

eferences

1] Millar JR, Smith DG, Marr WE, Kressman TRE. J Chem Soc 1963;218:218.
2] Seidl J, Malinsky J, Dusek K, Heitz W. Adv Polym Sci 1967;5:113.
3] Dusek K. In: Haward RN, editor. Developments in Polymerization 3. London: Applied Science, 1982. pp. 143.
4] Kun KA, Kunin R. J Polym Sci A-1 1968;6:2689.
5] Sederel WL, DeJong GJ. J Appl Polym Sci 1973;17:2835.
6] Jacobelli H, Bartholin M, Guyot A. J Appl Polym Sci 1979;23:927.
7] Howard GJ, Midgley GA. J Appl Polym Sci 1981;26:3845.
8] Wieczorek PP, Kolarz BN, Galina H. Angew Makromol Chem 1984;126:39.
9] Poinescu IC, Beldie C, Vlad C. J Appl Polym Sci 1984;29:23.
0] Okay O, Soner E, Gungor A, Balkas TI. J Appl Polym Sci 1985;30:2065.
1] Okay O, Balkas TI. J Appl Polym Sci 1986;31:1785.
2] Galina H, Kolarz BN, Wieczorek PP, Wojczynska M. Br Polym J 1985;17:215.
3] Okay O. J Appl Polym Sci 1986;32:5533.
4] Dragan S, Csergo D, Manolescu I, Carpov A. React Polym 1987;5:123.
5] Okay O. Angew Makromol Chem 1988;157:1.
6] Jun Y, Rongnan X, Juntan Y. J Appl Polym Sci 1989;38:45.
7] Coutinho FMB, Cid RCA. Eur Polym J 1990;26:1185.
8] Shea KJ, Stoddard GJ, Shavelle DM, Wakui F, Choate RM. Macromolecules 1990;23:4497.
[19] Cheng CM, Vanderhoff JW, El-Aasser, MS. J Polym Sci Polym Chem Ed 1992;30:245.
[20] Okay O, Gurun C. J Appl Polym Sci 1992;46:401.
[21] Wang QC, Svec F, Frechet JM. J Polym Sci Polym Chem Ed 1994;32:2577.
[22] Dusek K. J Polym Sci Polym Lett 1965;3:209.
[23] Dusek K. J Polym Sci C 1967;16:1289.
[24] Dusek K, Prins W. Adv Polym Sci 1969;6:1.
[25] Boots HMJ, Kloosterboer JG, Serbutoviez C, Touwslager FJ. Macromolecules 1996;29:7683.
[26] Flory PJ, Rehner Jr. J. J Chem Phys 1943;11:521.
[27] Frenkel J. Rubber Chem Technol 1940;13:264.
[28] Flory PJ. Principles of Polymer Chemistry. Ithaca, NY: Cornell University Press, 1953.
[29] Bastide J, Candau S, Leibler L. Macromolecules 1981;14:719.
[30] Horkay F, Zrinyi M. J Macromol Sci 1986;B25:307.
[31] Brochard F. J Phys 1981;42:505.
[32] De Gennes PG. Scaling Concepts in Polymer Physics. Ithaca, NY: Cornell University Press, 1979.
[33] Odian G. Principles of Polymerization. NY: McGraw-Hill, 1981 Ch. 6.
[34] Hild G, Okasha R. Makromol Chem 1985;186:93.
[35] Okay O. Polymer 1994;35:796.
[36] Hild G, Okasha R, Rempp P. Makromol Chem 1985;186:407.
[37] Orwoll RA. Rubber Chem Technol 1977;50:451.
[38] Okay O, Gurun C. J Appl Polym Sci 1992;46:421.
[39] Horie K, Otagawa A, Muraoka M, Mita I. J Polym Sci Polym Chem Ed 1975;13:445.
[40] Okay O. Polymer 1994;35:2613.

Pore Memory of Macroporous Styrene–Divinylbenzene Copolymers

EROL ERBAY,[1,2] OĞUZ OKAY[1,3]

[1] Kocaeli University, Department of Chemistry, 41300 Izmit, Kocaeli, Turkey

[2] PETKIM Petrochemicals Holding Inc., Research Center, P.O. Box 9, 41740 Korfez, Kocaeli, Turkey

[3] TUBITAK Marmara Research Center, Department of Chemistry, P.O. Box 21, 41470 Gebze, Kocaeli, Turkey

Received 20 January 1998; accepted 18 April 1998

ABSTRACT: The variation of the pore structure of styrene–divinylbenzene (S–DVB) copolymer beads with the drying conditions was investigated. Macroporous S–DVB copolymer beads with various DVB contents were prepared in the presence of toluene-cyclohexanol mixtures as a diluent. It was found that the pores of 10^1-nm radius, corresponding to the interstices between the microspheres, collapse upon drying of the copolymers from toluene. The collapsed pores reexpand if the copolymers were dried from methanol. The collapse–reexpansion process of the pores was found to be reversible, indicating that the actual pore structure formed during the crosslinking copolymerization is memorized by the copolymer network. The magnitude of the pore structure variation increased on worsening the polymer–diluent interactions during the gel formation process due to the simultaneous increase in crosslink density distribution.
 J Appl Polym Sci 71: 1055–1062, 1999

Key words: macroporous styrene–divinylbenzene copolymers; pore structure; pore memory; pore structure variation; crosslink density distribution

INTRODUCTION

Macroporous (heterogeneous) styrene–divinylbenzene (S–DVB) copolymer networks are widely used as starting materials for ion exchangers and as specific sorbents; therefore, they have been the subject of a large number of studies.[1–5] These materials are mainly prepared by free-radical crosslinking copolymerization of S and DVB monomers in the presence of an inert diluent. The diluent (a solvent, a nonsolvent, or a linear polymer) is included in the reaction system as a pore forming agent and plays an important role in the design of the pore structure of these crosslinked materials.[2]

If the diluent remains in the gel throughout the copolymerization, an expanded network structure is obtained. The expanded networks thus formed shrink during the removal of the diluent after their synthesis and therefore they are nonporous in the glassy state. Heterogeneities in the network structure appear if the diluent separates out of the gel phase during the polymerization reactions.[2,6–10] The incipient phase separation during the crosslinking copolymerization may occur before the onset of macrogelation; this results in the formation of a polymer dispersion in the liquid

Correspondence to: O. Okay, Istanbul Technical University, Department of Chemistry, 80626 Maslak, Istanbul, Turkey. (oguz@mam.gov.tr).

Contract grant sponsor: TUBITAK; contract grant number: TBAG-1561.

Journal of Applied Polymer Science, Vol. 71, 1055–1062 (1999)
 CCC 0021-8995/99/071055-08

phase. Otherwise, if the system phase separates beyond the gel point, the gel shrinks and results in a dispersion of the expelled liquid droplets in the network phase. In both cases, after complete conversion of the monomers a heterogeneous S–DVB network consisting of network and diluent phases is obtained. Removing the diluent from the network creates voids (pores) 1–1000 nm in size in the glassy state.

Relationships between the synthesis conditions and the structure of macroporous S–DVB networks have been the subject of intensive studies during the last four decades.[2,4,11–20] Experiments showed that a phase separation during the gel formation process is promoted; i.e., the volume of the diluent phase (pore volume) in the network increases as the concentration of the crosslinker (DVB) or that of the diluent increases, or as the solvating power of the diluent decreases. It was also shown that good solvents as a diluent create small pores and therefore a large specific surface area, whereas bad solvents or linear polymers produce materials with irregularly shaped large pores.

Although the final pore structure of a S–DVB network is fixed during the gel formation process when the network is in a rubbery state, its structural characterization is performed with the polymer sample in the glassy state. Krska et al. were the first to show the difference in the pore structure of S–DVB copolymers between the swollen and the dried states.[21] It was also found that the pore structure of these copolymers varies with the type of the solvent used to treat the network.[22–38] For instance, the copolymers dried from nonsolvents show a "maximum porosity," which is close to the porosity in the swollen state.[31] The drying process of the copolymers swollen in good solvents may lead to a partial or total collapse of the pores.[35,36] These experimental findings indicate that the swollen state porosity can be preserved in the dried state if the interactions between the polymer and the solvent are decreased before the drying process. It seems that the pore structure variation of S–DVB copolymers is closely related to the degree of inhomogeneity in crosslink distribution[29,31,35]; the pores in the loosely crosslinked (rubbery) regions of the material collapse during the drying process, whereas those in the highly crosslinked (glassy) regions remain unchanged.

This study seeks to obtain further insight into the pore structure variation in S–DVB copolymers, depending on the drying conditions. The reversibility of the pore structure variation and the size of the variable pores, as well as the magnitude of this variation, depending on the synthesis conditions, were investigated. Our primary aim was to determine the synthesis condition of macroporous S–DVB copolymers exhibiting a maximum memory of pores. For this purpose, a number of S–DVB copolymer beads with various DVB contents were prepared by the suspension polymerization technique. Cyclohexanol, toluene, and their mixture were used as a diluent. Toluene is a good solvent for polystyrene and its thermodynamic properties are the same as the monomers used in the polymerization. However, cyclohexanol has the solubility parameter value of 23.3 $(MPa)^{0.5}$ in contrast to the value of 15.6–21.1 $(MPa)^{0.5}$ for S–DVB copolymer,[39] which indicates that cyclohexanol is a nonsolvating diluent for the S–DVB copolymerization system. The changes in the pore structure of S–DVB copolymer beads were investigated by mercury porosimetry using copolymer samples dried from methanol and toluene.

EXPERIMENTAL

Materials

The S (Sabic), DVB (Riedel-de Haen), dibenzoyl peroxide (DBP, Elf Atochem), *tert*-butyl perbenzoate (TBP, Interchem), cyclohexanol (Merck), toluene (Merck), tricalcium phosphate (TCP, Budenheim), calcium chloride (Kemira Kemi), and dodecylbenzene sodiumsulfonate (DBS, Henkel) were used as received. Commercial DVB consisted of 62% DVB isomers with the rest being mostly ethylvinyl benzenes (35%). Fresh distilled water was used in the synthesis of the copolymers.

The S–DVB copolymer beads were obtained by the suspension polymerization technique.[40,41] Mixtures of cyclohexanol and toluene were used as the diluent of the organic phase. The volume fraction of the monomers in the organic phase (monomer–diluent mixture), v_2^{00}, was taken to be constant at 0.5 throughout the study, whereas the DVB concentration and the composition of the diluent were varied. The DVB concentrations were expressed in terms of the mole percent of the DVB isomers in the monomer mixture. DBP and TBP were used as the initiator of the low and high temperature period of the free-radical copolymerization, respectively. Suspension polymerization

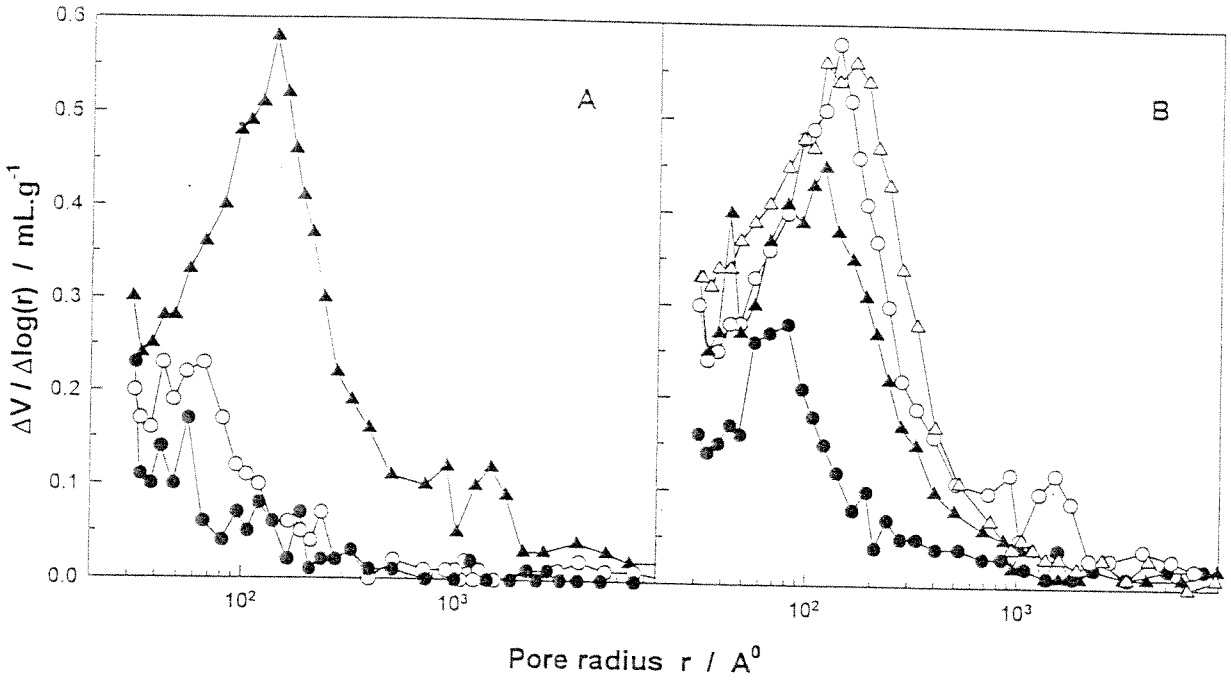

Figure 1 Effects of (A) the solvating power of the diluent and (B) the DVB concentration on the pore size distribution of macroporous S–DVB copolymers. $\nu_2^{00} = 0.5$. (A) DVB = 10%. Diluents: (●) toluene, (○) cyclohexanol/toluene [75/25 (v/v)], and (▲) cyclohexanol. (B) Diluent: cyclohexanol. DVB = (●) 5, (○) 10, (▲) 17.5, and (△) 24%.

was conducted in a 1-L Buchi jacketed glass reactor fitted with a mechanical stirrer, nitrogen inlet, condenser, and temperature and pressure indicators. A 3% aqueous NaCl solution (500 mL), the diluent (100 mL), and the S–DVB monomer mixture (100 mL) were first introduced into the reactor, heated to 70°C, and 100 mL of an aqueous suspension agent containing $CaCl_2$ (0.095 g), TCP (7.43 g), and DBS (0.017 g) were then added to the reactor under a nitrogen atmosphere at 300 rpm. The reaction mixture was heated to 90°C and the initiators DBP (0.50 g) and TBP (0.035 g) were fed to the mixture to initiate the polymerization reactions. The reaction was allowed to proceed at 90°C for 5.5 h and at 120°C for 1.5 h under a nitrogen atmosphere and at 300 rpm. After polymerization, a dilute HCl solution was added to the reactor to dissolve the TCP surrounding the beads. After filtration of the copolymer beads of 0.5–1.4 mm size, they were first washed with water and then extracted with acetone for 6 h in a Soxhlet apparatus.

Solvent Treatment

The copolymer beads thus obtained were swollen to equilibrium in toluene for at least 1 week. Then they were washed first with acetone and finally with pure methanol. Using this solvent exchange procedure, the good solvent toluene in the swollen gel was replaced with the nonsolvent methanol; thus, the gel was transferred from the rubbery to the glassy state before the drying process.[31] The copolymer beads after treatment with methanol as a final solvent were dried *in vacuo* at room temperature for 15 h. For comparison, part of the copolymer beads swollen in toluene were dried without the solvent exchange for 30 h at 80°C.

Methods

The pore volume and the pore size distribution of the copolymer beads were determined by mercury intrusion porosimetry on a Micromeritics 9305 model porosimeter. Cumulative pore volumes and the distribution function $\Delta V/\Delta\log(r)$ was used to express the pore size distribution, where ΔV is the pore volume change when the radius of a cylindrical pore was changed from r to $r - \Delta r$. The pore volume, V_p, and the total porosity, $P\%$, were calculated as

$$V_p = \frac{1}{d_0} - \frac{1}{d_2} \qquad (1)$$

$$P\% = \left(1 - \frac{d_0}{d_2}\right) \times 100 \qquad (2)$$

where d_0 is the apparent density of the copolymers and d_2 is the density of homogeneous S–DVB copolymers, taken as 1.06 g/mL.

To check the repeatability of the porosity measurements by the mercury porosimetry, three measurements were carried out on copolymer beads obtained at 44% DVB concentration and in the presence of toluene as a diluent. An average value of 0.355 mL/g for the pore volume with a standard deviation of 0.018 was obtained, indicating that the porosimeter gives reproducible results and the copolymer beads withstand the measurements of their pore structure.

RESULTS AND DISCUSSION

Macroporous S–DVB copolymer beads were prepared at a fixed monomer concentration (ν_2^{00} = 0.5). The synthesis parameters varied were the DVB concentration and the composition of the cyclohexanol–toluene diluent mixture (i.e., the solvating power of the diluent). Figure 1(A,B) illustrates the variation of the differential pore size distributions of S–DVB copolymers, depending on the quality of the diluent and the DVB concentration, respectively. Figure 1(A) shows that in copolymers with 10% DVB content the amount of pores of 10^1–10^2 nm in radius increases as the cyclohexanol content of the diluent increases (i.e., as the solvating power of the diluent decreases: (χ-induced syneresis[4]). Also, the average pore size becomes larger and the pore size distribution shifts toward the larger pores on worsening of polymer–diluent interactions as seen in Figure 1(A). From Figure 1(B) it is seen that with cyclohexanol as a diluent the porosity increases on raising the DVB concentration to 10% (ν-induced syneresis[4]) and then remains constant. Increasing the DVB content also shifts the pore size distribution toward the smaller pores. These results are expected and are in accord with previous reports.[2,4,31]

The pore size distributions of the copolymers shown in Figure 1 were measured using samples dried from methanol. Thus, Figure 1 represents the swollen state porosities, which are, the maximum porosities of the samples because the swelling agent toluene was replaced with the nonsolvent methanol before the drying process. Figure 2 compares the pore size distributions of copolymers with 10% DVB dried from methanol and from toluene. Cyclohexanol was used as the diluent during the synthesis. The pore sizes of 10^1-nm radius largely disappeared if the copolymers were swollen in toluene before the drying process (i.e., if they were dried in the rubbery state). To check the reversibility of the pore structure variation, the copolymers dried from toluene were swollen in toluene and then dried again from methanol and vice versa. The results of the

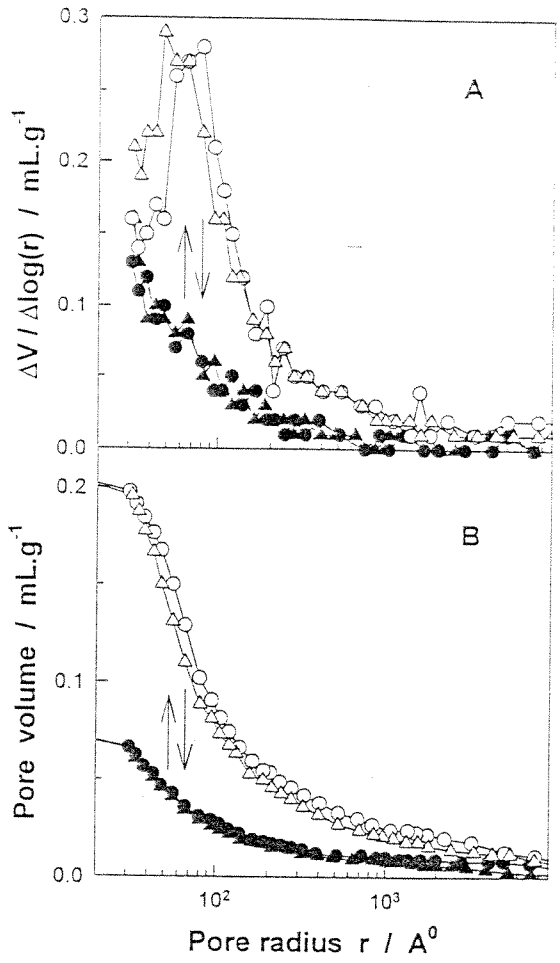

Figure 2 Pore size distribution of a macroporous S–DVB copolymer dried from toluene (filled symbols) and methanol (open symbols) in (A) differential and (B) integral modes. The copolymer samples dried from (●) toluene and (○) methanol. The sample dried from toluene was swollen again in toluene and thereafter dried from (△) methanol and (▲) vice versa. ν_2^{00} = 0.5. DVB = 10%. Diluent: cyclohexanol.

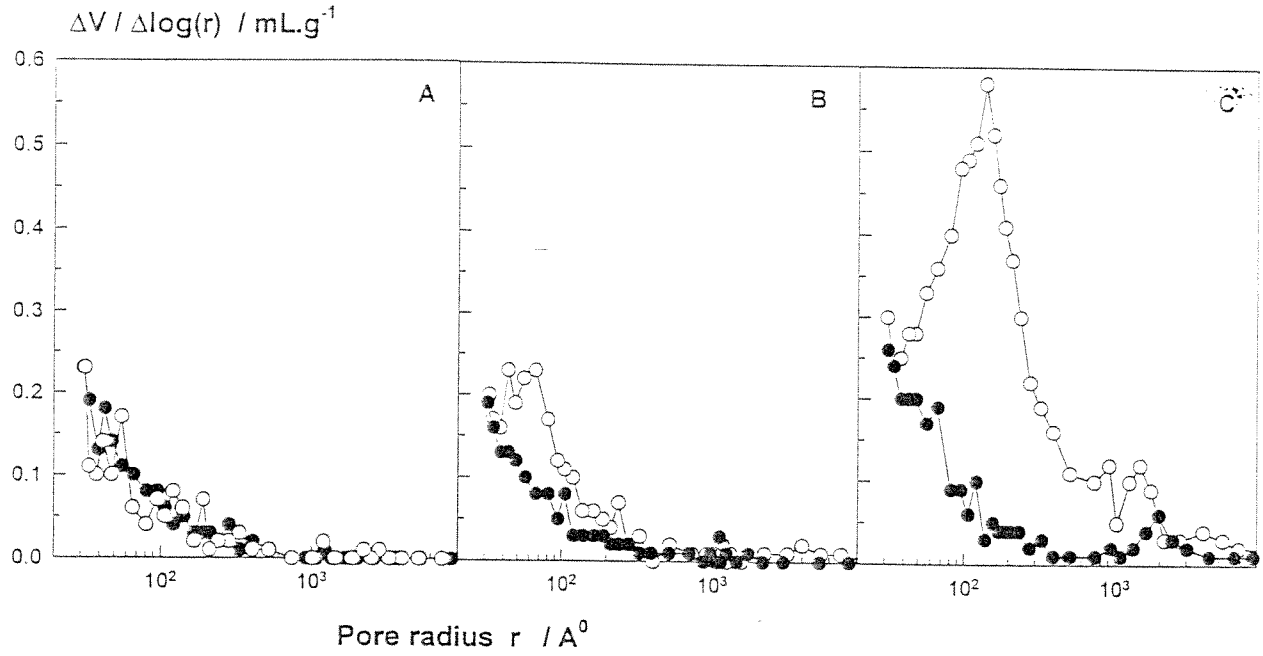

Figure 3 Effect of the solvating power of the diluent on the pore size distribution of macroporous S–DVB copolymers dried from (●) toluene and (○) methanol. $\nu_2^{00} = 0.5$. DVB = 10%. Diluents: (A) toluene, (B) cyclohexanol/toluene [75/25 (v/v)], and (C) cyclohexanol.

porosity measurements are also shown in Figure 2. It is seen that the collapse–reexpansion process of the pores of 10^1-nm radius is reversible. This indicates that the pore structure of S–DVB copolymers created during the crosslinking copolymerization is memorized by the copolymer network.

The structure of macroporous S–DVB copolymers is known to consist of globules[11]; the smallest, rather spherical particles of about 10–20 nm in diameter are the "nuclei," and the aggregation of these nuclei results in microspheres with diameters of 50–100 nm; the microspheres are aggregated again in particles of about 250–1000 nm in diameter. The pores are defined as the spaces between the nuclei and the particles and the microspheres and the particles. According to this picture, the variable pores of 10^1-nm radius shown in Figure 2 correspond to the interstices of the microspheres formed from the nuclei. This variation of the pore structure is mainly due to the higher reactivity of DVB compared to S in free-radical crosslinking copolymerization.[8] Because DVB monomer is incorporated into the polymer more rapidly than S, the parts of the network formed earlier (the nuclei and the inner part of the microspheres) are more highly crosslinked than those formed later. Therefore, the surface and the interstices of the microspheres formed at a later stage of the copolymerization (at which the reaction mixture is reached on the unreacted S monomer) are loosely crosslinked. The pores in these regions collapse during drying from toluene due to the cohesional forces between the solvated network chains. Thus, the reversibility of the pore structure variation originates from the crosslink density distribution, which is fixed for a given copolymer sample.

In Figures 3 and 4 the pore size distributions of S–DVB copolymers dried from toluene and methanol are shown as a function of the solvating power of the diluent and the DVB concentration, respectively. For a fixed amount of DVB, decreasing the solvating power of the diluent increases the magnitude of the pore structure variation (Fig. 3). As the diluent becomes poorer for the copolymer chains, pores of 10^1–10^2 nm radius start to appear. However, these pores are largely unstable and they collapse during the drying process. On the other hand, increasing DVB content to 10% increases the total porosity, as well as the amount of unstable pores (A and B in Fig. 4). A further increase in

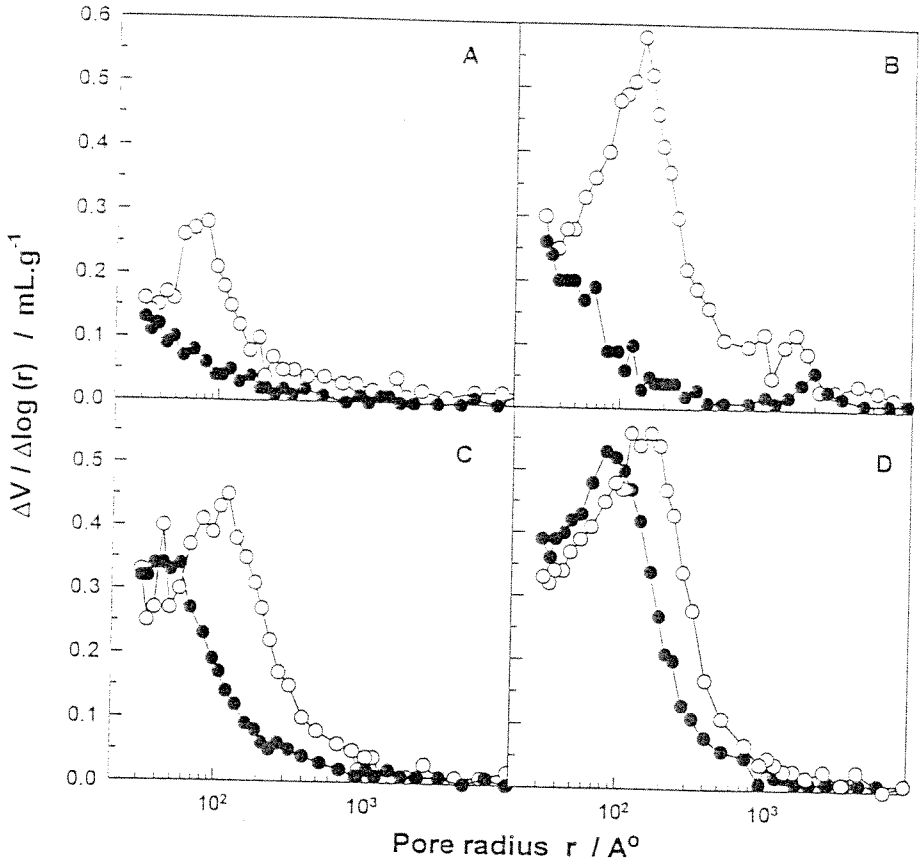

Figure 4 Effect of the DVB concentration on the pore size distribution of macroporous S–DVB copolymers dried from (●) toluene and (○) methanol. $\nu_2^{00} = 0.5$. Diluent: cyclohexanol. DVB = (A) 5, (B) 10, (C) 17.5, and (D) 24%.

the DVB concentration up to 24% does not change the total porosity much but increases the stability of the pores. These results can be explained as follows: a decrease in the solvating power of the diluent causes the process of phase separation to take place prior to gelation. This leads to an increase in the inhomogeneity in the final material (i.e., to an increase in the graduation of the crosslink distribution through the microspheres). As a result, the extent of the collapse–reexpansion process of the pores increases on decreasing the solvating power of the diluent. On the other hand, for a given type of diluent, increasing the DVB content promotes phase separation of the copolymers during the gel formation process and thus increases the inhomogeneity in the final copolymers. However, at high DVB contents even the less crosslinked regions of the network remain in the glassy state during drying due to the high overall crosslink density of the material. Thus, if the DVB concentration is sufficiently high [Fig. 4(D)], the pores remain almost stable and do not collapse on drying.

Defining $P_s\%$ as the fraction of stable pores,

$$P_s\% = \frac{P\%}{P_{max}\%} \times 100 \qquad (3)$$

where $P\%$ and $P_{max}\%$ are the total porosities of the copolymer samples dried from toluene and methanol, respectively, one may calculate the pore stability of S–DVB copolymer beads as a function of the synthesis conditions. Figure 5 shows the fraction of stable pores plotted as a function of the DVB concentration and the solvating power of the diluent. The solvating power of the diluent was estimated from $(\delta_1 - \delta_2)$, where δ_1 and δ_2 are the solubility parameters of the diluent

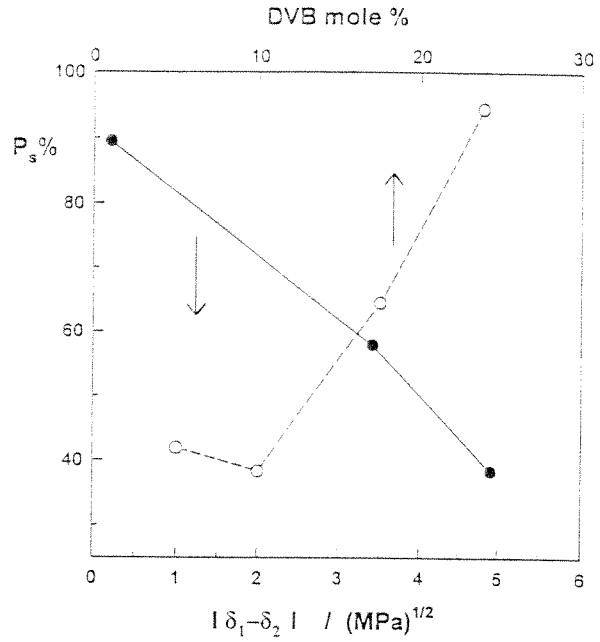

Figure 5 Fraction of stable pores in S–DVB copolymers, P_s%, shown as a function of the solvating power of the diluent ($\delta_1 - \delta_2$) and the DVB concentration. ν_2^{00} = 0.5. DVB = (●) 10%. Diluent: (○) cyclohexanol.

and the polymer, respectively. The solubility parameter of the diluent mixture was calculated from the solubility parameters of cyclohexanol and toluene as given previously.[17] Macroporous S–DVB copolymers with a stable pore structure form at high crosslinker concentrations or in the presence of good solvents as a diluent. Copolymers with a high number of variable pores are obtained in the presence of nonsolvating diluents and at medium DVB concentrations.

In summary, the present work shows the synthesis conditions of macroporous S–DVB copolymers that exhibit a reversible change in their pore structure. The reversible collapse–reexpansion phenomenon of pores of 10^1-nm radius occurs using copolymer beads with the methanol-toluene solvent pair as the posttreatment agent. The observed pore memory of S–DVB copolymers seems to widen their application area in size-selective separation of materials.

One of the authors (E.E.) wishes to thank PETKIM Petrochemicals Holding Inc. for permission to conduct this study in its laboratories.

REFERENCES

1. Millar, J. R.; Smith, D. G.; Marr, W. E.; Kressman, T. R. E. J Chem Soc 1963, 218, 218.
2. Seidl, J.; Malinsky, J.; Dusek, K.; Heitz, W. Adv Polym Sci 1967, 5, 113.
3. Kun, K. A.; Kunin, R. J Polym Sci 1968, A-1, 6, 2689.
4. Dusek, K. in Developments in Polymerization 3; Haward, R. N., Ed.; Applied Science: London, 1982; p. 143.
5. Guyot, A; Bartholin, M. Progr Polym Sci 1982, 8, 277.
6. Dusek, K. J Polym Sci Polym Lett 1965, 3, 209.
7. Dusek, K. J Polym Sci Part C 1967, 16, 1289.
8. Dusek, K.; Prins, W. Adv Polym Sci 1969, 6, 1.
9. Okay, O.; Gurun, C. J Appl Polym Sci 1992, 46, 421.
10. Okay, O.; Gurun, C. J Appl Polym Sci 1992, 46, 401.
11. Sederel,W. L.; DeJong, G. J. J Appl Polym Sci 1973, 17, 2835.
12. Jacobelli, H.; Bartholin, M.; Guyot, A. J Appl Polym Sci 1979, 23, 927.
13. Howard, G. J.; Midgley, G. A. J Appl Polym Sci 1981, 26, 3845.
14. Poinescu, I. C.; Beldie, C.; Vlad, C. J Appl Polym Sci 1984, 29, 23.
15. Okay, O.; Soner, E.; Gungor, A.; Balkas, T. I. J Appl Polym Sci 1985, 30, 2065.
16. Dragan, S.; Csergo, S.; Manolescu, I.; Carpov, A. React Polym 1987, 5, 123.
17. Okay, O. Angew Makromol Chem 1988, 157, 1.
18. Coutinho, F. M. B.; Cid, R. C. A. Eur Polym J 1990, 26, 1185.
19. Wang, Q. C.; Svec, F.; Frechet, J. M. J Polym Sci Polym Chem Ed 1994, 32, 2577.
20. Wojczynska, M.; Kolarz, B. N. J Appl Polym Sci 1995, 56, 433.
21. Krska, F.; Stamberg, J.; Pelzbauer, Z. Angew Makromol Chem 1968, 3, 149.
22. Haeupke, H.; Pientka, V. J Chromatogr 1974, 102, 117.
23. Hilgen, H.; DeJong, G. J.; Sederel, W. L. J Appl Polym Sci 1975, 19, 2647.
24. Galina, H.; Kolarz, B. N. Polym Bull 1980, 2, 235.
25. Baldrian, J.; Kolarz, B. N.; Galina, H. Coll Czech Chem Commun 1981, 46, 1675.
26. Kolarz, B. N.; Wieczorek, P. P.; Wojczynska, M. Angew Makromol Chem 1981, 96, 193.
27. Wieczorek, P. P.; Ilavsky, M.; Kolarz, B. N.; Dusek, K. J Appl Polym Sci 1982, 27, 277.
28. Wieczorek, P. P.; Kolarz, B. N.; Galina, H. Angew Makromol Chem 1984, 126, 39.
29. Galina, H.; Kolarz, B. N.; Wieczorek, P. P.; Wojczynska, M. Br Polym J 1985, 17, 215.
30. Okay, O.; Balkas, T. I. J Appl Polym Sci 1986, 31, 1785.

31. Okay, O. J Appl Polym Sci 1986, 32, 5533.
32. Poinescu, I.; Vlad, C.; Carpov, A.; Ionid, A. Angew Makromol Chem 1988, 156, 105.
33. Cheng, C. M.; Vanderhoff, J. W.; El-Aasser, M. S. J Polym Sci Polym Chem Ed 1992, 30, 245.
34. Okay, O. Angew Makromol Chem 1986, 143, 209.
35. Okay, O. Angew Makromol Chem 1987, 153, 125.
36. Okay, O. Angew Makromol Chem 1988, 157, 15.
37. Takeda, K.; Akiyama, M.; Yamamizu, T. Angew Makromol Chem 1988, 157, 123.
38. Jun, Y.; Rongnan, X.; Juntan, Y. J Appl Polym Sci 1989, 38, 45.
39. Grulke, E. A. in Polymer Handbook, 3rd ed.; Brandrup, J.; Immergut, E. H., Eds.; Wiley: New York, 1989; p. 519.
40. Erbay, E.; Bilgic, T.; Karali, M.; Savasci, O. T. Polym Plast Technol Eng 1992, 31, 589.
41. Erbay, E.; Bilgic, T. in Polymeric Materials Encyclopedia. Vol. 9; Salamone, J. C., Ed.; CRC Press: Boca Raton, FL, 1996; p. 6768.

Polymer Bulletin 41, 379–385 (1998)

Polymer Bulletin

Macroporous styrene-divinylbenzene copolymers: Formation of stable porous structures during the copolymerization

Erol Erbay[1,2], Oğuz Okay[1,3,*]

[1] Department of Chemistry, Kocaeli University, TR-41300 Izmit, Kocaeli, Turkey
[2] PETKIM Petrochemicals Holding Inc., Research Center, P.O. Box 9, TR-41740 Korfez, Kocaeli, Turkey
[3] TUBITAK Marmara Research Center, Department of Chemistry, P.O. Box 21, TR-41470 Gebze, Kocaeli, Turkey

Received: 27 February 1998/Revised version: 18 June 1998/Accepted: 18 June 1998

Summary

The variation of the pore structure of styrene-divinylbenzene (S-DVB) copolymer beads depending on the polymerization time was investigated. Macroporous S-DVB copolymer beads with 10 mol % DVB content were prepared in the presence of cyclohexanol as a diluent. It was found that the stable pores in S-DVB copolymers mainly form at an early stage of the copolymerization, i.e., at the gel point. Thus, the early phase separated portions of the network, where the crosslink density is locally high, do not collapse on drying and illustrate the stable part of the porosity of S-DVB copolymers. The number of stable pores does not change much during the whole course of the copolymerization. The maximum porosity first decreases on rising the post-gelation time due to the decreasing degree of dilution of the gel phase. Then, it increases continuously due to the increasing crosslink density of the gel. The pores formed at a later stage of the copolymerization are unstable and they collapse during the drying process. This is due to the lower crosslink density of the network regions forming later.

Introduction

Macroporous (heterogeneous) styrene - divinylbenzene (S-DVB) copolymer networks are widely used as starting materials for ion exchangers and as specific sorbents. These materials are prepared by free-radical crosslinking copolymerization of S and DVB monomers in the presence of an inert diluent (1-4). The diluent, which is a solvent, a nonsolvent, or a linear polymer, is included in the reaction system as a pore forming agent, and plays an important role in the design of the pore structure of these crosslinked materials. Heterogeneities in the network structure appear if the diluent separates out of the gel phase during the polymerization reactions. The incipient phase separation during the crosslinking copolymerization may occur before the onset of macrogelation; this results in the formation of a polymer dispersion in the liquid phase. Otherwise, if the system phase separates beyond the gel point, the gel shrinks and results in a dispersion of the expelled liquid droplets in the network phase (5,6). In both cases, after complete conversion of the monomers, a heterogeneous S - DVB network consisting of network and diluent phases is obtained. Removing of the diluent from the network creates voids (pores) of sizes 10 A^0 up to 1 μm in the glassy state. Relationships between the synthesis conditions and the structure of macroporous S-DVB networks have been the subject of intensive studies during the last four decades (1-4). Experiments showed that a phase separation during the gel formation process is promoted, i.e., the volume of the diluent

* Corresponding author: Department of Chemistry, Istanbul Technical University, TR-80626 Maslak, Istanbul, Turkey

phase (pore volume) in the network increases as the concentration of the crosslinker (DVB) or that of the diluent increases, or as the solvating power of the diluent decreases.

Although the final pore structure of a S - DVB network is fixed during the gel formation process, that is, when the network is in a rubbery state, its structural characterization is performed with the polymer sample in the glassy state. Krska et al. were first pointed out the difference in the pore structure of S-DVB copolymers between the swollen and the dried states (7). It was shown that the copolymers dried from nonsolvents such as methanol show a "maximum porosity", which is close to the porosity in the swollen state. The drying process of the copolymers swollen in good solvents such as toluene may lead to a partial or total collapse of the pores (8-15). These experimental findings indicate that the pore structure of S-DVB copolymers consists of two parts: the stable part which does not collapse during the post-treatment process, and the unstable part which collapses during the drying process in a rubbery state. It seems that the stability of the pores is closely related to the degree of inhomogeneity in crosslink distribution of the network; the pores in the loosely crosslinked (rubbery) regions of the material collapse during the drying process, whereas those in the highly crosslinked (glassy) regions remain unchanged.

This study aims to determine the polymerization times required for the formation of stable and unstable pores in S - DVB copolymers. These polymerization times are important because they also correspond to the formation times of network regions differing in crosslink density. For this purpose, S - DVB copolymerization reactions were carried by the suspension polymerization technique at 10 mol % DVB content. Cyclohexanol, a poor solvent for S - DVB copolymer was used as a diluent. The changes in the pore structure of S-DVB copolymer beads depending on the polymerization time were investigated by mercury porosimetry using copolymer samples dried from methanol and toluene.

Experimental

Materials

Styrene (S, Sabic), divinylbenzene (DVB, Riedel-de Haen), dibenzoyl peroxide (DBP, Elf Atochem), tert-butyl perbenzoate (TBP, Interchem), cyclohexanol (Merck), tricalcium phosphate (TCP, Budenheim), calcium chloride (Kemira Kemi), dodecylbenzene sodiumsulfonate (DBS, Henkel) were used as received. DVB consisted of 62 % DVB isomers with the rest being mostly ethylvinyl benzenes (35 %). Fresh distilled water was used in the synthesis of the copolymers.

The S-DVB copolymer beads were obtained by the suspension polymerization technique (16). Cyclohexanol was used as the diluent of the organic phase. The DVB concentration in the monomer mixture and the volume fraction of the monomers in the organic phase (monomer - diluent mixture) were taken to be constant at 10 mol % and 0.5, respectively. DBP and TBP were used as the initiator of the low and high temperature period of the free-radical copolymerization, respectively. Suspension polymerization was conducted in a 1 L Buchi jacketed glass reactor fitted with a mechanical stirrer, nitrogen inlet, condenser, temperature and pressure indicators. 550 mL of 3 % aqueous NaCl solution, the diluent cyclohexanol (100 mL) and the S - DVB monomer mixture (100 mL) were first introduced into the reactor, heated to 70^{0}C, and 100 mL of an aqueous suspension agent containing $CaCl_2$ (0.095 g), TCP (7.430 g), and DBS (0.017 g) were then added to the reactor under nitrogen atmosphere at 300 rpm. The reaction mixture was heated to 90^{0}C and the initiators DBP (0.500 g) and TBP (0.035 g) were feeded to the mixture to initiate the polymerization reactions. The reaction was allowed to proceed at 90^{0}C for 5.5 h and at 120^{0}C for 1.5 h under nitrogen atmosphere and at 300 rpm. In order to follow

the formation of porous structures and the monomer conversions during the copolymerization, at predetermined reaction times, samples of approximately 20 mL in volume were withdrawn from the reactor. One part of the sample was mixed with a dilute HCl solution to dissolve TCP surrounding the beads. After filtration of the copolymer beads, they were sieved using ASTM sieves under vibration. All the beads were within the size range of 0.5 to 1.4 mm in diameter. They were first washed with water and then extracted with acetone for 6 h in a Soxhlet apparatus. To determine the monomer conversion, another part of the sample taken from the reactor was also treated with HCl solution; then, the organic phase was separated and poured slowly into methanol under agitation. The precipitated copolymer was dried at 160 ^{0}C and then weighed. The fractional monomer conversion x was calculated as the amount of polymer formed per gram of the monomer present initially.

Solvent Treatment

The copolymer beads thus obtained were swollen to equilibrium in toluene for at least one week. Then, they were washed first with acetone and finally with pure methanol. Using this solvent exchange procedure, the good solvent toluene in the swollen gel was replaced with the nonsolvent methanol and, thus, the gel was transferred from the rubbery to the glassy state before the drying process. The copolymer beads after treatment with methanol as a final solvent were dried *in vacuo* at room temperature for 15 h. For comparison, part of the copolymer beads swollen in toluene was dried, without the solvent exchange, for 30 h at 80^{0}C.

Methods

The pore volume and the pore size distribution of copolymer beads were determined by mercury intrusion porosimetry on a Micromeritics 9305 model porosimeter. The distribution function $\Delta V / \Delta \log(r)$ was used to express the pore size distribution, where ΔV is the pore volume change when the radius of a cylindrical pore was changed from r to $r - \Delta r$. The total porosity, defined as the cumulative volume of the pores in one gram of the copolymer, was estimated from the intruded mercury volumes of the pores larger than 3 nm radius (intruded pressures smaller than 30000 psi).

Results and discussion

Macroporous S-DVB copolymer beads with 10 mol % DVB were prepared in the presence of cyclohexanol as an inert non-solvating diluent. The initial volume fraction of the monomers in the organic phase was taken to be constant at 0.5 throughout the present study, and only the polymerization time was varied. Figures 1A and 1B illustrate the differential pore size distribution curves of S - DVB copolymers isolated at different polymerization times. Open symbols in the figures represent the porosities of the copolymer samples dried from methanol; thus, they correspond to the swollen state ("maximum") porosities because the swelling agent toluene was replaced with the nonsolvent methanol before the drying process (10). The filled symbols belong to the copolymer samples dried from toluene, i.e., they represent the stable porosities.

At the very early stage of the copolymerization, the polymer was completely soluble in toluene. The insoluble material started to appear between a polymerization time of 20 and 25 min. The first sample for the porosity measurements was taken from the reactor after 30 min of polymerization. As seen from Figure 1A, this sample exhibits large number of pores of sizes 10^2 - 10^4 A° in radius, if it dried from methanol. However, these pores are unstable and, they totally disappear during the drying process from toluene.

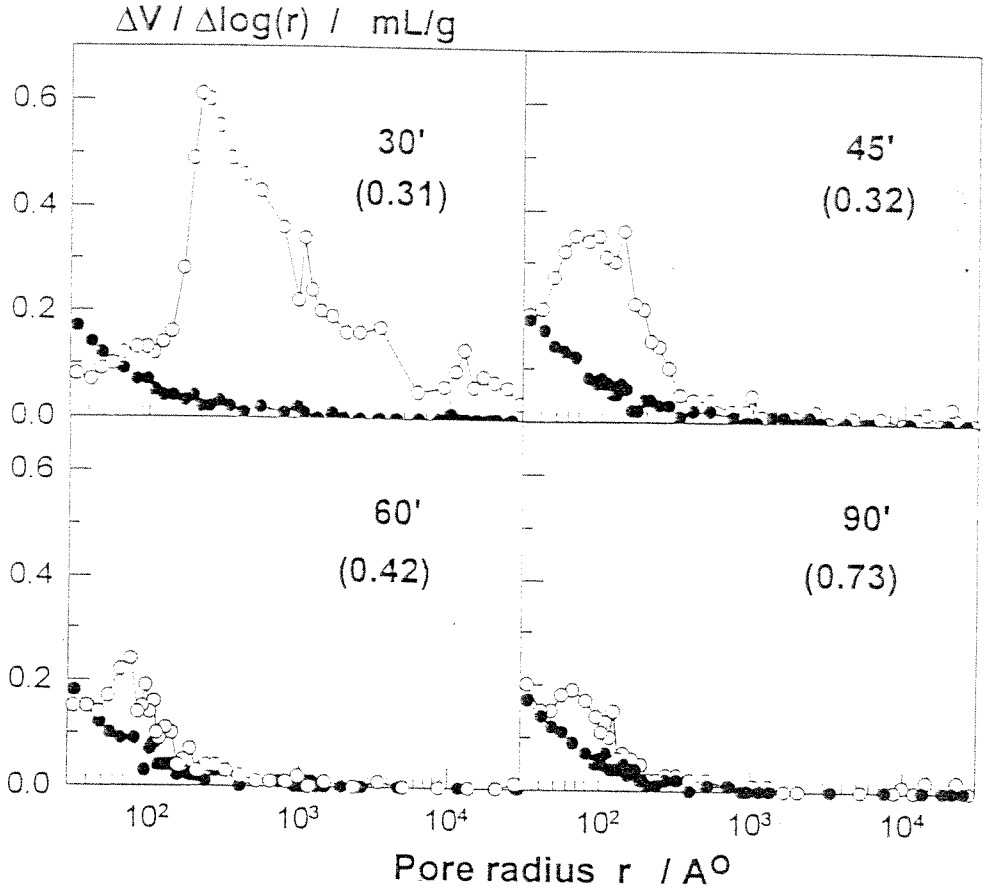

Fig. 1A. Differential pore size distribution of S-DVB copolymers dried from toluene (filled symbols) and from methanol (open symbols) at different reaction times. DVB = 10 mol %. Monomer concentration in the organic phase = 50 (v/v) %, Diluent = cyclohexanol. The reaction times and the monomer conversions (in parenthesis) are indicated in the figures.

As the polymerization time increases from 30 to 90 min, i.e., as the monomer conversion x increases from 0.3 to 0.7, the number of pores of 10^2 - 10^4 A° in radius found in the first sample decreases and finally disappears. Therefore, we may conclude that the pores of larger than 10^2 A^0 in radius appearing just beyond the gel point form due to the unreacted monomers and the sol polymers acting as an intrinsic diluent of the reaction system. Continuing polymerization converts monomer and sol polymer to the gel, so that the voids inside the network gradually fill up with the gel material, resulting in a decrease in porosity on increasing the polymerization time from 30 to 90 min.

Further polymerization up to 420 min creates new pores of 40 to 100 A^0 in radius (Figure 1B). The number of these pores increases and the pore size distribution shifts toward the larger pores on increasing the polymerization time. This increase in the porosity is first slight up to a polymerization time of 300 min but then ($x > 0.98$) rapid, due to the increasing crosslink density of the gel by the reaction of pendant vinyl groups with macroradicals to form crosslinks and multiple crosslinks. However, these pores formed at a later stage of the copolymerization are unstable and they collapse during the drying process.

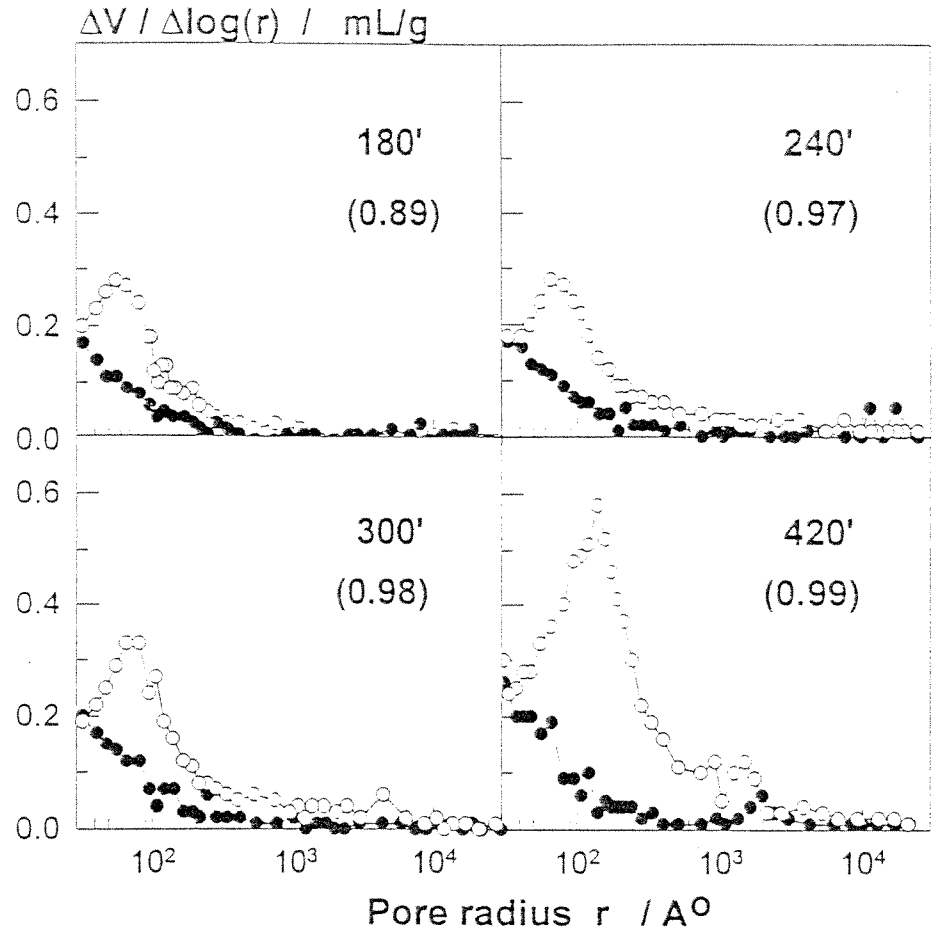

Fig. 1B. Differential pore size distribution of S-DVB copolymers dried from toluene (filled symbols) and from methanol (open symbols) at different reaction times. See Figure 1A caption for explanations.

Interesting is the observation that the stable pores of sizes less than 100 A^0 in radius appearing at the gel point exist during the whole course of the polymerization reaction (filled symbols in Figures 1A and 1B). These experimental results demonstrate that the stable pores in S-DVB copolymers form just beyond the macrogelation. This is probably due to the higher reactivity of the DVB monomers compared to styrene (17-21); at the beginning of the copolymerization, much more DVB is incorporated into the copolymer than is expected based on the initial composition of the monomer mixture. Accordingly, the first formed nuclei and their agglomerates (microspheres) are highly crosslinked than those formed in a later stage of the copolymerization when the major part of the DVB monomers have been used up. Thus, the pores inside the first formed regions of the network remain stable during the drying process because these regions will have higher crosslink density. However, the pores formed at higher monomer conversions are unstable due to the lower crosslink density of the network regions forming later.

In Figure 2, the total porosities of copolymers dried from methanol (expanded state) and toluene (collapsed state) are shown as a function of the polymerization time. It is seen that the stable porosity, i.e., the porosity of the copolymer dried from toluene does not change much during the whole course of the polymerization reactions. Its value is fixed with the onset of macrogelation. However, the maximum porosity first decreases on

rising the post-gelation time due to decreasing degree of dilution of the gel phase. Thereafter, it increases continuously on rising the reaction time due to the increasing crosslink density of the gel.

The structure of macroporous S-DVB copolymers is known to consist of globules (22); the smallest, rather spherical particles of about 100 - 200 A^0 in diameter are the nuclei, and the aggregation of these nuclei results in the microspheres. The pores are defined as the spaces between the nuclei, microspheres and the aggregated microspheres. According to this picture, the first formed nuclei and their agglomerates are stable whereas those formed later are unstable. The unstable pores in the copolymer collapse when it is dried from a good solvent like toluene. As we observed recently, the collapsed pores in S-DVB copolymer reexpand if the copolymer is swollen again in toluene and then dried from methanol (23). This collapse - reexpansion process of the unstable pores was found to be reversible, indicating that the actual pore structure formed during the crosslinking copolymerization is memorized by the copolymer network (23). According to Figure 2, a macroporous S - DVB copolymer with a maximum memory of pores, that is, with a maximum number of variable pores can be obtained if the network is isolated beyond the gel point.

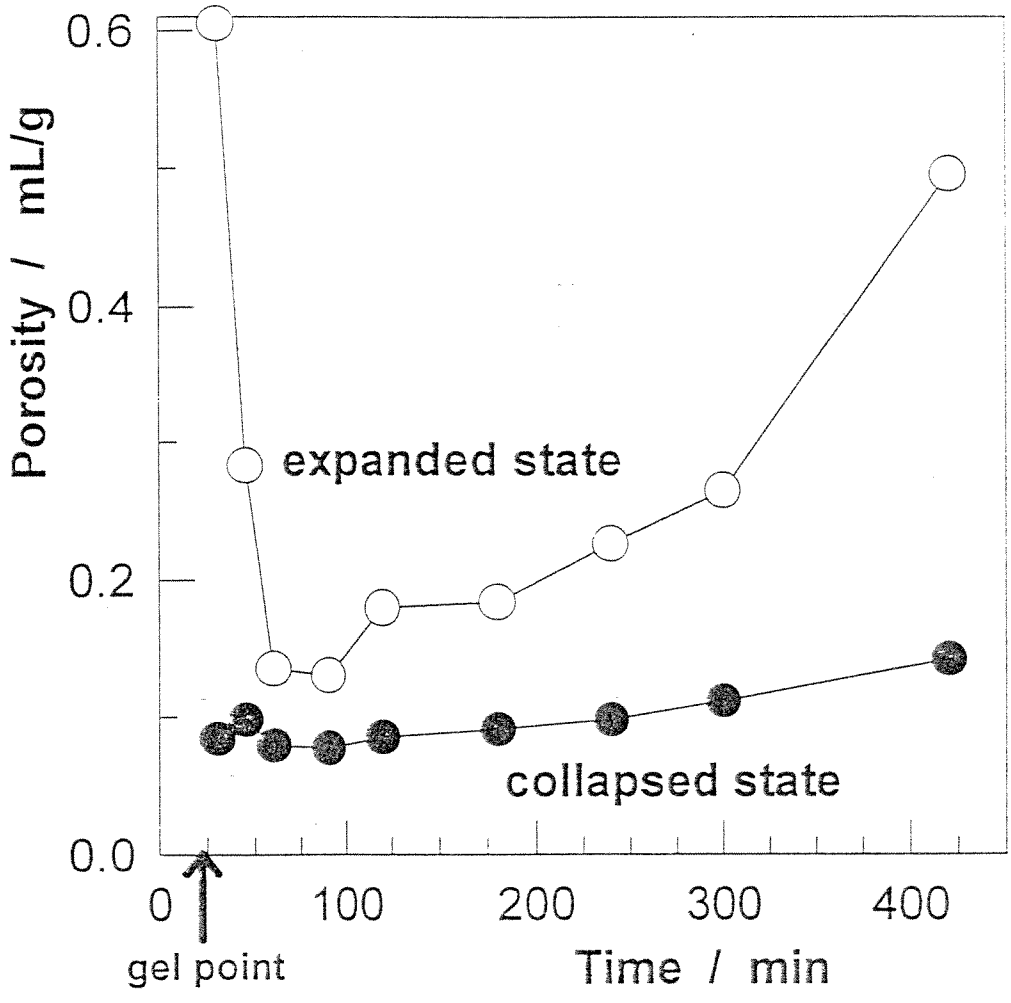

Fig. 2. Total porosity of copolymer samples dried from toluene (filled symbols) and from methanol (open symbols) shown as a function of the reaction time of S - DVB copolymerization.

Conclusions

1) Experimental data demonstrate that the stable pores in S-DVB copolymers mainly form at an early stage of the copolymerization, i.e., at the gel point. Thus, the early phase separated portions of the network, where the crosslink density is locally high, do not collapse on drying and illustrate the stable part of the porosity of S-DVB copolymers. The number of stable pores does not change much during the whole course of the copolymerization.

2) The maximum porosity first decreases on rising the post-gelation time due to the decreasing degree of dilution of the gel phase. Then, it increases continuously due to the increasing crosslink density of the gel. The pores formed at a later stage of the copolymerization are unstable and they collapse during the drying process. This is due to the lower crosslink density of the network regions forming later.

Acknowledgment

This work was supported by the Scientific and Technical Research Council of Turkey (TUBITAK) under Grand Number TBAG - 1561. One of the authors (EE) wishes to thank PETKIM Petrochemicals Holding Inc. for the permission to conduct this study in its laboratories.

References

1. Millar JR, Smith DG, Marr WE, Kressman TRE (1963) J Chem Soc 218:218
2. Seidl J, Malinsky J, Dusek K, Heitz W (1967) Adv Polym Sci 5:113
3. Kun KA, Kunin R (1968) J Polym Sci A1 6:2689
4. Dusek K (1982) In *Developments in Polymerization 3*, (ed RN Haward), Applied Science, London, p 143
5. Okay O, Gurun C (1992) J Appl Polym Sci 46:421
6. Okay O, Gurun C (1992) J Appl Polym Sci 46:401
7. Krska F, Stamberg J, Pelzbauer Z (1968) Angew Makromol Chem 3:149
8. Galina H, Kolarz BN, Wieczorek PP, Wojczynska M (1985) Br Polym J 17:215
9. Okay O, Balkas TI (1986) J Appl Polym Sci 31:1785
10. Okay O (1986) J Appl Polym Sci 32:5533
11. Poinescu I, Vlad C, Carpov A, Ionid A (1988) Angew Makromol Chem 156:105
12. Cheng CM, Vanderhoff CW, El-Aasser MS (1992) J Polym Sci Polym Chem Ed 30:245
13. Okay O (1986) Angew Makromol Chem 143:209
14. Okay O (1987) Angew Makromol Chem 153:125
15. Okay O (1988) Angew Makromol Chem 157:15
16. Erbay E, Bilgic T (1996) In *Polymeric Materials Encyclopedia*, (ed JC Salamone), CRC Press, Vol 9, FL, p 6768
17. Wiley RH, Devenuto G (1965) J Polym Sci A3:1959
18. Wiley RH, Mathews WK, O'Driscoll KF (1967) J Macromol Sci Chem A1:503
19. Malinsky J, Klaban J, Dusek K (1969) Coll Czech Chem Comm 34:711
20. Soper B, Haward RN, White EFT (1972) J Polym Sci A1 10:2545
21. Hild G, Okasha R (1985) Makromol Chem 186:93
22. Jacobelli H, Bartholin M, Guyot A (1979) J Appl Polym Sci 23:927
23. Erbay E, Okay O, J Appl Polym Sci (in press)

Subject:
Date: 22 Jan 99 16:35 EST
From: Heide.Roth@wiley.com
To: okayo@itu.edu.tr

With our compliments, to follow please find a recent issue of our publication, 'Advanced Coatings & Surface Technology Alert' in which your company appeared.

'Advanced Coatings & Surface Technology Alert' reports and puts into perspective significant developments in coatings and surface modification across a broad range of industry lines. Emphasis is on advanced coatings techniques - lasers, vapor deposition, and vacuum techniques, offering interdisciplinary analyses of those that have true commercial potential. This service includes patent coverage.

This service is available for individual use as a monthly newsletter for the annual subscription price of $620($680 outside N.A.). 'Advanced Coatings & Surface Technology Alert' is also available via weekly electronic delivery on a corporate-wide license basis for distribution on a computer network. A corporate license allows for electronic dissemination of the information to an unlimited amount of people within a company while also archiving the information for future searches.

There are 15 other services available covering the following topics: industrial r&d, microelectronics technology, advanced manufacturing, sensor technology, industrial bioprocessing, chemical processing, high-tech materials, bio/med devices, genetic technology, emerging technologies, food safety, nutrition research, nanotechnology, science & government, and food technology.

If any of these areas are of interest to you and you would like to see a sample, please let us know.

TECHNICAL INSIGHTS ALERT
Phone: 201-568-4744

ADVANCED COATINGS & SURFACE TECHNOLOGY ALERT
JANUARY 15, 1999

GROW HIGHLY-ORIENTED PT FILMS IN TWO STEPS
CVD DIAMOND FILM IN DOSIMETERS
REVERSIBLE PORES FOR BETTER S-DVB SORBENTS
SURFACE TREATMENT IMPROVES PVC PLASTICIZER
FULLY FLUORINATED LUBRICANTS AVAILABLE
SOME IMPORTANT PATENTS FOR YOU TO CHECK

****
To get further details on the advances noted below,
just call/write/fax/e-mail the contact named
at the end of each briefing.
****

GROW HIGHLY-ORIENTED PT FILMS IN TWO STEPS

The next generation of high-density, dynamic random access memory (DRAM) devices depends on oxide films with a high dielectric constant. Ferroelectric oxide films are especially important for nonvolatile ferroelectric random access memory, or FRAM, for use in infrared sensors and actuators. The preferred orientation of such films, which effects their physical properties, is affected by the orientation of the electrode films that they are grown on. Platinum is one of the best materials for the bottom electrode because it remains stable during subsequent oxide deposition processes, is less leaky than RuO_2, and provides better nucleation sites for ferroelectric oxide films. However, Pt is usually oriented in (111) planes.

micrometer in diameter. The responses of these diamond tips were tested at low X-ray energies (50-250 keV) and at relatively high energies (6-15 MeV), both in terms of sensitivity (collected charge with respect to the absorbed do se) and linearity, as a function of X-ray fluence.

Results show that sensitivities larger than 2 nC/Gy are achieved, with a good linearity in the dose rate range used in applications. The researchers hope to use the device as a profilometer to determine the X-ray beam profile from a linear accelerator with a spatial resolution of 0.1 mm, and to make a microdosimeter for in vivo detection. The device would be applied under the skin, and give an electrical signal proportional to the real absorbed dose. They currently have made and tested a couple of prototypes.

The next step in this line of research is to continue characterizing the CVD diamond thermoluminescence dosimeter and to find the expertise to make the dosimeters commercially available.

The Copernicus Project, the General Physics Institute of Moscow, and the Universities of Antwerp and Bucharest fund this research. So far, a patent application has not been filed. Researchers are very interested in development partners, licensees, and R&D funding.

Details: Ettore Vittone, Dipartmento di Fisica Sperimentale, Universita d Torina, via P. Giuria 1, 10125 Torino, Italy. Phone: +39-11-670-7317. Fax: +39-11-669-1104. E-mail: vittone@to.infn.it. URL: www.dfs.unito.it/solid/PUBBLICAZIONI/pub_HFCVD.html.

C990014

110299

REVERSIBLE PORES FOR BETTER S-DVB SORBENTS

Macroporous styrene-divinylbenzene (S-DVB) copolymers are widely used as starting materials for ion exchange resins and sorbents. S-DVB is usually made by free-radical cross-linking of styrene and divinylbenzene in the presence of an inert diluent, which acts as a pore-forming agent. When the diluent (a solvent, a nonsolvent, or a linear polymer) remains in the gel throughout polymerization, an expanded network structure forms. This network shrinks during the removal of diluent and creates a nonporous glassy state. If the diluent separates out of the gel phase during polymerization, heterogeneities in the network structure appear. However, in both cases, after complete conversion of monomers, a heterogeneous S-DVB network phase is obtained. Removing the diluent from the network at this phase creates pores 1-1000 nm in size in the glassy state. In addition, pore structure of copolymers varies with the type of solvent used to treat the S-DVB network.

Researchers have been working on understanding the relationships between synthesis conditions and the structure of macroporous S-DVB networks for the last 20 years. Recently, they have focused on the ability of swollen state porosity to be preserved in the dried state if the interactions between the polymer and solvent are decreased before the drying process.

Chemists in Turkey examined the pore structure variation in S-DVB copolymers under different drying conditions, and found that the variation of the porosity in these materials is reversible under specific synthesis conditions. They did this by preparing a number of S-DVB beads with various DVB contents. Cyclohexanol, toluene, and their mixture were used in different combinations as a diluent, and the samples were dried with methanol and toluene. The resulting changes in the pore structure of the copolymer beads were analyzed by mercury porosimetry.

Results show that for a fixed amount of DVB, decreasing the solvating power of the diluent increases the magnitude of the pore structure variation and creates unstable pores that collapse during the drying process. They also found that increasing DVB content to 10% increases the total porosity and the amount of unstable pores, but increasing it up to 24% stabilizes the pores.

What this means for the consumer or manufacturer is that with one material, you can create pores, control pores, or remove pores. This makes it easier to selectively trap biological molecules or organic materials, depending on the size of the particle and the size of the pores.

The next step is to synthesize polymer beads with monodisperse pores that can collapse and regenerate.

A patent application will be filed for this technology, which is available for licensing. Development partnerships or funding are sought as well.

Details: Oguz Okay, Tubitak Marmara Research Center, Department of Chemistry, PO Box 21, Gebze, Kocaeli-Turkey. Phone: +90-212-2853156. Fax:

Swelling Behavior of Anionic Acrylamide-Based Hydrogels in Aqueous Salt Solutions: Comparison of Experiment with Theory

OĞUZ OKAY,[1,2] SAFIYE B. SARIIŞIK,[1] SIBEL D. ZOR[1]

[1] Department of Chemistry, Kocaeli University, 41300 Izmit, Kocaeli, Turkey

[2] Department of Chemistry, TUBITAK Marmara Research Center, P.O. Box 21, 41400 Gebze, Kocaeli, Turkey

Received 17 November 1997; accepted 2 March 1998

ABSTRACT: A series of hydrogels were prepared from acrylamide and 2-acrylamido-2-methylpropanesulfonic acid (AMPS) monomers with 0–80 mol % AMPS and using *N,N'*-methylenebis(acrylamide) as the crosslinker. The swelling capacities of hydrogels were measured in water and in aqueous NaCl solutions. The volume swelling ratio q_v of hydrogels in water increases sharply when the mole fraction f_c of AMPS increases from 0 to 0.06. At higher values of f_c from 0.06 up to 0.18, no change in the swelling capacities of hydrogels was observed; in this range of f_c, q_v becomes nearly constant at 750. However, as f_c further increases, q_v starts to increase again monotonically over the entire range of f_c. At a fixed value of f_c, the swelling ratio of hydrogels decreases with increasing salt concentration in the external solution. The results of the swelling measurements in aqueous salt solutions were compared with the predictions of the Flory–Rehner theory of swelling equilibrium. It was shown that the theory correctly predicts the swelling behavior of hydrogels up to 80 mol % charge densities. The method of estimation of the network parameters was found to be unimportant in the prediction of the experimental swelling data. The network parameters used in the simulation only correct the deficiency of the swelling theory. © 1998 John Wiley & Sons, Inc. J Appl Polym Sci 70: 567–575, 1998

Key words: anionic hydrogels; polyacrylamide; 2-acrylamido-2-methylpropanesulfonic acid; swelling; swelling theory

INTRODUCTION

In recent years, hydrophilic gels called hydrogels have received considerable attention for use as specific sorbents and as support carriers in biomedical engineering. Hydrogels are mainly prepared by free-radical crosslinking copolymerization of acrylamide (AAm) and a divinyl monomer (crosslinker) in aqueous solutions. To increase the swelling capacity of hydrogels, an ionic monomer is also included in the monomer mixture. The desired property of hydrogels, such as their swelling capacity, is obtained by adjusting the concentration as well as the composition of the initial monomer mixture.

Investigations of the swelling behavior of hydrogels have been reported in the last 4 decades. Most of these studies have been concentrated on hydrogels containing weakly ionizable groups such as the carboxylate groups.[1–7] The swelling properties of these weak polyelectrolyte gels strongly vary depending on the pH of the solution.

Correspondence to: O. Okay, Istanbul Technical University, Department of Chemistry, Maslak, Istanbul, Turkey.

Contract grant sponsor: Scientific and Technical Research Council of Turkey; contract grant number: TBAG-1561.

Journal of Applied Polymer Science, Vol. 70, 567–575 (1998)

CCC 0021-8995/98/030567-09

However, hydrogels with strong electrolytes dissociate completely in the overall pH range and, therefore, exhibit pH independent swelling behavior. Sulfonic acid containing hydrogels represent a class of strong polyelectrolyte gels with a high degree of ionization. It was shown that the linear polymers with sulfonate groups derived from 2-acrylamido-2-methylpropanesulfonic acid (AMPS) exhibit extensive coil expansion in aqueous solutions;[7] even in 5*M* NaCl solution, the expansion of polymer coils due to charge repulsion cannot be totally screened.[7] Liu and colleagues[8] investigated the swelling properties of the corresponding hydrogels and observed a similar behavior. Highly concentrated salt solutions were required to screen the charge interactions within the hydrogel derived from AMPS and *N,N*-dimethylacrylamide (DMAA).

Tong and Liu[9] observed a constant swelling capacity of AMPS/DMAA hydrogels in the whole pH range and concluded that the AMPS content of the hydrogel corresponds to its charge density. Their calculation results showed a large discrepancy between the measured swelling data in water and that predicted by the Flory–Rehner theory of swelling equilibrium. Hooper and colleagues[10] and Baker and colleagues[11,12] investigated the swelling properties of strong polyelectrolyte AAm-based cationic and ampholytic hydrogels in water and in aqueous salt solutions. In contrast to Tong and Liu, they observed a good agreement between the Flory–Rehner theory and experiment. It seems that the approximations of the swelling theory cancel each other, so that it correctly predicts the swelling behavior of their hydrogels with charge densities below 5 mol %.

The scope of the present work was to establish whether it is possible to predict the swelling behavior of highly swollen hydrogels with charge densities up to 80 mol % using the Flory–Rehner theory. It was also of interest to clarify the sensitivity of the theory's predictions to the estimation method of the network parameters. For this purpose, we prepared a series of strong polyelectrolyte AAm-AMPS hydrogels with various ionic group content and measured their swelling capacities in water and in aqueous NaCl solutions ranging in concentration from 10^{-5} to 1*M*. Instead of DMAA, AAm was used as a comonomer of AMPS to increase the swelling capacity of our hydrogels. The measured swelling data of the hydrogels were compared with that predicted by the Flory–Rehner theory. As will be shown, this simple theory correctly predicts the swelling behavior of hydrogels with swelling capacities up to 2 L of water per mL of dry hydrogel.

EXPERIMENTAL

Materials

AAm (Merck), *N,N'*-methylenebis(AAm) (BAAm; Merck), AMPS (AKSA), ammonium persulfate (APS; Merck), *N,N,N',N'*-tetramethylethylenediamine (TEMED; Merck), and NaCl (Merck) were used as received. Double distilled and deionized water were used in hydrogel preparation and in swelling measurements.

Hydrogel Synthesis

Hydrogels were prepared by free-radical crosslinking copolymerization of AAm and AMPS with a small amount of BAAm as a crosslinker in aqueous solution. APS and TEMED were, respectively, the initiator and accelerator. Reactions were conducted at room temperature (21 ± 2°C). Gels were prepared according to the following scheme.

5 g AAm-AMPS mixture, NaOH (in the amount corresponding to the number of moles of AMPS), 133 mg BAAm, and 40 mg APS were dissolved in double distilled water under cooling to give a total volume of 100 mL. After addition of 0.24 mL of TEMED, the solution was transferred to small tubes of 5.8 mm in diameter. Polymerization was conducted for 24 h. Homologous series of anionic hydrogels were prepared in this way, allowing systematic variation of the AMPS concentration between 0 and 80 mol % (with respect to the monovinyl monomers). The total monomer concentration and the crosslinker ratio *X* (mole ratio of vinyl to divinyl monomers) were fixed at 5 w/v % and 82, respectively. It must be pointed out that, due to the electrostatic repulsion between the AMPS monomer and the growing chains, one may expect a lesser reactivity for AMPS compared with AAm in free-radial crosslinking copolymerization. Therefore, the microstructure concerning the composition of the network chains in the hydrogels may be heterogeneous.

After polymerization, hydrogel samples were cut into specimens of ~ 10 mm in length. The samples (usually 10 pieces) were then immersed in a large excess of distilled water for at least 1 week; during this period, water was replaced every other day to remove the unreacted species. It was found that the sol fraction in the gels is

<0.1% after extraction with water. Half of the gel samples were then subjected to swelling measurements, whereas the remaining samples were dried according to the following procedure: the swollen gel samples were successively washed with solutions whose compositions were changed gradually from water to pure methanol. This solvent exchange process facilitates final drying of the gel samples. The collapsed samples after the treatment with methanol as a final solvent were dried in vacuum at 60°C to constant weight. The weight swelling ratio of hydrogels after preparation, q_F, was calculated as

$$q_F = \frac{\text{mass gel after preparation}}{\text{mass dry gel}} \quad (1)$$

Swelling Measurements

The swollen hydrogel samples from the same gel (usually five pieces) were immersed in vials (100 mL) filled with water. The vials were set in a temperature-controlled bath at 25 ± 0.1°C. To reach the equilibrium degree of swelling, the gels were immersed in water at least for 1 week; the swelling equilibrium was tested by weighing the samples. The gels were then weighed in the swollen state and transferred to vials containing the most concentrated aqueous NaCl solution. The concentration of NaCl solutions ranged from 1.0*M* to 10^{-5}*M*. Gel samples were allowed to swell in the solution at least for 1 week, during which aqueous NaCl was refreshed to keep the concentration as feeded. After the swelling equilibrium is established, the samples were weighed and then transferred into the next dilute NaCl solution. The swelling measurements in aqueous NaCl were conducted both in direction of decreasing salt concentration from 1*M* to water and in reverse direction from water up to 1*M* NaCl. No systematic variation in the recorded swelling data was observed. The weight swelling ratios of hydrogels in water and in aqueous NaCl, q_w (mass gel after swelling/mass dry gel), were calculated using the equations

$$q_w(\mathrm{H_2O}) = q_F \frac{\text{mass gel in water}}{\text{mass gel after preparation}} \quad (2a)$$

$$q_w(\mathrm{NaCl}_{aq}) = q_w(\mathrm{H_2O}) \frac{\text{mass gel in aqueous NaCl}}{\text{mass gel in water}} \quad (2b)$$

The volume swelling ratio of hydrogels, q_v, was calculated as

$$q_v = 1 + \frac{(q_w - 1)\rho}{d} \quad (3)$$

where ρ and d are the densities of polymer and solution, respectively. The values ρ and d used were 1.35 g mL^{-1} and 1 g mL^{-1}, respectively. Each swelling ratio reported in this article is an average of at least five separate measurements; standard deviations of the measured swelling ratios were <4% of the mean.

THEORY OF SWELLING EQUILIBRIUM

The state of equilibrium swelling of a polymer network immersed in a solvent is obtained when the solvent inside the network is in thermodynamic equilibrium with that outside. This equilibrium state is described by the equality of the solvent chemical potential μ_1 in both phases. Thus, at swelling equilibrium, we have

$$\Delta\mu_1^g = \Delta\mu_1^s \quad (4)$$

where the superscripts g and s denote the gel and solution phases, respectively. In terms of the osmotic pressure π, eq. (4) can also be written as

$$\pi = -\frac{\mu_1^g - \mu_1^s}{V_1} = 0 \quad (5)$$

where V_1 is the molar volume of solvent. Osmotic pressure π of a gel determines whether the gel tends to expand or to shrink. When nonzero, π provides a driving force for gel volume change. Solvent moves into or out of the gel until π is 0 (i.e., until the forces acting on the gel are balanced). During the swelling process, there are at least three forces acting on an ionic gel: those due to polymer-solvent mixing (*mix*), due to deformation of network chains to a more elongated state (*el*), and due to the nonuniform distribution of mobile counterions between the gel and the solution (*ion*). Within the framework of the Flory–Rehner theory, the osmotic pressure π of a gel is the sum of these three contributions[13,14]:

$$\pi = \pi_{mix} + \pi_{el} + \pi_{ion} \quad (6)$$

According to the Flory–Huggins theory, π_{mix} is given by[15]

$$\pi_{mix} = -\frac{RT}{V_1}(\ln(1 - v_2) + v_2 + \chi v_2^2) \quad (7)$$

where v_2 is the volume fraction of polymer in the hydrogel (i.e., $v_2 = 1/q_v$), χ is the polymer–solvent interaction parameter, R is the gas constant, and T is temperature. To describe the elastic contribution π_{el} to the swelling pressure, several theories are available.[16–22] We will use here the simplest affine network model to describe the behavior of our gels[15]:

$$\pi_{el} = -\frac{RT}{V_1}N^{-1}(v_2^{1/3}v_2^{02/3} - v_2/2) \quad (8)$$

where N is the average number of segments in the network chain and v_2^0 is the volume fraction of polymer network after preparation. Ionic contribution π_{ion} to the swelling pressure is caused by the concentration difference of counterions between the gel and the outer solution. To describe this effect completely, one should consider the ion–ion, ion–solvent, and ion–polymer interactions. The ideal Donnan theory ignores these interactions and gives π_{ion} as the pressure difference of mobile ions inside and outside the gel[15]:

$$\pi_{ion} = RT\sum_i (C_i^g - C_i^s) \quad (9)$$

where C_i is the mobile ion concentration of species i. According to ideal Donnan equilibria, the chemical potential of an ionic species i inside the hydrogel must be equal to that outside. Thus, for aqueous solutions of univalent salts, we have the equality

$$C_+^g C_-^g = C_+^s C_-^s = C_{salt}^{s\,2} \quad (10)$$

where C_{salt}^s represents the salt concentration in the external solution. On the other hand, the condition of electroneutrality inside an anionic hydrogel requires

$$C_-^g = C_+^g + C_{fix} \quad (11)$$

where C_{fix} is the concentration of fixed charges in the gel.

Using eqs. (4)–(11), we obtain the following system of equations describing equilibrium value of v_2 of hydrogels in aqueous salt solution and the distribution coefficient K of counterions between the gel and solution phases:

$$\ln(1 - v_2) + v_2 + \chi v_2^2 + N^{-1}(v_2^{1/3}v_2^{02/3} - v_2/2) - 2(K - 1)V_1C_{salt}^s - V_1C_{fix} = 0 \quad (12a)$$

$$K(K + C_{fix}/C_{salt}^s) - 1 = 0 \quad (12b)$$

where $K = C_-^g/C_{salt}^s$. Let f be the mole fraction of charged units in the network and $\bar{V}_r$ the molar volume of a polymer repeat unit, C_{fix} equals to

$$C_{fix} = \frac{f}{\bar{V}_r}v_2 \quad (12c)$$

In the case of swelling of hydrogels in water free of ionic species ($C_{salt}^s = 0$), eq. (12a) reduces to

$$\ln(1 - v_2) + v_2 + \chi v_2^2 + N^{-1}(v_2^{1/3}v_2^{02/3} - v_2/2) - V_1C_{fix} = 0 \quad (13)$$

Note that, for $C_{salt}^s < 10^{-6}M$, the contribution of the salt concentration in the external solution to the swelling equilibrium represented by eqs. (12a) and (12b) becomes negligible; thus, eq. (12a) also reduces to eq. (13) for $C_{salt}^s < 10^{-6}M$.

Moreover, for highly swollen hydrogels, since $v_2 \ll 1$, eqs. (12a) and (12b) can also be written as

$$-(0.5 - \chi)v_2^2 + N^{-1}v_2^{02/3}v_2^{1/3} - 2V_1C_{salt}^s(K - 1) - V_1C_{fix} = 0 \quad (14)$$

where

$$K = 0.5\left(\sqrt{\left(\frac{C_{fix}}{C_{salt}^s}\right)^2 + 4} - \frac{C_{fix}}{C_{salt}^s}\right) \quad (14a)$$

Calculations

The system of eqs. (12a) and (12b), in combination with eq. (12c), was solved numerically to calculate the equilibrium swelling ratio of hydrogels in aqueous salt solutions ($q_v = 1/v_2$) and the distribution coefficient of counterions K. For calculations, the values used were $V_1 = 18$ g mL^{-1}

and $\bar{V}_r = 52.6 + 117 f$ (obtained using the values 71 and 229 g mol^{-1} for the molecular weights of AAm and AMPS units, respectively, and using $\rho = 1.35$ g mL^{-1}). The χ parameter value for polyacrylamide (PAAm)–water system was recently evaluated from the swelling data for uncharged PAAm hydrogels swollen in water.[10] A best-fit value for χ of 0.48 was obtained.[11] This value of the χ parameter provided a good fit to the experimental swelling data of AAm-based anionic, cationic, and ampholytic hydrogels of various compositions.[11,12] In the following calculations, χ was held constant at this value. The volume fraction of polymer network after preparation, v_2^0, was calculated from the experimental q_F values as

$$v_2^0 = \left[1 + \frac{(q_F - 1)\rho}{d}\right]^{-1} \tag{15}$$

The experimental value of v_2^0 increased from 0.038 to 0.070 with increasing AMPS content from 0 to 80 mol %. C_{salt}^s is the independent variable of eqs. (12a) and (12b), which was varied between $10^{-5}M$ and $1.0M$ in our experiments.

To solve eqs. (12a) and (12b) for the two unknowns, $q_v = 1/v_2$ and K, the values of the network parameters f and N characterizing the hydrogels must also be known. The f and N values of hydrogels can be estimated by two different approaches.

Chemically Fixed Crosslink Density of Hydrogels

Because both the crosslinker ratio X (mole ratio of monomer to crosslinker) and the total monomer concentration were fixed in our experiments, whereas only the mole fraction of AMPS varies between the hydrogels, it is reasonable to assume a constant crosslink density for all the hydrogels. Thus, using the swelling ratio of nonionic gel in water $q_v = 40.9$ and using eq. (13) for $C_{fix} = 0$, we calculated N as 1.2×10^3, which should be valid for all other ionic hydrogels. After calibration of the gels, that is, after finding their crosslink densities in terms of N, f value of the ionic hydrogels obtained at the same chemical crosslink density was calculated from their swelling ratio in water and using eq. (13) for the condition $N = 1.2 \times 10^3$. Note that this method of estimation of the network parameters assumes that the addition of AMPS in the comonomer mixture does not change the network topology.

Chemically Varied Charge Density of Hydrogels

Because AMPS is a strong dissociating electrolyte, the amount of AMPS used in the hydrogel preparation should be equal to its charge density. Thus, f in eq. (12c) is given by

$$f = \frac{\text{AMPS mol \%}}{100} \tag{16}$$

From the equilibrium swelling ratio of hydrogels in water and using eqs. (13) and (16), one may calculate the crosslink densities of hydrogels in terms of N. Note that this method of estimation of network parameters neglects counterion condensation[6,23] and assumes that the ionization degree of AMPS units equals to unity. Also, it is assumed that AMPS completely reacts during the gel formation, and no reactions such as the hydrolysis reaction of AAm units take place during the swelling measurements.

In the following section, we will use both approaches to evaluate the network parameters and to compare the predictions of the theory with the experimental data.

RESULTS AND DISCUSSION

Figure 1 shows the volume swelling ratio q_v of AMPS/AAm hydrogels in water and in aqueous salt solutions plotted as a function of f_c, the mole fraction of AMPS used in the gel preparation. As expected, q_v increases sharply when the mole fraction f_c of AMPS increases from 0 to 0.06. This is due to the fact that, as f_c increases, the mobile ion (Na^+) concentration inside the gel also increases to maintain the electroneutrality condition. As a result, the difference between the mobile ion concentration inside and outside the gel increases with increasing f_c, which creates an additional osmotic pressure that expands the gel. Also expected is the decreased swelling ratio of hydrogels with increasing salt concentration in the external solution; this is due to decrease in the concentration difference of counterions inside and outside the hydrogel. In $1.0M$ NaCl solution, the swelling ratio is almost independent on the AMPS content of hydrogels due to screening of charge interactions within the hydrogel.

Interestingly, at higher values of f_c from 0.06 up to 0.18, no change in the swelling capacities of hydrogels was observed; in this range of f_c, q_v becomes nearly constant at 750. This may be a

result of counterion condensation, as was observed previously in carboxylate-containing AAm hydrogels.[6] However, as f_c further increases, q_v starts to increase again monotonically over the entire range of f_c. This swelling behavior of hydrogels with $f_c > 0.2$ may be a result of their high swelling ratios. The network chains in these swollen hydrogels are in 9- to 10-fold expanded configuration with respect to dry state, so that a destruction of the chains may occur during the swelling process. For AMPS/DMAA hydrogels, Tong and Liu also obtained a similar swelling curve as given in Figure 1. However, due to their insufficient data points in the range of $f_c < 0.20$, they interpreted the results as a monotonic increase of q_v over the entire f_c range from 0 to 0.90. However, the present results clearly illustrate the plateau in the swelling curve between $f_c = 0.06$ and 0.18.

Using the equilibrium swelling data q_v of hydrogels in water, we can now evaluate the network parameters f and N, describing the average number of charged units and of segments in a network chain, respectively. First, the value $q_v = 40.9$ found by experiments for nonionic gels in water yields $N = 1.2 \times 10^3$, compared with its chemical value $N_c = 41$ calculated from the crosslinker ratio $X = 82$. Comparison of these two values indicates that >90% of the crosslinker BAAm used in the gel synthesis were consumed in cycles and/or in multiple crosslinks. This is in accord with our previous results.[24,25] Second, to evaluate f and N values of ionic hydrogels, we will use both approaches explained in the previous section.

Chemically Fixed Crosslink Density

Assuming that $N = 1.2 \times 10^3$ is valid for all other hydrogels, eq. (13) can be solved for f using the experimental q_v data of ionic hydrogels. The calculated values of f are shown in Figure 2(A) as filled symbols plotted as a function of mole fraction of AMPS in the gel synthesis f_c. In the figure, the dotted line represents the relation $f/f_c = 1$ (i.e., in this line AMPS content of hydrogels equals to their charge density). It is seen that, in up to 1% AMPS content, all AMPS units act as charged units in the gel swelling. However, as f_c further increases, deviations appear from the straight line dependence, and f approaches a limiting value of 0.25.

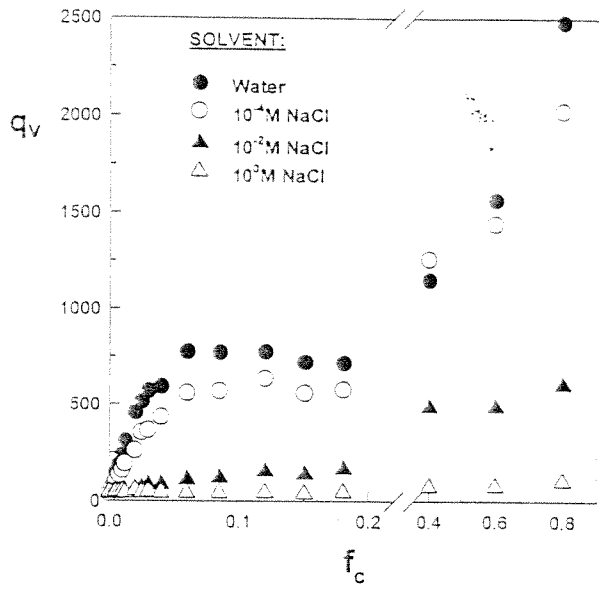

Figure 1 Variation of the volume swelling ratio q_v of AAm/AMPS hydrogels in water and in aqueous NaCl solutions with the mole fraction of AMPS used in the gel preparation f_c.

Chemically Varied Charge Density

Assuming that $f = f_c$, eq. (13) can be solved for N using the experimental q_v data of ionic hydrogels. The calculated values of N are also shown in Figure 2(B) as open symbols plotted as a function of f_c. N strongly decreases on rising f_c and approaches its stochiometric value of $N_c = 41$, shown in Figure 2(B) as the horizontal dashed line.

It is seen that the two approaches used in the estimation of the network parameters f and N yield totally different values. We will use now both approaches to predict the swelling capacities of hydrogels in aqueous NaCl solution. The results are collected in Figures 3 and 4. Herein, the volume swelling ratios q_v of hydrogels are shown as a function of the NaCl concentration. The experimental data are shown as symbols. The solid curves were calculated using eqs. (12a) and (12b) and using f and N values evaluated from the first approach. The dotted curves were calculated in the same way; but we used f and N values evaluated from the second approach. It is seen that both approaches provide good agreement with the experimental data up to 1.5 mol % AMPS (Fig. 3). In this range of AMPS concentration, the first approach (solid curves, N fixed) provides a slightly better agreement with the experimental

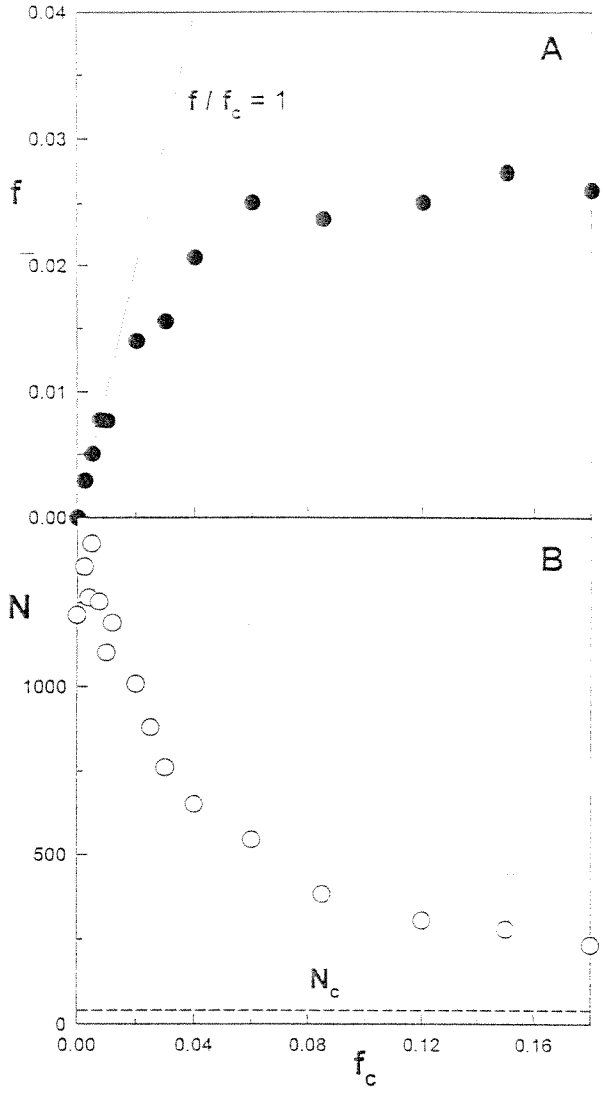

Figure 2 Variation of the network parameters f and N with the AMPS content of hydrogels f_c. In (A), the crosslink density of hydrogels is assumed to be constant (chemically fixed crosslink density), whereas in (B) the charge density of hydrogels is assumed to be equal to their AMPS content (chemically varied charge density). The f and N values were evaluated from the swelling ratio of hydrogels in pure water and using eq. (13).

data. Agreement between theory and experiment becomes qualitative at high AMPS contents (>18%; Fig. 4); Herein, the second approach ($f = f_c$) provides a better fit to the experimental data. We can conclude that both estimation methods of the network parameters can be used to predict the swelling behavior of hydrogels in aqueous salt solutions. In fact, due to the several assumptions and approximations of the Flory–Rehner and Flory–Huggins theories, no agreement between theory and experiment can be expected, especially in case of highly swollen hydrogels. This is, of course, in the case, where the actual values of f and N were used in the calculations.[9,11] The present results indicate that the deficiency of the theories are compensated by the values of the parameters f and N used in the fit. Thus, it must be pointed out that the values of f and N generated from the experimental swelling data should only be considered as fit parameters.

Another interesting point that is not visible in the magnification of Figures 3 and 4 is illustrated in Figure 5. The equilibrium swelling ratio q_v of hydrogels with <3 mol % AMPS content increases again, when the salt concentration further increases from 0.01M to 1.0M. This interesting feature, not predicted by the theory, was also observed previously by Baker and colleagues[12] in ampholytic and nonionic AAm-based hydrogels. Specific interactions between AAm and mobile ions seem to be responsible for this behavior.

Figure 6 shows the calculated distribution coefficient K of mobile counterions Cl^- between inside and outside the gel phase plotted as a function of the NaCl concentration in the external

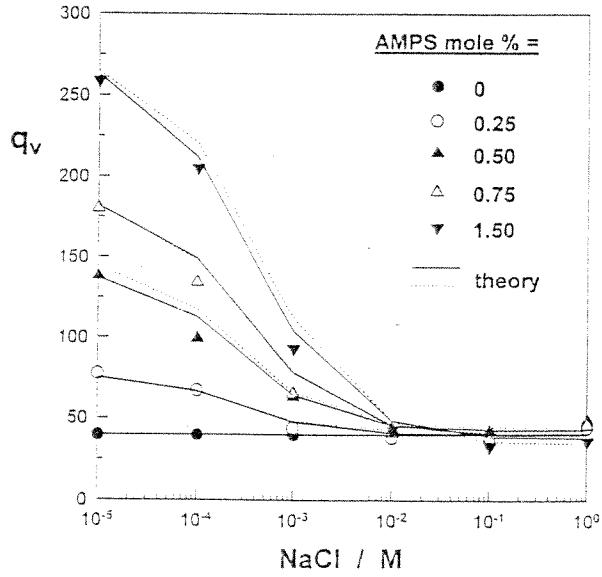

Figure 3 Variation of the volume swelling ratio q_v of hydrogels with the NaCl concentration in the external solution. Experimental data are shown as symbols. Curves were calculated using the swelling theory. Calculations were for fixed N (solid curves) and for $f = f_c$ (dotted curves).

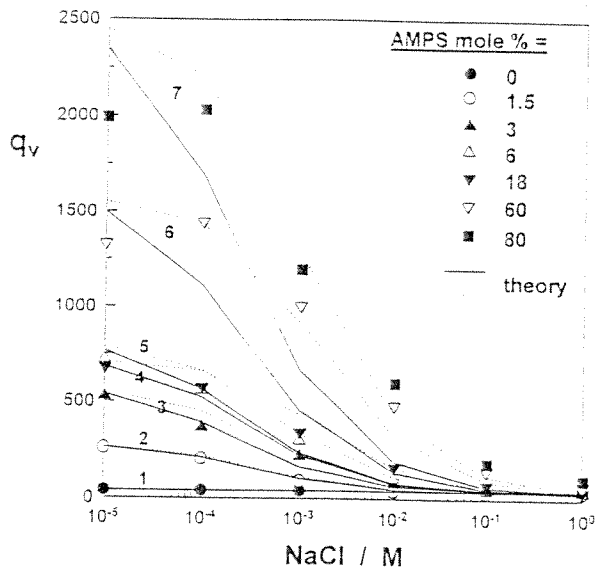

Figure 4 Variation of the volume swelling ratio q_v of hydrogels with the NaCl concentration in the external solution. Experimental data are shown as symbols. Curves were calculated using the swelling theory. Calculations were for fixed N (solid curves) and for $f = f_c$ (dotted curves). AMPS mole % = 0 (1), 1.5 (2), 3 (3), 6 (4), 18 (5), 60 (6), and 80 (7).

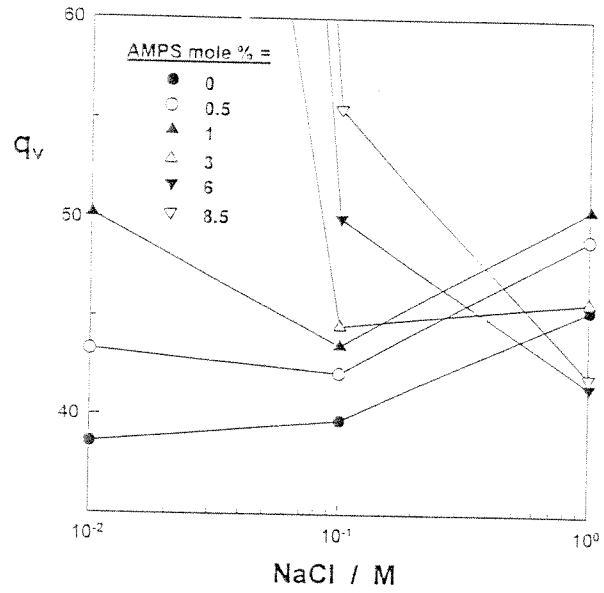

Figure 5 Variation of the volume swelling ratio q_v of hydrogels with the NaCl concentration in the external solution. Experimental data are shown as symbols. Curves only show the trend of data.

solution. Calculations were using the network parameters generated by the first approach and for hydrogels with 0–18 mol % AMPS content. Here, $K = 1$ means that the anion concentration inside the anionic gel is equal to that in the solution, whereas $K = 0$ means that the anionic gel excludes all the anions. Figure 6 indicates that a large amount of Cl^- ions penetrate into the gel if the salt concentration in the outer solution is high. Decreasing salt concentration in the solution decreases the K ratio, and it approaches 0 for NaCl concentrations $<10^{-5}M$. Thus, if the concentration of NaCl in the outer solution is sufficiently low, the Cl^- ion does not penetrate inside the hydrogel.

CONCLUSIONS

A series of hydrogels from AAm and AMPS monomers were prepared by free-radical crosslinking copolymerization using BAAm as the crosslinker. The swelling capacities of the hydrogels were measured in water and in aqueous salt solutions ranging in concentration from 10^{-5} to $1M$. The volume swelling ratio q_v of hydrogels in water increases sharply as the mole fraction f_c of AMPS increases from 0 to 0.06. At higher values of f_c from 0.06 up to 0.18, no change in the swelling capacities of hydrogels was observed. However, as

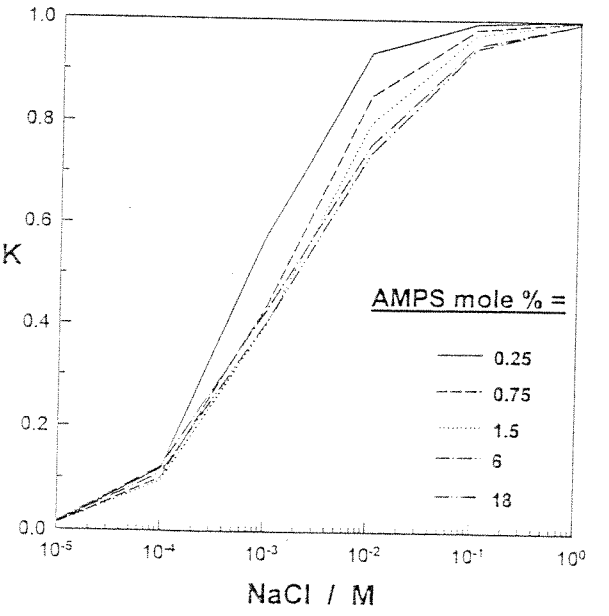

Figure 6 Variation of the calculated distribution coefficient K of Cl^- ions between the gel and solution phases as a function of the NaCl concentration. Calculations were for a fixed crosslink density N.

f_c further increases, q_c starts to increase again monotonically over the entire range of f_c. The results of swelling measurements of hydrogels in aqueous NaCl solutions were compared with the theory of swelling equilibrium. It was shown that the theory correctly predicts the swelling behavior of hydrogels up to 80 mol % charge densities. The method of estimation of the network parameters was found to be insignificant in the simulation of the experimental swelling data. The network parameters only correct the deficiency of the swelling theory.

REFERENCES

1. A. Katchalsky and I. Michaeli, *J. Polym. Sci.*, **15**, 69 (1955).
2. J. Hasa and M. Ilavsky, *J. Polym. Sci., Polym. Phys. Ed.*, **13**, 263 (1975).
3. T. Tanaka, *Phys. Rev. Lett.*, **40**, 820 (1978).
4. M. Ilavsky, K. Dusek, J. Vacik, and J. Kopecek, *J. Appl. Polym. Sci.*, **23**, 2073 (1979).
5. W. Oppermann, S. Rose, and G. Rehage, *Br. Polym. J.*, **17**, 175 (1985).
6. C. Konak and R. Bansil, *Polymer*, **30**, 677 (1989).
7. L. W. Fisher, A. R. Sochor, and J. S. Tan, *Macromolecules*, **10**, 949 (1977).
8. X. Liu, Z. Tong, and O. Hu, *Macromolecules*, **28**, 3813 (1995).
9. Z. Tong and X. Liu, *Macromolecules*, **27**, 844 (1994).
10. H. H. Hooper, J. P. Baker, H. W. Blanch, and J. M. Prausnitz, *Macromolecules*, **23**, 1096 (1990).
11. J. P. Baker, L. H. Hong, H. W. Blanch, and J. M. Prausnitz, *Macromolecules*, **27**, 1446 (1994).
12. J. P. Baker, H. W. Blanch, and J. M. Prausnitz, *Polymer*, **36**, 1061 (1995).
13. P. J. Flory and J. Rehner, Jr., *J. Chem. Phys.*, **11**, 521 (1943).
14. J. Frenkel, *Rubber Chem. Technol.*, **13**, 264 (1940).
15. P. J. Flory, *Principles of Polymer Chemistry*, Cornell University Press, Ithaca, NY, 1953.
16. P. J. Flory, *Proc. R. Soc. London, Ser. A*, **351**, 351 (1976).
17. P. J. Flory, *Macromolecules*, **12**, 119 (1979).
18. P. J. Flory and B. Erman, *Macromolecules*, **15**, 800 (1982).
19. B. Erman and P. J. Flory, *Macromolecules*, **15**, 806 (1982).
20. N. W. Tschoegl and C. Gurer, *Macromolecules*, **18**, 680 (1985).
21. S. F. Edwards and Th. Vilgis, *Polymer*, **27**, 483 (1986).
22. K. Iwata, *J. Chem. Phys.*, **76**, 6363, 6375 (1982).
23. Z. Tong and X. Liu, *Eur. Polym. J.*, **5**, 705 (1993).
24. O. Okay, N. K. Balimtas, and H. J. Naghash, *Polym. Bull.*, **39**, 233 (1997).
25. H. J. Naghash and O. Okay, *J. Appl. Polym. Sci.*, **60**, 971 (1996).

Polymer Bulletin 40, 491–498 (1998)

Polymer Bulletin

Effects of cyclization and electrostatic interactions on the termination rate of macroradicals in free-radical crosslinking copolymerization

Muzaffer Keskinel [1], Oğuz Okay [2,*]

[1] Kocaeli University, Department of Chemistry, TR-41300 Izmit, Kocaeli, Turkey
[2] TUBITAK Marmara Research Center, Department of Chemistry, P.O. Box 21, TR-41470 Gebze, Kocaeli, Turkey

Received: 15 December 1997/Accepted: 13 February 1998

Summary

Effects of cyclization and ionic group contents on the termination rate of macroradicals formed at zero monomer conversion were investigated. For this purpose, the pregel regime of free-radical methyl methacrylate / ethylene glycol dimethacrylate (MMA/EGDM) and acrylamide / N,N'-methylenebisacrylamide (AAm/BAAm) copolymerization systems was studied by means of the dilatometric technique. To eliminate the chain-length dependent variation of the termination rates, different sets of experiments were carried out each at a fixed monomer and initiator concentration. At low crosslinker contents, the termination rate of zero-conversion macroradicals was enhanced in crosslinking copolymerizations compared to linear polymerization. This is due to the cyclization reactions which reduce the size of the macroradical coils and thus, enhance the termination rates due to the lowering of the thermodynamic excluded volume effect. As the amount of the crosslinker increases, an enhancement in the initial rate of polymerization is observed in all series of experiments, indicating that steric effects on segmental diffusion dominate at high crosslinker contents. The results also indicate a slower rate of termination of ionic macroradicals compared to the non-ionic radicals of the same molecular weight and points the significance of the thermodynamic excluded volume effect on rising the ionic group content.

Introduction

Free-radical crosslinking copolymerization (henceforth referred as FCC) of vinyl/divinyl monomers is a commonly used procedure for preparing polymer gels. To predict the final properties of polymer gels, their structural characteristics are extremely important, and these in turn depend on the history of the gel formation process by FCC. Previous studies have shown that the mechanism of gel formation in FCC differs appreciably from the prediction of the gel formation theories (1). The difference between the actual and predicted behaviour of FCC has mainly been attributed to cyclization and to diffusion control, which are not properly accounted for in the gel formation theories.

Cyclization is a characteristic feature of FCC especially at zero conversion, at which it strongly influences the polymer structure. A cycle during FCC forms when a macroradical attacks a double bond pendant in the same kinetic chain. Cyclization is responsible for the formation of compact intramolecularly crosslinked structures, called microgels, in the pregel regime of FCC (2). On the other hand, termination reactions during the gel formation process by FCC are known to be diffusion controlled right down

* Corresponding author

to zero conversion. It is usual to distinguish two diffusion steps in the termination process (3): (1) translational diffusion of the center-of-mass of the macroradicals toward each other through the solvent, and (2) segmental diffusion of two segments bearing radical ends to a position in which they are able to react each other; this occurs by translational and rotational diffusion or by micro-Brownian motion of these segments. Most evidence points out that the second diffusion step, namely the segmental diffusion is rate controlling at low monomer conversions (4-6). The diffusion rate of segments is affected by both the size and the structure of macroradical coils, which we will define as thermodynamic and steric excluded volume effects, respectively. In larger coils, the segmental diffusion of the radical center out of the coil to encounter another radical becomes difficult; as a result, in larger coils a radical will be found more difficult by other radicals due to the thermodynamic excluded volume effect. On the other hand, in compact macroradicals, the mobility of segments is reduced so that the diffusion of radical centers toward each other is restricted due to the steric excluded volume effect (Figure 1).

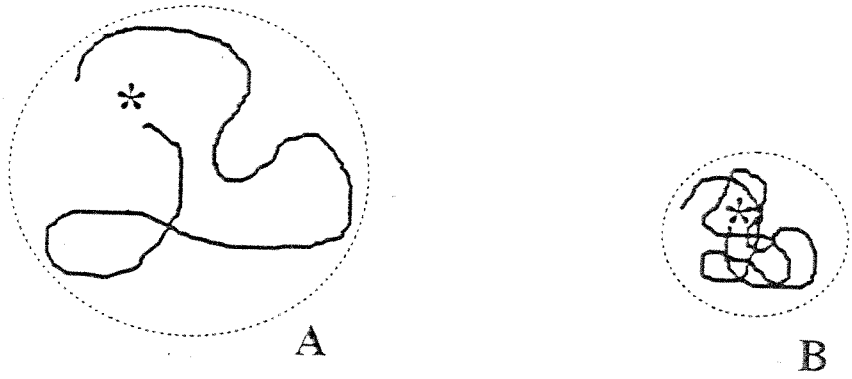

Fig. 1. Two macroradical coils having the same kinetic chain length with expanded (A) and shrinked (B) conformations. Thermodynamic and steric excluded volumes determine the process of the segmental diffusion in coils A and B, respectively.

In the present study, we intend to elucidate the relative contributions of thermodynamic and steric excluded volumes on the termination rate of macroradicals during FCC. For this purpose, we investigated the termination rate of polymer radicals formed at zero monomer conversion, at which the second order reactions such as the crosslinking and multiple crosslinking reactions do not occur. To eliminate chain-length dependent variation of the termination rates, different sets of experiments were carried out each at a fixed monomer and initiator concentration. Macroradicals of the same kinetic chain length but of different sizes and structure were obtained by including into the reaction mixture a crosslinker or an ionic comonomer, both in small quantities. Addition of a crosslinker in the feed leads, at zero monomer conversion, to the formation of cycles, which reduces the size of the macroradicals formed. Addition of an ionic comonomer in the feed causes formation of ionic macroradicals, that exhibit, compared to the nonionic macroradicals, an expanded conformation in solution due to the electrostatic interactions. Two commonly used comonomer systems for the gel synthesis were selected for this purpose, namely methyl methacrylate / ethylene glycol dimethacrylate (MMA/EGDM) and acrylamide / N,N'-methylenebisacrylamide (AAm/BAAm) systems. The pregel regime of FCC reactions was studied by means of the dilatometric technique. Polymerization solvents, toluene and water for MMA/EGDM and AAm/BAAm systems respectively,

were used at a high concentration to ensure that strong cyclization occurs during the reaction (2).

Experimental

Materials

Commercially available MMA, EGDM, AAm, acrylic acid (AAc), 2-acrylamido-2-methylpropanesulfonic acid (AMPS) and BAAm monomers and the initiators 2,2' azobisisobutyronitrile (AIBN) and potassium peroxodisulfate ($K_2S_2O_8$) were purified by usual methods. The ionic comonomers sodium acrylate (NaAc) and AMPS sodium salt (NaAMPS) were prepared *in situ* by adding equimolar amounts of sodium hydroxide and AAc or AMPS in the polymerization mixture, respectively. The polymerization solvents toluene (Merck p.a.) and water were twice distilled before use. Sodium hydrogen carbonate ($NaHCO_3$) and sodium thiosulfate ($Na_2S_2O_3$) (both analytical grades) were used without further purification.

Polymerization procedure

MMA - EGDM copolymerizations were carried out at a monomer concentration of 2.3 M (24.4 v/v %) in toluene at 60±0.1°C with AIBN as the initiator. AAm - BAAm copolymerizations were carried out at a monomer concentration of 0.5 M (35g/L) in water at 40 $\pm 0.1^{\circ}C$ with $K_2S_2O_8$ / NaS_2O_3 redox initiator system in the presence of $NaHCO_3$ buffer. Concentrations used were $1x10^{-3}$ M for $K_2S_2O_8$, NaS_2O_3, and $NaHCO_3$. NaAc and NaAMPS were used as the ionizable comonomer of AAm. The conversion of monomers up to the onset of macrogelation was followed by dilatometry. The dilatometers consisted of a blown glass bulb, approximately 25 ml in volume connected to a 30 cm length of 1.5 mm precision-bore capillary tubing with a ground-glass joint. The meniscus was read with a millimetric paper to 0.2 mm. The polymerization technique used was described in detail elsewhere (7). The reproducibility of the kinetic data was checked by repeating the experiments. The deviation in the initial slopes of time versus conversion data between two runs was always less than 3%.

Different series of experiments were carried out. In the first series of experiments, monomer ($[M]_0$) and initiator ($[I]_0$) concentrations were held constant while the mole fraction of the crosslinker in the monomer mixture (f_{2o}) was varied from 0 to $0.12x10^{-2}$. In the second series of experiments, monomer (AAm), crosslinker (BAAm), and initiator concentrations were held constant while the mole fraction of the ionic comonomer NaAc or NaAMPS was varied from 0 to 0.08. Typical monomer conversion x versus time t plots for various crosslinker (f_{2o}) and NaAc contents are shown in Figures 2A and 2B, respectively. The initial polymerization rates, $(dx/dt)_0$, were estimated from the lines drawn through the data points for $x < 0.10$ by using a least-squares fit.

Results and discussion

Figure 3A shows the variation of the initial rate of polymerization $(dx/dt)_0$ in MMA/EGDM and AAm/BAAm systems with the crosslinker concentration (f_{2o}). In each series of experiments shown in the figure, the total monomer and the initiator concentrations were held constant, so that the chain length of macroradicals was fixed. At low crosslinker contents, the initial rates are slow compared with the linear polymerization. As the amount of crosslinker increases, an enhancement in the initial rate of polymerization is observed in all series of experiments. The enhancement of the rate of polymerization with increasing f_{2o} has also been observed previously for moderate to high

crosslinker concentrations (1,8-12). However, reduced polymerization rate at low crosslinker contents was recently observed by us and the present results shown in Figure 3A confirm this phenomenon (7). Figure 3B shows the initial rates in AAm/BAAm copolymerization plotted as a function of the concentration of the ionic comonomer NaAc and NaAMPS. It is seen that the initial rate strongly depends on the amount of the ionic comonomer and it increases on rising NaAc or NaAMPS concentration in the feed.

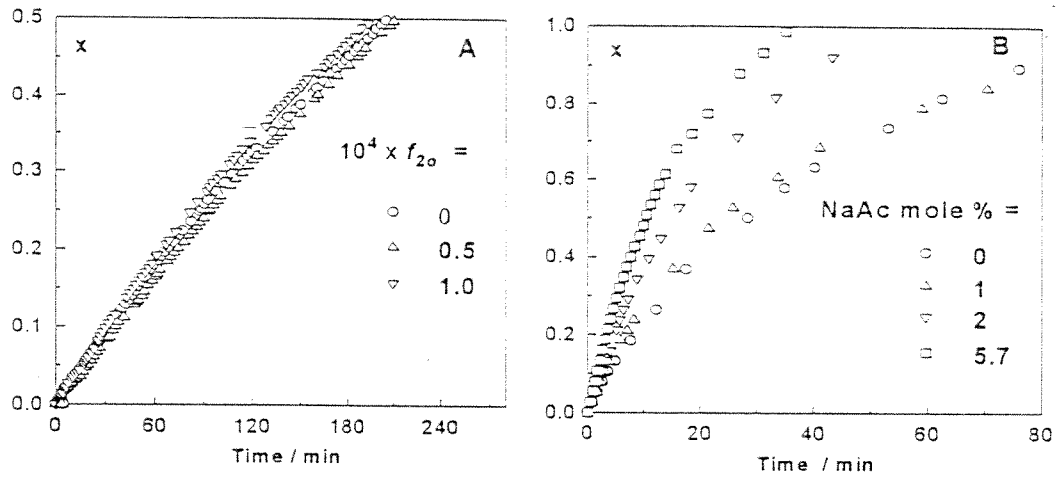

Fig. 2. Variation of the conversion x versus time histories in FCC with the crosslinker (A) and the ionic comonomer concentration (B). **(A)** MMA/EGDM system. $[I]_0 = 0.02$ M. **(B)** AAm/BAAm system. $f_{2o} = 5 \times 10^{-4}$.

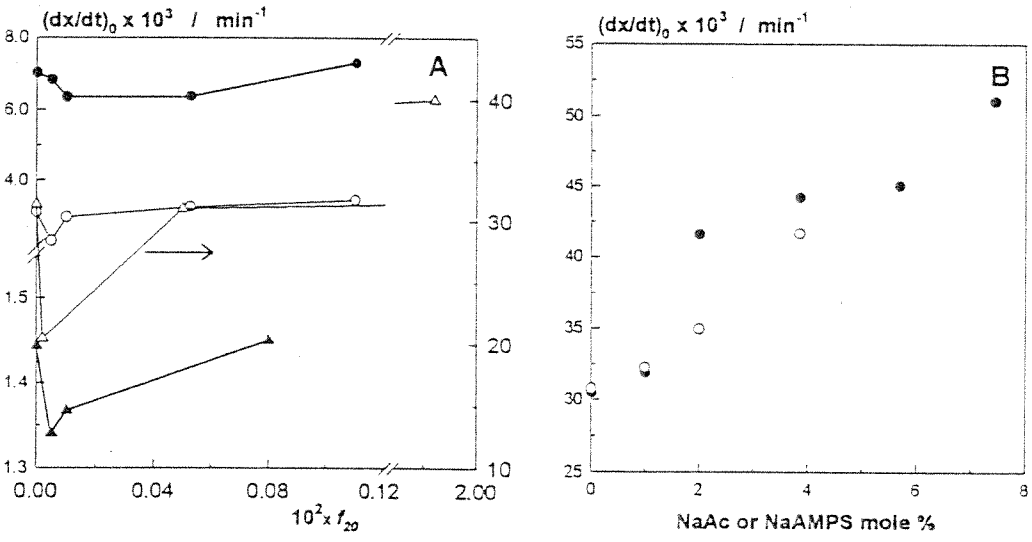

Fig. 3. Variation of the initial rate of polymerization $(dx/dt)_0$ with the crosslinker (f_{2o}) and ionic comonomer (NaAc or NaAMPS) concentration. (A) MMA/EGDM system: $[I]_0$ = 0.1 (●), 0.02 (○), and 3.75×10^{-3} M (▲). AAm/BAAm system: (Δ). (B) AAm/BAAm system: $f_{2o} = 5 \times 10^{-4}$, Ionic comonomer = NaAc (●), NaAMPS (○).

Invoking steady-state approximation for radicals R^*, the expression for the rate of polymerization in FCC is given by (12):

$$dx/dt = k_p[R^*](1-x) \tag{1}$$

$$[R^*] = \left(2f\ k_d[I]/k_t\right)^{0.5} \tag{1a}$$

where k_p and k_t are the instantaneous rate constants for propagation and termination, respectively, f is the initiator efficiency, and k_d is the decomposition rate constant of the initiator I. The instantaneous propagation rate constant k_p relates to the propagation rate constant for the homopolymerization of monovinyl monomer k_{p1} through the equation (12):

$$k_p = k_{p1}\left[1+\left(2r_{21}-1\right)f_2\right] \tag{1b}$$

where f_2 is the mole fraction of the divinyl monomer (crosslinker) in the reaction mixture, and r_{21} is the reactivity ratio of vinyls on divinyl to monovinyl monomer. The expression for the initial rate of polymerization follows from eq (1) as:

$$\left(dx/dt\right)_0 = k_{p0}[R^*]_0 \tag{2}$$

$$[R^*]_0 = \left(2f\ k_d[I]_0/k_{t0}\right)^{0.5} \tag{2a}$$

where the subscript o holds for the initial values. Previous experimental studies showed that the vinyl group reactivities in MMA/EGDM and in AAm/BAAm copolymerization systems are almost equal, i.e., $r_{21} \cong 1$ (13-15). Furthermore, since $f_{20} << 1$ in the present study, it is reasonable to assume a constant k_{p0} in each series of experiments (constant initial concentrations of the total monomer and the initiator). Thus, the relative initial termination rate constant, $k_{t0,rel}$, which is the ratio of k_{t0} of crosslinking polymerization to that of the linear polymerization at the same reaction condition, can be calculated from eq (2) as:

$$k_{t0,rel} = \frac{k_{t0}}{k_{t0,l}} = \left(\frac{\left(dx/dt\right)_{0,l}}{\left(dx/dt\right)_0}\right)^2 \tag{3}$$

where the subscript l denotes the linear polymerization. In Figures 4A, $k_{t0,rel}$ values calculated using eq (3) are shown as a function of the crosslinker concentration. $k_{t0,rel}$ is greater than unity at low crosslinker contents, i.e., the termination rate constant of zero conversion macroradicals k_{t0} was enhanced in crosslinking copolymerizations compared to linear polymerization. Since we are dealing with zero conversion polymer radicals, i.e., with the polymer radicals in the absence of preformed polymers, the basic difference between linear and crosslinking copolymerization is the incorporation of cycles in the growing polymer. Cyclization reactions reduce the size of the macroradical coils; this is reflected in Figure 4A with the enhancement of the termination rates due to the lowering of the thermodynamic excluded volume effect. It must be noted that the delayed onset of gelation in good solvents as observed by Matsumoto et al. in several FCC systems is also a

result of this thermodynamic excluded volume effect (16); the reactivity of pendant vinyl groups for intermolecular reactions is much lower in good solvents than in poor solvents due to the excluded volume of the molecule. The present results suggest the significance of the thermodynamic excluded volume effect at very low crosslinker contents (f_{20} < $1x10^{-4}$). As the crosslinker concentration (f_{20}) further increases, $k_{t0,rel}$ decreases monotonically, indicating that steric effects on segmental diffusion dominate at high crosslinker contents. As f_{20} increases, the local concentration of pendant vinyls within a coil should increase. Thus, the growing radicals would tend to form more cycles and exhibit more compact structure. According to the experimental data, the reduction in the termination rate of radicals due to the steric effects compensates more than the rate enhancement due to the decrease of the coil size.

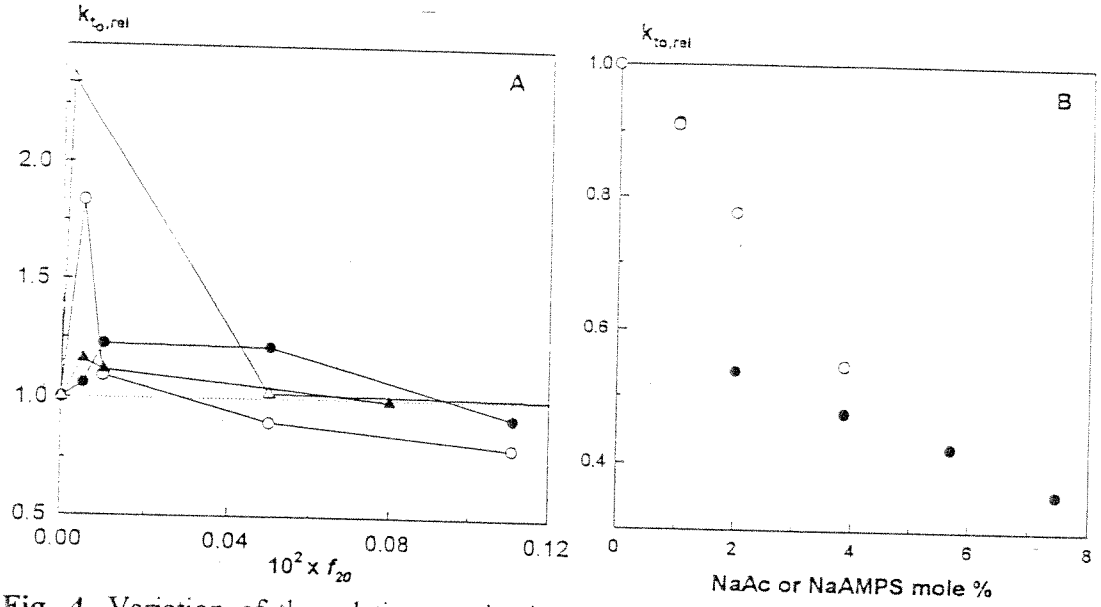

Fig. 4. Variation of the relative termination rate constant of zero conversion polymer radicals, $k_{t0,rel}$, with the crosslinker (f_{20}) and ionic comonomer (NaAc or NaAMPS) concentration. **(A)** MMA/EGDM system: $[I]_0$ = 0.1 (●), 0.02 (○), and $3.75x10^{-3}$ M (▲). AAm/BAAm system: (Δ). **(B)** AAm/BAAm system: $f_{20} = 5x10^{-4}$, Ionic comonomer = NaAc (●), NaAMPS (○).

Another feature shown in Figure 4A is a much more steeper increase of $k_{t0,rel}$ in AAm/BAAm system compared to the MMA/EGDM system. This is probably due to the higher extent of cyclization in AAm/BAAm copolymerization (80 % compared to 30 % in MMA/EGDM system (7,9,17)), which leads to a greater decrease in the coil size at the same crosslinker concentration. Experimental data obtained at various initiator concentrations give no evidence on the chain-length dependent variation of the thermodynamic excluded volume effect.

For ionic FCC at low ionic comonomer contents, one may define $k_{t0,rel}$ as the ratio of k_{t0} of ionic FCC to that of the non-ionic FCC at the same reaction condition. In Figure 4B, $k_{t0,rel}$ values calculated for AAm/BAAm copolymerization are shown as a function of the concentration of NaAc and NaAMPS. $k_{t0,rel}$ decreases continuously on rising the ionic comonomer concentration. This indicates a slower rate of termination of ionic macroradicals compared to the non-ionic radicals of the same molecular weight and points the significance of the thermodynamic excluded volume effect on rising the ionic group content.

The results presented so far demonstrate separate contributions of thermodynamic and steric excluded volumes of zero-conversion macroradicals on their rate of termination. However, at non-zero monomer conversions, the rate of termination reactions in FCC is mainly determined by the steric effects. Figure 5A shows monomer conversion x versus time plots for the homopolymerizations of MMA (open symbols) and EGDM (filled symbols) at two different initial monomer concentrations. It is seen that EGDM polymerizes much more rapidly than MMA and, the difference between their rates of polymerization increases as the initial monomer concentration decreases. Using the experimental data shown in Figure 5A and using eqs (1) - (2), we calculated the normalized termination rate constants k_t / k_{t0}, and they are shown in Figure 5B as a function of the monomer conversion. A steeper decrease in k_t observed at $x < 0.05$ in EGDM polymerization compared to the MMA polymerization points the significance of the steric effect on the segmental diffusion. In EGDM polymerization, we always observed the appearance of a turbidity in the reaction mixture after a short reaction time. This indicates spatial inhomogeneities in the reaction solution due to the formation of microgels. The crosslink density of microgels is known to increase on rising the degree of dilution (18); this is reflected in Figure 5B with the extent of the diffusion control which is more pronounced at lower monomer concentration.

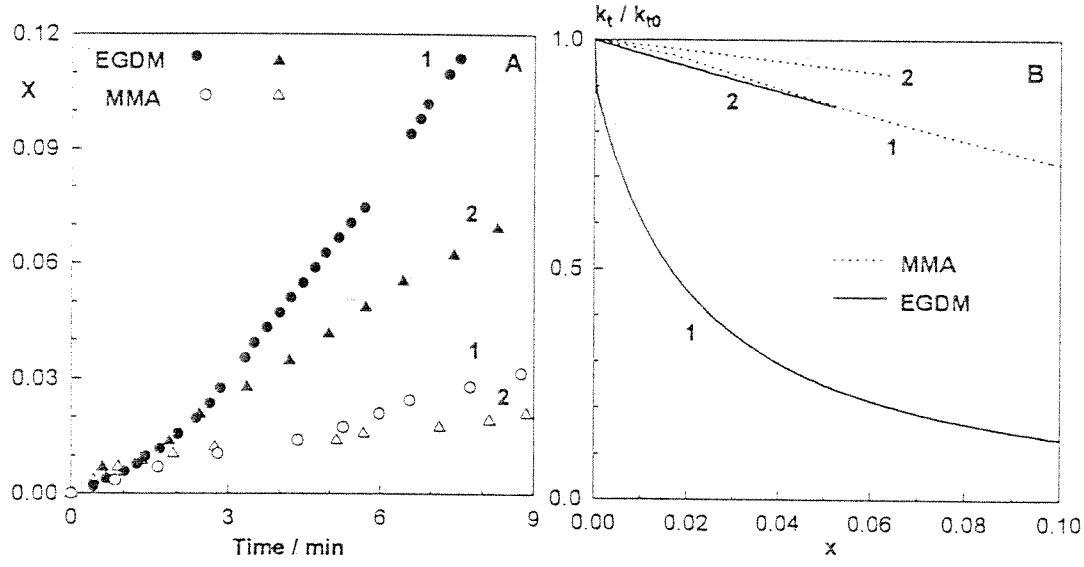

Fig. 5. Variation of the monomer conversion x versus time and k_t / k_{t0} versus conversion x in MMA and EGDM homopolymerizations. $[M]_0 = 0.53$ (1) and 1.06 M (2). $[I]_0 = 0.02$ M

In summary, the present work introduces a technique that enables to vary the size of macroradical coils while their kinetic chain length remains unchanged. The results presented demonstrate separate contributions of thermodynamic and steric excluded volumes on the termination rate of macroradicals formed at zero monomer conversion. At non-zero monomer conversions, only steric effects determine the termination rates.

Acknowledgment

This work was supported by the Scientific and Technical Research Council of Turkey (TUBITAK) under Grand Number TBAG - 1561.

References

1. Dusek K (1982) In *Developments in Polymerization - 3;* (ed RN Haward), Applied Science, London, p 143
2. Funke W, Joos-Muller B, Okay O, Adv Polym Sci (in press)
3. Benson SW, North AM (1962) J Am Chem Soc 84: 935
4. Mita I, Horie K (1987) J Macromol Sci C 27: 91
5. Mahabadi HF, O'Driscoll KF (1977) J Polym Sci Polym Chem Ed 15: 283
6. O'Driscoll KF (1981) Pure & Appl Chem 53: 617
7. Okay O, Naghash H, Capek I (1995) Polymer 36: 2413
8. Horie K, Otagawa A, Muraoka M, Mita I (1975) J Polym Sci Polym Chem Edn 13: 445
9. Tobita H, Hamielec AE (1990) Polymer 31: 1546
10. Dotson NA, Diekman T, Macosko CW, Tirrel M (1992) Macromolecules 25: 4490
11. Shah AC, Parsons IW, Haward RN (1980) Polymer 21: 825
12. Naghash HJ, Okay O, Yagci Y (1997) Polymer 38: 1187
13. Li WH, Hamielec AE, Crowe CM (1989) Polymer 30: 1513
14. Mao R, Liu Y, Huglin MB, Holmes PA (1995) Macromolecules 28: 6739
15. Nieto JL, Baselga J, Hernandez-Fuentes I, Llorente MA, Pierola IF (1987) Eur Polym J 23: 551
16. Matsumoto A (1995) Adv Polym Sci 123: 41
17. Naghash HJ, Okay O (1996) J Appl Polym Sci 60: 971
18. Okay O, Kurz M, Lutz K, Funke W (1995) Macromolecules 28: 2728

Polymer Bulletin 41, 363–370 (1998)

Polymer Bulletin

Heterogeneities in polyacrylamide gels immersed in acetone-water mixtures

Oğuz Okay[1,2], Ufuk Akkan[3]

[1] Department of Chemistry, Istanbul Technical University, TR-80626 Maslak, Istanbul, Turkey
[2] TUBITAK Marmara Research Center, P.O. Box 21, TR-41470 Gebze, Kocaeli, Turkey
[3] Department of Chemistry, Kocaeli University, TR-41300 Izmit, Kocaeli, Turkey

Received: 14 April 1998/Revised version: 17 June 1998/Accepted: 17 June 1998

Summary

Immersion of polyacrylamide gels in acetone-water mixtures with a high content of acetone leads to the formation of heterogeneous structures. The extent of heterogeneity increases as the initial swelling degree of the gel increases, or, as the polarity of the nonsolvent decreases. The nature of the deswelling curves indicates that the polymer-rich regions of the gel formed by the collapse transition block the solvent diffusion outside the gel. This prevents the equilibration of the gel volume with surroundings.

Introduction

Hydrophilic gels called hydrogels have received considerable attention for use as specific sorbents and as support carriers in biomedical engineering. In recent years, attention has turned to the swelling and collapse phenomena that are observed when a hydrogel network is brought into contact with a solvent. The possibility of a first-order phase transitions in polymer gels has been predicted theoretically (1) and proved experimentally on hydrolyzed polyacrylamide (PAAm) gels immersed in acetone - water mixtures (2).

Theoretical analysis of the experimental swelling data of polymer gels assumes that the gel immersed in a liquid attains its thermodynamic equilibrium state with the surrounding solution after a finite time, i.e., usually after a few weeks. Thereafter, since the chemical potentials of all diffusable components in and outside the gel sample are equal, theories predict the equilibrium volume of the gel phase as a function of the solvent composition. However, due to the prolonged relaxation time of the network chains compared to that of linear chains, nonequilibrium states may appear in polymer gels. These nonequilibrium states may be fixed if additional crosslinks are introduced into the gel (3) or, if these states become kinetically frozen (4). Ilavky (5) showed that, if PAAm gels are immersed in mixtures with a high content of acetone, the gel samples remain heterogeneous even after 2 months of observation. No further details or experimental data were given by this author. Philippova et al. (6) also observed the appearance of heterogeneities in swollen ionic gels immersed in poor solvents. They showed that water swollen gels immersed in water-ethanol mixtures with ethanol contents higher than 70 % exhibit kinetically frozen nonequilibrium structures. Formation of non-equilibrium structures was also observed by Siegel et al. in pH-sensitive gels (7). Recently, we have shown formation of heterogeneous structures in PAAm gels immersed in aqueous solutions of poly(ethylene glycol) (8).

The present work aims to describe the conditions for the formation of nonequilibrium structures in PAAm gels. For this purpose, a series of PAAm gels with different ionic

group contents were prepared by solution polymerization technique. The gels were then subjected to swelling/deswelling experiments, starting from three different initial states: a) the dry state, b) the state after preparation, and c) the equilibrium swollen state in pure water. The solvents used for the experiments were acetone-water mixtures of various compositions, methanol, ethanol, and n-butanol. Assuming that a gel sample attains its equilibrium state in a given solvent, the final mass of the gel should be independent on its initial state. Deviations from this condition will give information about the extent of heterogeneities in PAAm gels. Here, we report the effects of the number of ionic groups and of crosslinks in the gel as well as the polarity of the nonsolvent on the degree of the heterogeneities in PAAm gels.

Experimental

PAAm gels

PAAm gels were prepared by free-radical crosslinking copolymerization of acrylamide with a small amount of N,N'-methylenebis(acrylamide) (BAAm) in aqueous solution. Sodium acrylate (NaAc) was used as the ionizable comonomer and prepared *in situ* by adding equimolar amounts of sodium hydroxide (NaOH) and acrylic acid (Ac) in the polymerization mixture. Ammonium persulfate (APS) and N,N,N',N'-tetramethyl-ethylenediamine (TEMED) were respectively the initiator and the accelerator. The reactions were carried out at room temperature (21±2°C). The gels were prepared according to the following scheme: 5 g acrylamide, 133 mg BAAm, 40 mg APS and varying amounts of NaOH and Ac were dissolved in double distilled water to give a total volume of 100 mL. After addition of 0.24 mL of TEMED, the solution was transferred to small tubes of 5.8 mm in diameter. The gelation took place within 5 min. After 3 hours, the gels were cut into specimens of approximately 10 mm in length and divided into two parts. The first part of the gel samples, which we shall call thereafter "gels after synthesis", was subjected to swelling experiments without further treatment. The second part of the gel samples was immersed in a large excess of distilled water to remove the unreacted species. It was found that the sol fraction in the gels is less than 0.1 % after extraction with water. Then, a part of the equilibrium swollen gels in water, called "preswollen gels", were used for swelling experiments. Another part of the preswollen gels was successively washed with acetone-water mixtures containing increasing amounts of acetone and, finally with pure acetone. Using this solvent exchange procedure, the good solvent water in the preswollen gels was gradually replaced by the nonsolvent acetone; thus, the gel was transferred from rubbery to the glassy state without the appearance of heterogeneities. The gels were then dried in vacuum at room temperature. Thereafter the gel specimens, called "dry gels" were used for the swelling experiments. Swelling experiments were also carried out using gel samples dried in vacuum at room temperature after their preparation. The swelling behavior of these samples was found to be the same as that of the dry gels.

Swelling measurements

For the swelling measurements, PAAm gel samples of different initial states (preswollen gels, dry gels, and gels after synthesis) were immersed in vials (100 mL) filled with acetone-water mixtures. The volume of solution in the vial was much larger than the gel volume so that the concentration of the acetone-water mixture was practically unchanged. For the swelling experiments in nonsolvents (acetone, methanol, ethanol and n-butanol), the nonsolvent was refreshed every other day over a period of one week to keep the concentration constant. The swelling experiments were carried out at 21±2°C.

In order to reach the apparent equilibrium degree of swelling, the gels were immersed in solutions at least for one week. The relative mass of the gel after swelling is expressed in terms of the swelling ratio related to the network formation state, q_w, which is defined as $q_w = m / m_0$, where m and m_0 are the masses of the gel after swelling and after preparation, respectively. Each swelling ratio reported in this paper is an average of at least two separate measurements; standard deviations of the measured swelling ratios were less than 10 and 5% of the mean for swollen and collapsed gels respectively.

Results and Discussion

In Figure 1, the relative masses of PAAm gels, q_w, of different initial states are shown as a function of the acetone concentration in the outer acetone-water mixtures. The concentrations of the ionic comonomer NaAc in the monomer mixture were 0, 4.6, and 28 mol % in A, B, and C, respectively. The filled and empty circles belong to dry and preswollen gels respectively, whereas the filled triangles to the gels after synthesis. As expected (9,10), the PAAm gel without any ionizable groups exhibits a continuous change in the relative mass over the entire range of acetone concentration, whereas ionic PAAm gels undergo a discontinuous phase transition at a critical acetone concentration. For acetone concentrations at or below the critical acetone content for phase transition, all gel samples exhibit similar behavior within the limits of experimental error; all are in a swollen state below the critical acetone concentration, whereas a sudden change in the relative mass of the gel was observed at the critical acetone content. These results indicate that all the gel samples are at equilibrium in this range of acetone concentrations. The discrepancy in the relative masses of the gels appears after passing the phase transition point. The "dry" gels slightly decrease their relative masses as the acetone content of the solvent mixture further increases, whereas the preswollen gels cannot deswell up to the equilibrium state. The swelling degree of PAAm gels immersed in acetone-water mixtures after their preparation lies between the two sets of experiments. Comparison of the ionic gel masses in acetone indicates that the amount of solvent in the preswollen gels is about tenfold larger than in the gels after synthesis or after drying.

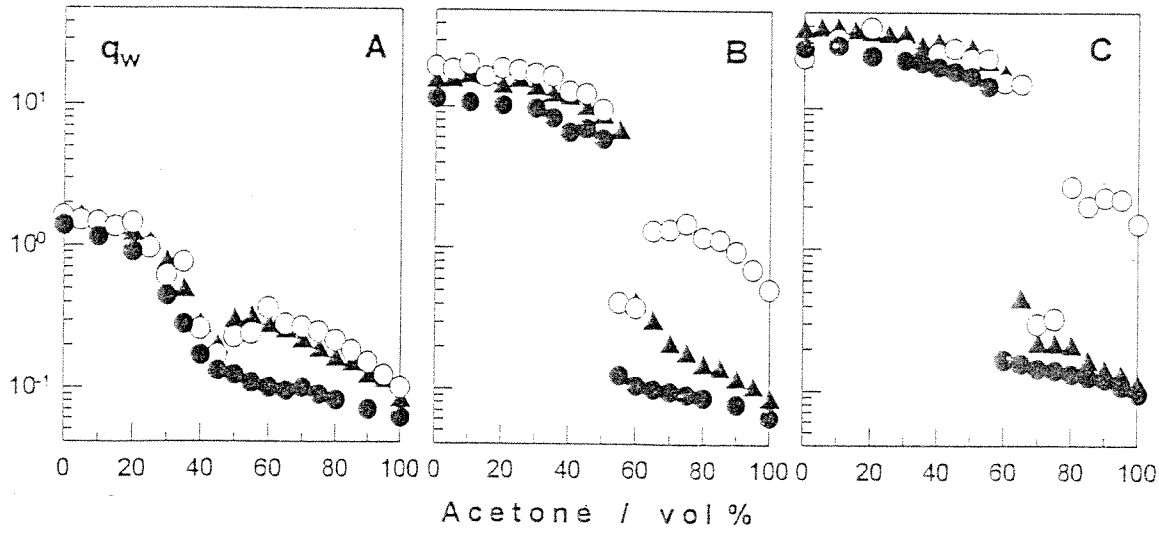

Fig. 1. The relative masses, q_w, of PAAm gels of different initial states shown as a function of the acetone concentration in the acetone-water mixtures. BAAm = 1 mol %, NaAc = 0 (A), 4.6 (B), and 28 mol % (C). Initial states of the gel = dry (●), preswollen (○), after synthesis (▲).

Even after 7 months of immersion times in acetone, no change in the relative mass of the preswollen gels was observed, indicating that they are at an "apparent equilibrium state" in acetone. Thus, the originally swollen gel fails to deswell to the same mass as is observed when deswelling is from the dry or after synthesis states. Assuming that the volume of the gel in acetone does not change on removing the extra solvent, for instance, by freeze-drying, this process would lead to a porous hydrogel in which the porous structure was created during the posttreatment of the gel samples.

According to the above results, heterogeneity in PAAm gels starts to appear after the phase transition point is crossed. Visual observations showed that heterogeneous gel samples exhibit both swollen (rubbery) and unswollen (glassy) regions; thus, both swollen and collapsed states coexist in a single sample beyond the critical point. A series of gels containing varying amounts of the ionic comonomer NaAc between 0 and 28 mol % were prepared and then subjected to swelling experiments starting from different initial states. All gel samples exhibited similar behavior in acetone-water mixtures, as illustrated in Figure 1. In Figure 2, the relative masses of the gels, q_w , in water as well as in acetone are shown as a function of their NaAc contents. As expected, q_w of PAAm gels in water increases as the ionic group content increases because of the additional swelling due to the osmotic pressure of counterions. At NaAc contents as high as 17%, q_w in water becomes rather insensitive to the ionic group content of the gel as a result of the counterion condensation (11) or due to the finite extensibility of the network chain. In acetone, the relative mass of dry gels or gels after synthesis remains constant over the entire range of NaAc concentration; this is due to the low polarity of acetone compared to water which facilitates formation of ion pairs on the network chains and prevents the extra swelling of ionic gels. However, the relative mass of preswollen gels in acetone increases with increasing NaAc content of the gel up to about 17 mol % and then remains constant.

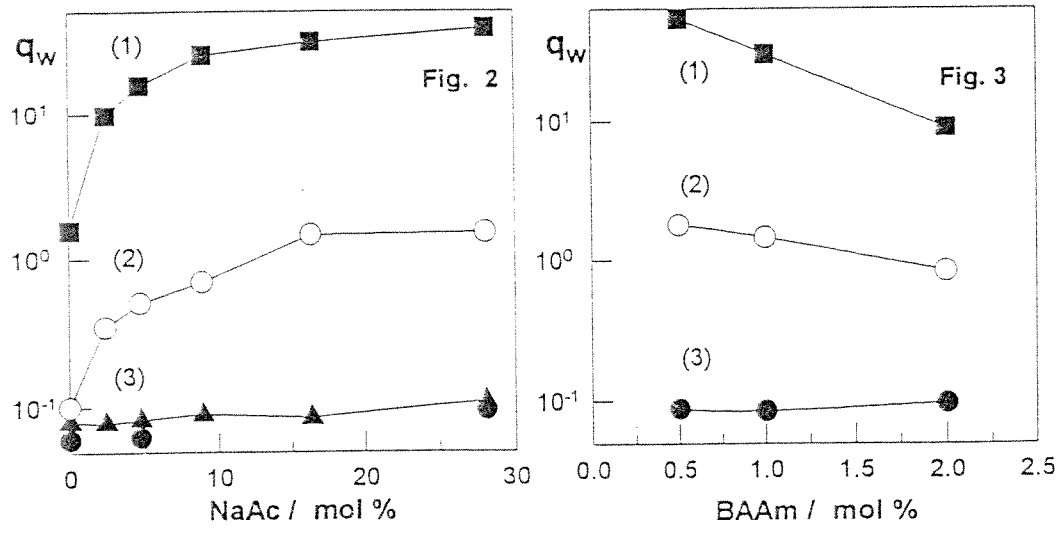

Fig. 2. The relative masses of PAAm gels, q_w , shown as a function of their NaAc contents. The curve (1) concerns the gels in water while the other two curves (2, 3) demonstrate the behavior of the gels in acetone. Initial states of the gel: dry (●), preswollen (○), after synthesis (▲). BAAm = 1 mol %.

Fig. 3. The relative masses of PAAm gels, q_w , shown as a function of their BAAm content. NaAc = 16.5 mol %. See legend to Figure 2 for the explanations.

The heterogeneity in the gel may be characterized by the difference between the relative masses of the preswollen and dry gels. According to Figure 2, this difference increases with increasing ionic group content of the gel. This means that increasing swelling ratio in water also increases the extent of heterogeneities in preswollen PAAm gels immersed in acetone. In Figure 2, increase in the water absorption capacity of the gels was achieved by replacing some of the acrylamide units in the network chains with the ionic comonomer NaAc. Similar results were also obtained by decreasing the crosslink density of PAAm gels. In Figure 3, the relative masses of the gel in water and in acetone are shown as a function of the amount of the crosslinker BAAm used in the gel synthesis. Decrease in BAAm content increases the swelling capacity of PAAm gels in water and thus, increases the extent of heterogeneities in PAAm gels immersed in acetone.

In Figure 4, variation of the relative mass of ionic PAAm gel with 28 mol % NaAc content is shown as a function of the contact time with pure acetone. The empty symbols belong to the preswollen gels, whereas the filled symbols are for gel samples used after synthesis. In all ionic gel samples immersed in acetone after their preparation, a two stage deswelling process was observed; a fast initial period which corresponds to release of water from the excess volume of the rubbery polymer, followed by a slow second stage of deswelling. The gels reach their final swelling state within a couple of days. In preswollen gels, however, the second stage of deswelling was not observed. One may expect that, in the initial period of deswelling, the diffusion of solvent controls the deswelling process and about half of the water content of the gel is released within this period. As deswelling commences and the gel loses water, the glass transition temperature of the polymer/solvent mixture approaches to the temperature of the experiment and the polymer requires a finite time to relax to its final contracted state. Thus, the relaxation time of polymer in response to changes in solvent composition inside the gel becomes rate limiting in the second stage of deswelling.

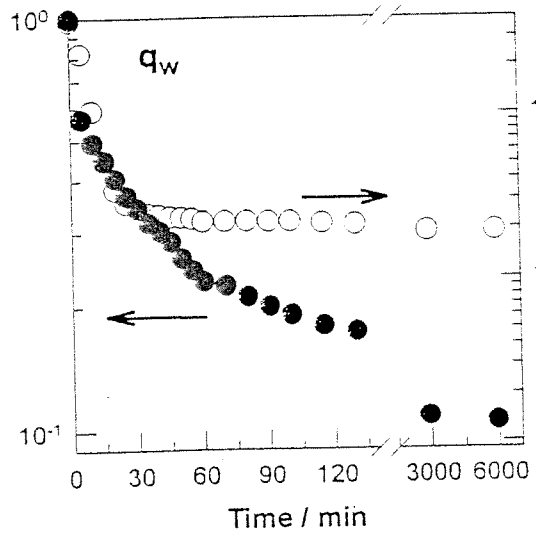

Fig. 4. Variation of q_w of ionic PAAm gel with 28 mol % NaAc shown as a function of the contact time with pure acetone. Initial states of the gel: preswollen (○),after synthesis (●).

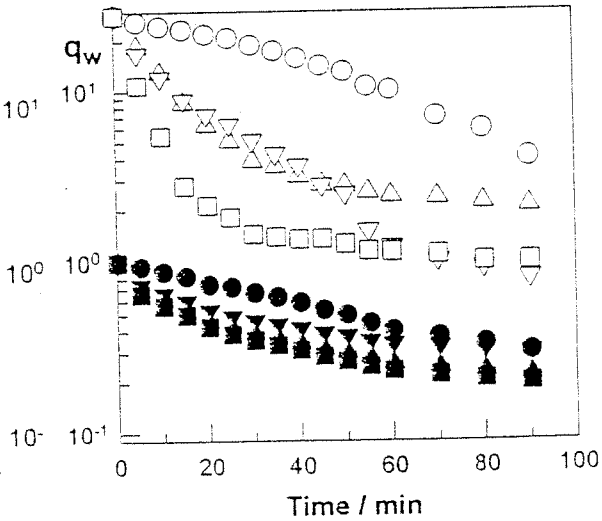

Fig. 5. Variation of q_w of ionic PAAm gel with 16.5 mol % NaAc shown as a function of the contact time with a series of nonsolvents. The empty and filled symbols belong to preswollen gels and gels after synthesis, respectively. Nonsolvents: n-butanol (○), ethanol (△), methanol (▽), acetone (□).

According to the experimental results, since the second stage of deswelling was not observed in gels from the swollen state, the glassy regions formed by the collapse transition seems to block the equilibration of the gel volume with surroundings. Thus, the discrepancy in the final relative masses of the gels can be accounted for different relaxation times of the network chains in both gels. Deswelling process from the dry or after synthesis states proceeds by slow relaxation of the whole network chains and further deswelling of the macroscopic sample so that an equilibrium state can be approached. However, in deswelling process from the swollen state, the swollen gel sample on contact with the poor solvent first segregates into a solvent-rich and a polymer-rich phase; if the polymer-rich regions of the sample are in the glassy state, they can block solvent diffusion and so, further deswelling of the whole sample. Thus, microdomains in a glassy state will appear which are embedded in polymer-poor regions in rubbery state so that an equilibrium cannot be reached and the heterogeneous structure is stabilized.

In Figure 5, variation of the relative mass of ionic PAAm gels with 16.5 mol % NaAc content is shown as a function of the contact time with a series of nonsolvents. The empty and filled symbols belong to preswollen gels and gels after synthesis respectively. The form of the deswelling curves strongly depends on the nature of the nonsolvent used. The rate of deswelling increases in the order n-butanol < methanol and ethanol < acetone. In order to understand the type of deswelling curves it is useful to consider the extent of interactions between the nonsolvents and the PAAm segments. According to the Hildebrand theory (12), the solvating (swelling) power of a polymer-solvent medium can be estimated from $(\delta_1 - \delta_2)^2$, where δ_1 and δ_2 are the solubility parameters for the solvent and the polymer, respectively. The solubility of a polymer in a solvent is favored when $(\delta_1 - \delta_2)^2$ is minimized, i.e., when the solubility parameters of the two components are most closely matched. A more detailed solubility parameter approach proposed by Hansen (13) separates the solubility parameter into components due to dispersion (nonpolar) forces (δ_d), polar forces (δ_p), and hydrogen-bonding interactions (δ_h). Materials having similar (Hansen) solubility parameters have high affinity for each other. Thus, the values $\Delta\delta_d^2 = (\delta_{d,1} - \delta_{d,2})^2$, $\Delta\delta_p^2 = (\delta_{p,1} - \delta_{p,2})^2$, and $\Delta\delta_h^2 = (\delta_{h,1} - \delta_{h,2})^2$ are important in determining the extent of interactions for a solvent (1) - polymer (2) system.

Since water is a good solvent for PAAm, its solubility parameter components can be taken as those of PAAm. Literature data (14) indicate that the dispersion solubility parameter values ($\delta_{d,1}$) of the nonsolvents used are quite similar; thus, nonpolar interactions cannot be responsible for the features of the deswelling kinetics shown in Figure 5. However, polar and H-bonding components of the solubility parameter vary considerable depending on the type of the nonsolvents (14). In Figure 6, the difference between the relative masses of the preswollen gels and the gels after synthesis, Δq_w, after a deswelling time of 1.5h is plotted as functions of $\Delta\delta_p^2$ and $\Delta\delta_h^2$. Since Δq_w is equal to the amount of "frozen solvent" inside the preswollen gels, Figure 6 illustrates the dependence of the degree of heterogeneity in PAAm gels on the extent of polar and H-bonding interactions in gel - nonsolvent system. The heterogeneity appears intensively in butanol, i.e., in nonsolvent with the smallest polarity, and, the degree of heterogeneity decreases as the polarity of the medium increases, i.e. as the value of $\Delta\delta_p^2$ decreases. Previous theoretical studies (15,16) showed that the degree of ion pairs formation strongly depends on the polarity of the medium; in relatively nonpolar solvents such as in n-butanol, the degree of dissociation of ion pairs in the gel is very small. Thus, decrease in polarity of the nonsolvent increases the probability of ionpairing in the polymer-rich regions of the sample with subsequent shrinkage of these regions. As a result, the polymer-rich regions of the gel will pass into the glassy state earlier, i.e., at higher relative masses, as the

polarity of the nonsolvent decreases; this blocks increasingly the release of water from the polymer-poor regions.

The results shown in Figures 5 and 6 also indicate that the gel deswells rapidly in acetone and the degree of heterogeneity in the gel created by this nonsolvent is relatively low. Comparison of the $\Delta\delta_p^2$ values show that acetone is more polar than ethanol and n-butanol (Figure 6); as a result, it induces relatively low degree of heterogeneity in PAAm gels. On the other hand, in contrast to the alcohols used, acetone - PAAm system exhibits a high $\Delta\delta_h^2$ value, i.e., acetone forms weak H-bonds with the acrylamide units of the network chains (Figure 6). This facilitates the movement of individual solvent and nonsolvent molecules through the network and results in the observed rapid deswelling of PAAm gels in acetone (Figure 5).

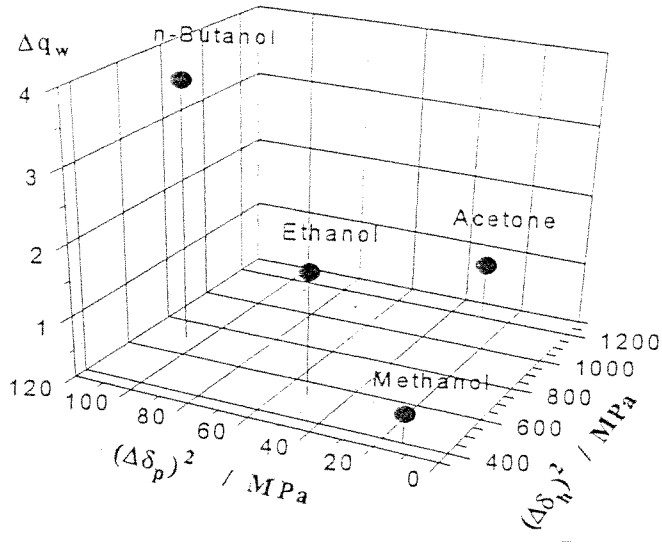

Fig. 6. The difference between the relative masses of the preswollen gels and the gels after synthesis, Δq_w, after a deswelling time of 1.5h shown as functions of $\Delta\delta_p^2$ and $\Delta\delta_h^2$.

Conclusions

Heterogeneous (porous) crosslinked polymers have usually been prepared by crosslinking copolymerization of monomers in the presence of an inert diluent. A phase separation during the copolymerization and crosslinking reactions is responsible for the formation of heterogeneous structures (17,18). The results presented here introduce a novel technique to produce heterogeneous hydrogels in which the heterogeneity was created during the posttreatment of the gel with nonsolvents. The extent of heterogeneity in PAAm gels increases as the initial swelling degree of the gel increases or, as the polarity of the nonsolvent decreases. The nature of the deswelling curves in nonsolvents indicates that the polymer-rich regions of the gel formed by the collapse transition block the solvent diffusion inside the gel. This prevents the equilibration of the preswollen gel volume with surroundings.

It must be noted that the experimental results presented here were obtained using cylindrical PAAm gel samples of 10 mm in length and 5.8 mm in diameter. Since the relaxation time of the network chains is proportional to the macroscopic gel size (10), the data obtained in the non-equilibrium region may not be reproducible for PAAm gel samples of different shape and volumes.

Acknowledgment
This work was supported by the Scientific and Technical Research Council of Turkey (TUBITAK) under Grand Number TBAG - 1561.

References

1. Dusek K, Patterson D (1968) J Polym Sci A2 6: 1209
2. Tanaka T (1978) Phys Rev Lett 40: 820
3. Dusek K (1971) In *Polymer Networks. Structure and Mechanical Properties;* (eds AJ Chompff, S Newman), Plenum Press, NY, p 245
4. Okay O (1986) J Appl Polym Sci 32: 5533
5. Ilavsky M (1982) Macromolecules 15: 782
6. Philippova OE, Pieper TG, Sitnikova NL, Starodoubtsev SG, Khokhlov AR, Kilian HG (1995) Macromolecules 28: 3925
7. Siegel RA (1993) Adv Polym Sci 109: 233
8. Kayaman N, Okay O, Baysal BM (1997) Polymer Gels and Networks 5: 339
9. Tanaka T, Fillmore D, Sun S-T, Nishio I, Swislow G, Shah A (1980) Phys Rev Lett 45: 1636
10. Shibayama M, Tanaka T (1993) Adv Polym Sci 109: 1
11. Tong Z, Liu X (1993) Eur Polym J 29: 705
12. Gardon JL (1965), In *Encyclopedia of Polymer Science and Technology,* (eds HF Mark, NG Gaylord, NM Bikales), Interscience, NY, Vol 3, p 833
13. Hansen CM, Beerbower A (1971), In *Kirk-Othmer Encyclopedia of Chemical Technology, Supplement Volume,* (ed A Standen), Interscience, NY, p 889
14. Hansen CM (1995), In *ASTM Manual 17,* Paint and Coating Testing Manual, American Society for Testing and Materials, 35, p 383
15. Khokhlov AR, Kramarenko EY (1996) Macromolecules 29: 681
16. Khokhlov AR, Kramarenko EY (1994) Macromol Theory Simul 3: 45
17. Dusek K (1982) in *Developments in Polymerization 3,* (ed RN Haward), Applied Science, London, p 143
18. Okay O, Gurun C (1992) J Appl Polym Sci **46:** 421

PERGAMON

European Polymer Journal 00 (1999) 1–7

EUROPEAN POLYMER JOURNAL

Swelling behavior of poly(acrylamide-co-sodium acrylate) hydrogels in aqueous salt solutions: theory versus experiments

Oğuz Okay[a,b,*], Safiye B. Sariisik[c]

[a] *Department of Chemistry, Istanbul Technical University, 80626 Maslak, Istanbul, Turkey*
[b] *TUBITAK Marmara Research Center, P.O. Box 21, 41470 Gebze, Kocaeli, Turkey*
[c] *Department of Chemistry, Kocaeli University, 41300 Izmit, Kocaeli, Turkey*

Received 4 August 1998; received in revised form 4 January 1999; accepted 29 January 1999

Abstract

The predictions of the Flory–Rehner theory of swelling equilibrium including the ideal Donnan equilibria were compared with the experimental swelling data obtained from poly(acrylamide-co-sodium acrylate) hydrogels swollen in water and in aqueous salt (NaCl) solutions. For this comparison, the fraction of counterions which are effective in the gel swelling was taken into account. The ionic hydrogels were prepared from acrylamide and sodium acrylate (NaAc) monomers with 0 to 5 mol% NaAc and using *N,N'*-methylenebis(acrylamide) as the crosslinker. As expected, at a fixed crosslinker ratio, the volume swelling ratio of hydrogels in water increases sharply when the mole fraction of NaAc increases or the NaCl concentration in the external solution decreases. Taking into account the wasted counterions within the hydrogels, the theory correctly predicts the swelling behavior of hydrogels in water and in aqueous salt solutions. Not predicted by the theory is the increased swelling ratio of hydrogels with less than 4 mol% NaAc content with increasing salt concentration from 10^{-1} to 10^{0} M.

1. Introduction

Hydrophilic gels called hydrogels are crosslinked materials absorbing large quantities of water without dissolving. Investigations of the swelling behavior of acrylamide (AAm)-based hydrogels have received considerable attention in the last four decades. These hydrogels are prepared by free-radical crosslinking copolymerization of AAm monomer with a small amount of a hydrophilic crosslinker, e.g., *N,N'*-methylenebis(acrylamide) (BAAm). In order to increase their swelling capacity, an ionic comonomer is also included into the reaction mixture [1,2]. The equilibrium swelling degree of hydrogels is known to depend on the crosslink and charge densities of the network as well as on the polymer network concentration after the gel preparation. These three factors are related to the concentrations of BAAm, the ionic comonomer and the total monomers in the initial reaction mixture, respectively. The Flory–Rehner theory including the ideal Donnan equilibria gives the following well-known relation between the equilibrium swelling ratio of hydrogels in water and the three synthesis parameters [3]:

* Corresponding author. Fax: +90-0262-6412300.
E-mail address: oquz@mam.gov.tr (S.B. Sariisik)

0014-3057/99/$ - see front matter
PII: S0014-3057(99)00058-0

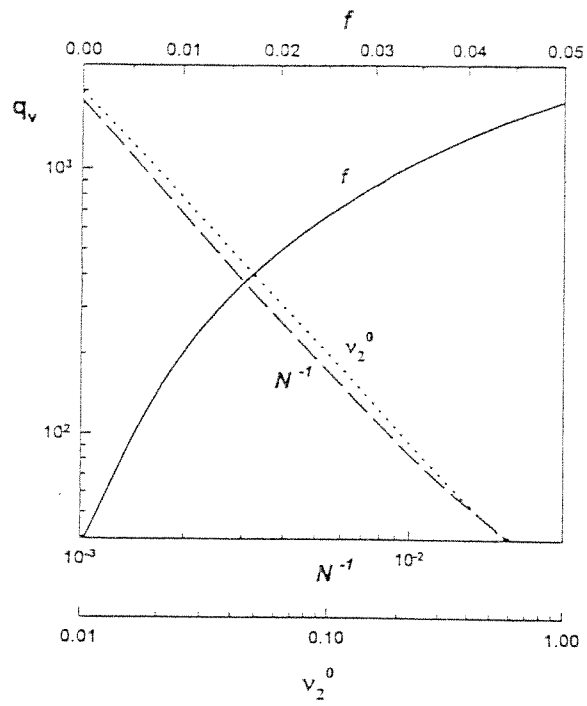

Fig. 1. The prediction of the Flory–Rehner theory [3] for the volume swelling ratio q_v of hydrogels in water shown as a function of the crosslink density N^{-1}, the effective charge density of the network f, and the polymer network concentration after gel preparation υ_2^0. Calculations were using Eq. (1) with $\chi = 0.48$, $V_1 = 18$ ml/mol, and $\bar{V}_r = 53$ ml/mol. Solid curve: $N^{-1} = 10^{-3}$, $\upsilon_2^0 = 0.04$. Dashed curve: $f = 0.05$, $\upsilon_2^0 = 0.04$. Dotted curve: $N^{-1} = 10^{-3}$, $f = 0.02$.

$$\ln(1-v_2) + v_2 + \chi v_2^2 + N^{-1}\left[\upsilon_2^{1/3}\left(\upsilon_2^0\right)^{2/3} - \upsilon_2/2\right] - V_1\frac{f}{\bar{V}_r}v_2 = 0 \quad (1)$$

where v_2 is the volume fraction of polymer in the equilibrium swollen hydrogel, i.e., the inverse of the volume swelling ratio q_v, χ is the polymer–solvent interaction parameter, N is the number of segments between two successive crosslinks of the network, υ_2^0 is the volume fraction of polymer network after preparation, V_1 and $\bar{V}_r$ are the molar volumes of solvent (water) and the polymer repeat unit, respectively, and f is the mole fraction of effective charged units in the network.

The calculated equilibrium volume swelling ratio q_v versus crosslink density (N^{-1}), effective charge density (f), and the polymer concentration (υ_2^0) plots shown in Fig. 1 indicate that, according to the theory, highly swollen hydrogels can be obtained at high network charge densities f, at low crosslink densities N^{-1}, or at low monomer concentrations υ_2^0. Superabsorbent materials with q_v in the order of 10^3 could be obtained by adjusting one of the three network parameters.

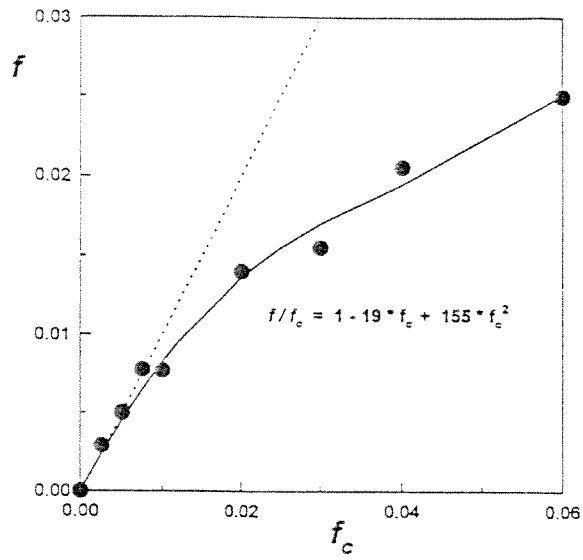

Fig. 2. Variation of the effective network charge density f with the chemical charge density f_c in AAm/AMPS hydrogels. The dotted line represents the relation $f = f_c$.

Experimental results indicate, however, only qualitative agreement between the experimental swelling data and the theoretical curves shown in Fig. 1 [4–7]. In fact, due to the several assumptions and approximations of the classical theory, no agreement between theory and experiment can be expected, especially in case of highly swollen hydrogels [8,9]. This is, of course, for the case where the experimental values of f and N^{-1} obtained from the condition of gel preparation were used in the calculations [5,7]. Although many new theories have been proposed to modify the classical theory [10–17], recent results show a good agreement between the classical theory and the experimental swelling data, if the parameters N^{-1} and f are taken as adjustable parameters [5]. Recently, we have also shown that the classical theory correctly predicts the swelling behavior of strong polyelectrolyte AAm/2-acrylamido-2-methylpropanesulfonic acid (AMPS) hydrogels swollen in water and in aqueous salt solutions [18]. For AMPS mole fractions $f_c < 0.05$, a good agreement between the measured and calculated results was obtained if f is taken as a fit parameter, which was found to be a function of the AMPS mole fraction f_c [18]. The variation of the effective charge density f with chemical charge density f_c found in Ref. [18] is illustrated in Fig. 2 as filled circles. In the figure, the dotted line represents the relation $f/f_c = 1$, i.e., on this line the ionic group content of hydrogels is equal to their effective charge density. It is seen that up to 1%

AMPS content ($f_c = 0.01$), all AMPS units act as charged units in the gel swelling. However, as f_c further increases, deviations appear from the straight line dependence. A polynomial regression yields:

$$\frac{f}{f_c} = 1 - 19f_c + 155f_c^2 \quad (2)$$

in the range of $f_c \leq 0.06$ (solid curve in Fig. 2). Eq. (2) suggests that not all the fixed charges inside the gel are effective in the gel swelling. Thus, only a certain fraction of mobile counterions (f/f_c) inside the gel are effective in creating an osmotic pressure that expands the gel. According to Fig. 2, the fraction of effective counterions decreases on raising the chemical charge density of the network. This experimental finding is in accord with recent experimental and theoretical results indicating the existence of 'osmotically passive' counterions inside the swollen gel which do not contribute to the swelling process [5,19].

The scope of the present work was to establish whether it is possible to predict the swelling behavior of weak polyelectrolyte AAm/sodium acrylate (NaAc) hydrogels using the empirical equation (2). For this purpose, we prepared a series of AAm/NaAc hydrogels with chemical charge densities f_c between 0 and 0.05 and measured their swelling capacities in water and in aqueous NaCl solutions ranging in concentration from 10^{-5} to 1 M. The measured swelling data of the hydrogels were compared with that predicted by the Flory–Rehner theory in combination of Eq. (2). As will be shown below, the theory correctly predicts the swelling behavior of hydrogels in water and in aqueous NaCl solutions if the fraction of effective counterions given by Eq. (2) is taken into account.

2. Experimental

2.1. Materials

Acrylic acid (AA, Fluka) was distilled under a vacuum. Acrylamide (AAm, Merck), *N,N'*-methylenebis(acrylamide) (BAAm, Merck), ammonium persulfate (APS, Merck), *N,N,N',N'*-tetramethylethylenediamine (TEMED, Merck), and NaCl (Merck) were used as received. Sodium acrylate (NaAc) was prepared in situ by adding equimolar amounts of AA and NaOH in the polymerization mixture. Double distilled and deionized water was used in the hydrogel preparation and in the swelling measurements.

2.2. Hydrogel synthesis

The hydrogels were prepared by free-radical crosslinking copolymerization of AAm and NaAc with a small amount of BAAm as a crosslinker in aqueous solution. APS and TEMED were respectively the initiator and the accelerator. The reactions were carried out at room temperature (21 ± 2°C). The gels were prepared according to the following procedure.

Five grams of AAm–AA mixture, NaOH (in amount corresponding to the number of moles of AA), 133 mg BAAm, and 40 mg APS were dissolved in double distilled water under cooling to give a total volume of 100 ml. After addition of 0.24 ml of TEMED, the solution was transferred to small tubes of 5.8 mm in diameter. The polymerization was conducted for 24 h. Homologous series of anionic hydrogels were prepared in this way allowing systematic variation of the NaAc concentration between 0 and 5 mol% (with respect to the monovinyl monomers). The total monomer concentration and the crosslinker ratio X (mole ratio of divinyl to vinyl monomers) were fixed at 5% (w/v) and 82^{-1}, respectively.

After polymerization, hydrogel samples were cut into specimens of approximately 10 mm in length. The samples (usually 10 pieces) were then immersed in a large excess of distilled water for at least one week; during this period, water was replaced every other day to remove the unreacted species. It was found that the sol fraction in the gels is less than 0.1% after extraction with water. Half of the gel samples were then subjected to swelling measurements, whereas the remaining samples were dried according to the following procedure: the swollen gel samples were successively washed with solutions whose compositions were changed gradually from water to pure methanol. This solvent exchange process facilitates final drying of the gel samples. The collapsed samples after the treatment with methanol as a final solvent were dried in vacuum at 60°C to constant weight. The weight swelling ratio of hydrogels after preparation, q_F, was calculated as:

$$q_F = \frac{\text{mass gel after preparation}}{\text{mass dry gel}} \quad (3)$$

The volume fraction of polymer network after preparation, v_2^0, was calculated from q_F values as:

$$v_2^0 = \left[1 + \frac{(q_F - 1)\rho}{d}\right]^{-1} \quad (4)$$

where ρ and d are the densities of polymer and solution, respectively. The values ρ and d used were 1.35 and 1 g/ml, respectively. The experimental value of v_2^0 was found to be 0.056 and 0.039 ± 0.002 for non-ionic and ionic hydrogels, respectively.

2.3. Swelling measurements

The swollen hydrogel samples from the same gel

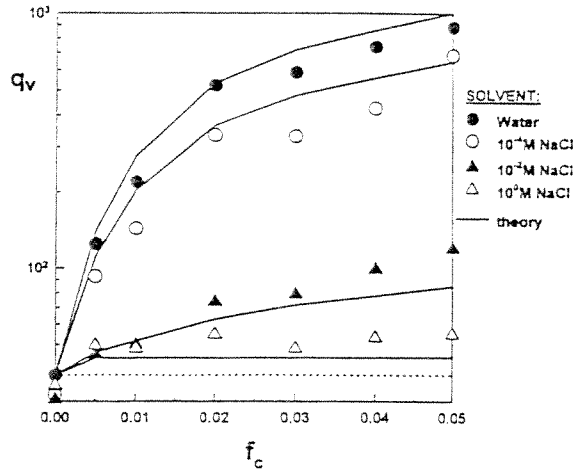

Fig. 3. Variation of the volume swelling ratio q_v of AAm/NaAc hydrogels in water and in aqueous NaCl solutions with the mole fraction of NaAc used in the gel preparation f_c. The experimental data are shown as symbols. The solid lines were calculated using the swelling theory and using Eq. (2). The dotted line represents the prediction of the theory without the Donnan term (Eq. (10)).

(usually five pieces) were immersed in vials (100 ml) filled with water. The vials were set in a temperature-controlled bath at 25 ± 0.1°C . In order to reach the equilibrium degree of swelling, the gels were immersed in water at least for one week; the swelling equilibrium was tested by weighing the samples. The gels were then weighed in the swollen state and transferred to vials containing the most concentrated aqueous NaCl solution. The concentration of NaCl solutions ranged from 1.0 to 10^{-5} M. The gel samples were allowed to swell in the solution at least for one week, during which aqueous NaCl was refreshed to keep the concentration as feeded. After the swelling equilibrium was established, the samples were weighed and then transferred into the next dilute NaCl solution. The swelling measurements in aqueous NaCl were carried out both in direction of decreasing salt concentration from 1 M to water and in reverse direction from water up to 1 M NaCl. No systematic variation in the recorded swelling data was observed. The weight swelling ratios of hydrogels in water and in aqueous NaCl q_w, mass gel after swelling/mass dry gel, were calculated using the equations:

$$q_{w(H_2O)} = q_F \frac{\text{mass gel in water}}{\text{mass gel after preparation}} \tag{5a}$$

$$q_{w(NaCl_{aq})} = q_{w(H_2O)} \frac{\text{mass gel in aqueous NaCl}}{\text{mass gel in water}} \tag{5b}$$

The volume swelling ratio of hydrogels, q_v, was calculated as:

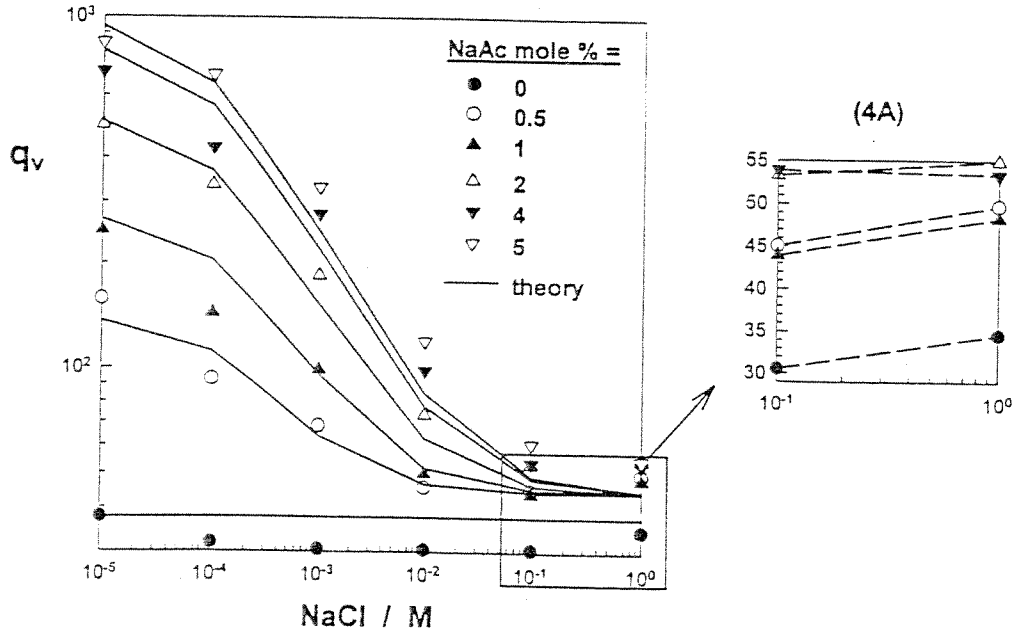

Fig. 4. Variation of the volume swelling ratio q_v of hydrogels with the NaCl concentration in the external solution. The experimental data are shown as symbols. The curves were calculated using the swelling theory and using Eq. (2). Fig. 4A is a magnification of the small box. The dashed lines in Fig. 4A only show the trend of data.

$$q_v = 1 + \frac{(q_w - 1)\rho}{d} \tag{6}$$

Each swelling ratio reported in this paper is an average of at least five separate measurements; standard deviations of the measured swelling ratios were less than 4% of the mean.

3. Results and discussion

Fig. 3 shows the equilibrium volume swelling ratio q_v of AAm/NaAc hydrogels in water and in aqueous NaCl solutions plotted as a function of f_c, the mole fraction of NaAc used in the hydrogel preparation. In Fig. 4, q_v of hydrogels is shown as a function of the NaCl concentration in the external solution. The experimental data are shown as symbols. As expected, q_v increases sharply when the mole fraction f_c of NaAc increases from 0 to 0.05 (Fig. 3). This is due to the fact that, as f_c increases, the mobile ion (Na^+) concentration inside the gel also increases to maintain the electroneutrality condition. As a result, the difference between the mobile ion concentration inside and outside the gel increases with increasing f_c, which creates an additional osmotic pressure that expands the gel.

Also expected is the decreased swelling ratio of hydrogels with increasing salt concentration in the external solution (Fig. 4); this is due to a decrease in the concentration difference of counterions inside and outside the hydrogel. The decrease in q_v is first rapid up to 10^{-2} M NaCl concentration. As the NaCl concentration further increases, the decrease in q_v slows down and, between 10^{-1} and 10^0 M NaCl, q_v remains almost constant or slightly increases with increasing salt concentration (Fig. 4A).

To interpret the experimental swelling data shown in Figs. 3 and 4 within the framework of the Flory–Rehner theory, the osmotic pressure π of a hydrogel during swelling is given as the sum of the pressures due to polymer–solvent mixing (mix), due to deformation of network chains to a more elongated state (el), and due to the nonuniform distribution of mobile counterions between the gel and the external solution (ion) [20,21]:

$$\pi = \pi_{mix} + \pi_{el} + \pi_{ion} \tag{7}$$

According to the Flory–Huggins theory, π_{mix} is given by [3]:

$$\pi_{mix} = -\frac{RT}{V_1}\left(\ln(1 - v_2) + v_2 + \chi v_2^2\right) \tag{8}$$

where R is the gas constant and T is temperature. To describe the elastic contribution π_{el} to the swelling pressure, we will use here the simplest affine network model to describe the behavior of our gels [3]:

$$\pi_{el} = -\frac{RT}{V_1} N^{-1}\left[v_2^{1/3}\left(v_2^0\right)^{2/3} - v_2/2\right] \tag{9}$$

Ionic contribution π_{ion} to the swelling pressure is caused by the concentration difference of counterions between the gel and the outer solution. The ideal Donnan theory gives π_{ion} as the pressure difference of mobile ions inside and outside the gel [3]:

$$\pi_{ion} = RT \sum_i \left(C_i^g - C_i^s\right) \tag{10}$$

where C_i^g and C_i^s are the concentrations of the mobile ions of species i inside and outside the gel, respectively. According to ideal Donnan equilibria, for aqueous solutions of univalent salts, we have the equality:

$$C_+^g C_-^g = C_+^s C_-^s = \left(C_{salt}^s\right)^2 \tag{11}$$

where C_{salt}^s represents the salt concentration in the external solution. On the other hand, the condition of electroneutrality inside an anionic hydrogel requires:

$$C_+^g = C_-^g + \frac{f}{\bar{V}_r} v_2 \tag{12}$$

Solution of Eqs. (7)–(12) for the thermodynamic equilibrium state of a gel ($\pi = 0$) gives the following system of equations describing the equilibrium value of v_2 of hydrogels in aqueous salt solution and the distribution coefficient K of counterions between the gel and solution phases:

$$\ln(1 - v_2) + v_2 + \chi v_2^2 + N^{-1}\left[v_2^{1/3}\left(v_2^0\right)^{2/3} - v_2/2\right] - 2(K - 1)V_1 C_{salt}^s - V_1 \frac{f}{\bar{V}_r} v_2 = 0 \tag{13a}$$

$$K\left(K + \frac{f v_2}{\bar{V}_r C_{salt}^s}\right) - 1 = 0 \tag{13b}$$

where $K = C_-^g / C_{salt}^s$. Note that, in the case of swelling of hydrogels in water free of ionic species ($C_{salt}^s = 0$), Eq. (13a) reduces to Eq. (1) given in Section 1.

The system of equations (13a) and (13b) were solved numerically to calculate the equilibrium swelling ratio of AAm/NaAc hydrogels in aqueous salt solutions ($q_v = 1/v_2$). For calculations, the values used were $V_1 = 18$ ml/mol and $\bar{V}_r = 52.6 + 17 f_c$ (obtained using the values 71 and 94 g/mol for the molecular weights of AAm and NaAc units, respectively). The χ-parameter value for PAAm–water system was recently

Table 1
Calculated effective charge densities f of AAm/NaAc hydrogels with various chemical charge densities f_c

$10^2 \times f_c$	$10^2 \times f$
0.50	0.45
1.0	0.83
2.0	1.36
3.0	1.71
4.0	1.95
5.0	2.19

evaluated from the swelling data for uncharged PAAm hydrogels swollen in water [22]. A best-fit value for χ of 0.48 was obtained [5]. This value of χ-parameter provided a good fit to the experimental swelling data of acrylamide-based anionic, cationic, and ampholytic hydrogels of various compositions [5,6]. In the following calculations, χ was held constant at this value. The f value of the hydrogels was calculated using Eq. (2) derived from the equilibrium swelling degrees of AAm/AMPS hydrogels in water [18]. Table 1 shows the f values used in the calculations. C^s_{salt} (and mM) is the independent variable of Eqs. (13a) and (13b), which was varied between 10^{-5} and 1.0 M in our experiments (Fig. 3 Fig. 4).

In order to solve Eqs. (13a) and (13b), the crosslink density of the network N^{-1} characterizing the hydrogels must also be known. Both the crosslinker ratio X (mole ratio of crosslinker to monomer) and the total monomer concentration were fixed in our experiments, while only the mole fraction of NaAc varied between the hydrogels from 0 to 0.05. Therefore, it is reasonable to assume a constant crosslink density for all the hydrogels. Thus, using the swelling ratio of non-ionic gel in water $q_v = 37.9$ and using Eq. (1) for $f = 0$, we calculated N as 1.5×10^3, which should be valid for all other ionic hydrogels. In fact, from the crosslinker ratio $X = 82^{-1}$ used in the hydrogel synthesis, one may expect the chemical value of N as 41, if all BAAm molecules form effective crosslinks in the final hydrogel. It is seen that more than 90% of BAAm used in the hydrogel synthesis were consumed in cycles, multiple crosslinks or, in units with pendant vinyl groups. This high fraction of wasted BAAm monomer is in accord with our previous result on PAAm gels [23]. For the same copolymerization system, Tobita et al. [24] and Naghash et al. [25] used an analytical titration technique to calculate the fraction of BAAm units involved in formation of cycles. They showed that, in AAm/BAAm copolymerization, at least 80% of the pendant acryl groups are consumed by cyclization reactions, which is also comparable with the present result. However, contrary to these results Baselga et al. pointed out that the difference in the vinyl group reactivity leading to the spatial inhomogeneity in PAAm gels is mainly responsible for the observed deviations and cyclization has a very low probability [26,27].

Calculation results using Eqs. (13a) and (13b) are shown in Figs. 3 and 4 as the solid curves. The dotted line in Fig. 3 represents the prediction of the theory without the Donnan term (Eq. (10)). It is seen that the predictions of the classical theory including the ideal Donnan equilibria agree reasonably well with the experimental swelling data of hydrogels in water and in aqueous salt solutions. It must be pointed out that no adjustable parameter was used in the calculation of the swelling data of ionic hydrogels. This good agreement also means that the fraction of effective counterions found in AAm/AMPS hydrogels also corresponds to that in the present hydrogels. We can thus conclude that the empirical Eq. (2) in connection with the Flor—Rehner theory can be used to predict the swelling behavior of hydrogels in aqueous salt solutions.

Another point shown in Fig. 4A is that the equilibrium swelling ratio q_v of hydrogels with less than 4 mol% NaAc content increases again, when the salt concentration further increases from 0.1 to 1.0 M. This interesting feature, not predicted by the theory, was also observed previously in ampholytic, cationic, and non-ionic AAm-based hydrogels [6,22] and in AAm/AMPS hydrogels [18]. Specific interactions between AAm units and mobile ions seem to be responsible for this behavior.

4. Conclusions

A series of hydrogels from AAm and NaAc monomers were prepared by free-radical crosslinking copolymerization using *N,N'*-methylenebis(acrylamide) as the crosslinker. The swelling capacities of the hydrogels were measured in water and in aqueous salt solutions ranging in concentration from 10^{-5} to 1 M. The volume swelling ratio q_v of hydrogels increases sharply as the mole fraction f_c of NaAc increases from 0 to 0.05, or as the NaCl concentration in the external solution decreases. The results of swelling measurements were compared with the theory of swelling equilibrium. It was shown that the theory correctly predicts the swelling behavior of hydrogels in water and in aqueous salt solutions if their effective charge densities are taken into account.

Acknowledgements

This work was supported by the Scientific and Technical Research Council of Turkey (TUBITAK) under Grand Number TBAG-1561. The authors wish

to thank Dr. Sibel Zor from the Kocaeli University for the technical assistance during a part of this work.

References

[1] Ilavsky M, Dusek K, Vacik J, Kopecek J. J. Appl. Polym. Sci 1979;23:2073.
[2] Oppermann W, Rose S, Rehage G. Br. Polym. J 1985;17:175.
[3] Flory PJ. Principles of polymer chemistry. Ithaca, NY: Cornell University Press, 1953.
[4] Katchalsky A, Michaeli I. J. Polym. Sci 1955;15:69.
[5] Baker JP, Hong LH, Blanch HW, Prausnitz JM. Macromolecules 1994;27:1446.
[6] Baker JP, Blanch HW, Prausnitz JM. Polymer 1995;36:1061.
[7] Tong Z, Liu X. Macromolecules 1994;27:844.
[8] Matsuo ES, Orkisz M, Sun ST, Li Y, Tanaka T. Macromolecules 1994;27:6791.
[9] Skouri R, Schosseler F, Munch JP, Candau SJ. Macromolecules 1995;28:197.
[10] Katchalsky A, Lifson S. J. Polym. Sci 1953;11:409.
[11] Michaeli I, Katchalsky A. J. Polym. Sci 1957;23:683.
[12] Hasa J, Ilavsky M, Dusek K. J. Polym. Sci. Polym. Phys. Ed 1975;13:253.
[13] Hasa J, Ilavsky M. J. Polym. Sci. Polym. Phys. Ed 1975;13:263.
[14] Konak C, Bansil R. Polymer 1989;30:677.
[15] Tong Z, Liu X. Eur. Polym. J 1993;5:705.
[16] Prange MM, Hooper HH, Prausnitz JM. AIChE J 1989;35:803.
[17] Hino T, Prausnitz JM. J. Appl. Polym. Sci 1996;62:1635.
[18] Okay O, Sariisik SB, Zor SD. J. Appl. Polym. Sci 1998;70:567.
[19] Philippova OE, Rulkens R, Koutunenko BI, Abramchuk SS, Khokhlov AR, Wegner G. Macromolecules 1998;31:1168.
[20] Flory PJ, Rehner Jr J. J. Chem. Phys 1943;11:521.
[21] Frenkel J. Rubber Chem. Technol 1940;13:264.
[22] Hooper HH, Baker JP, Blanch HW, Prausnitz JM. Macromolecules 1990;23:1096.
[23] Okay O, Balimtas NK, Naghash HJ. Polym. Bull 1997;39:233.
[24] Tobita H, Hamielec AE. Polymer 1990;31:1546.
[25] Naghash HJ, Okay O. J. Appl. Polym. Sci 1996;60:971.
[26] Baselga J, Llorente MA, Fuentes IH, Pierola IF. Eur. Polym. J 1989;25:471.
[27] Baselga J, Llorente MA, Fuentes IH, Pierola IF. Eur. Polym. J 1989;25:477.

Formation of Macroporous Styrene - Divinylbenzene Copolymer Networks: Theory versus Experiments

Oğuz OKAY

Istanbul Technical University, Department of Chemistry, 80626 Maslak, Istanbul, and TUBITAK Marmara Research Center, P.O. Box 21, 41470 Gebze, Kocaeli, Turkey

ABSTRACT: A kinetic - thermodynamic model is presented to predict the total porosities of macroporous copolymer networks formed by free-radical crosslinking copolymerization of styrene (S) and commercial divinylbenzene (DVB, a mixture of meta and para DVB isomers and ethylstyrene). The kinetic part of the model predicts, based upon the method of moments, the concentration of the reacting species, the gel and sol properties as a function of the monomer conversion. The thermodynamic part of the model describes the phase equilibria between the gel and separated phases during the S - DVB copolymerization and predicts the volume of the separated phase, which is the pore volume of the crosslinked material, as a function of the monomer conversion. Calculation results show that the porosity of S - DVB networks increases as the polymer - diluent interaction parameter increases, or, as the initial monomer concentration decreases. Porosity also increases on increasing the DVB content of the monomer mixture. Both the polymerization temperature and the initiator concentration affect significantly the kinetics of S - DVB copolymerization. However, the final porosity of S - DVB copolymers is largely insensitive to the

amount of the initiator and to the polymerization temperature. All calculation results are in accord with the experimental data published previously.

Keywords: porosity formation, phase separation, macroporous styrene - divinylbenzene copolymer networks, kinetic-thermodynamic modeling, free-radical crosslinking copolymerization.

Contract grant sponsor: Scientific and Technical Research Council of Turkey (TUBITAK), contract grant number: TBAG - 1561.

BİBLİYOGRAFİK BİLGİ FORMU	
1- Proje No: TBAG - 1561	2- Rapor Tarihi: Haziran 1999
3- Projenin Başlangıç ve Bitiş Tarihleri: 1.03.1997 - 28.02.1999	
4- Projenin Adı: MAKROGÖZENEKLİ POLİMERİK JEL SENTEZLERİ	
5- Proje Yürütücüsü ve Yardımcı Araştırıcılar:	Prof. Dr. O. Okay Y.K. Selda Durmaz Prof. Dr. A. Erarslan Prof. Dr. H. Ağırbaş Yard. Doç. Dr. S. Zor
6- Projenin Yürütüldüğü Kuruluş ve Adresi: Kocaeli Üniversitesi, Fen-Edeb. Fak., Kimya Böl, İzmit, Kocaeli ve İstanbul Teknik Üniv., Fen-Edeb. Fak., Kimya Böl., Maslak, İstanbul.	
7- Destekleyen Kuruluş(ların) Adı ve Adresi: -	
8- Öz (Abstract): Makrogözenekli stiren - divinilbenzen kopolimer kürecikleri suspansiyon polimerizasyonu yöntemi ile sentezlendi ve karakterize edildi. Cıvalı porozimetre ile yapılan ölçümler yardımı ile polimerik jellerin sentez şartlarına bağlı olarak gözenek yapılarındaki değişmeler incelendi. Gözenek yapılarındaki dayanıklı ve dayanıksız gözeneklerin oluşma şartları aydınlatıldı. Sentez şartlarının uygun bir şekilde seçimi ile tersinir gözenekli polimerlerin sentezlenebileceği gösterildi. Termodinamik ve kinetik açıdan gözenekli yapı oluşumu incelenerek kopolimer sentez şartları ile kopolimerin gözenek yapısı arası bağıntıyı veren teorik bir model geliştirildi ve bu model stiren-divinilbenzen sistemine uygulandı. Diğer yandan poliakrilamid esaslı iyonik jeller sentez sonrası iyi çözücü-kötü çözücü karışımları ile muamele edilerek heterojen hale dönüştürüldü. 2-Akrilamido-2-metilpropan sulfonik asit (AMPS) esaslı kuvvetli elektrolit hidrojeller sentezlendi ve bu jellerin su ve tuzlu sulardaki şişme oranları belirlendi. 1 mL si 2,5 litreye kadar su emebilen AMPS esaslı jellerin sentezleri gerçekleştirildi. Deneysel şişme değerlerinin açıklanabilmesi için Flory-Rehner teorisi ile ideal Donnan dengesi göz önüne alındı. Ağ yapının çapraz bağ yoğunluğu veya iyonik grup sayısı bir ayarlama parametresi olarak alındığında teori ile deney arasında uyum sağlandı ve bulguların sodyum akrilat esaslı zayıf elektrolit jeller için de geçerli olduğu gösterildi. **Anahtar Kelimeler:** Polimerik jel, makrogözenekli polimer ağ yapılar, gözenek yapılar, hidrojeller, şişme	
9- Proje ile ilgili Yayın/Tebliğlerle İlgili Bilgiler: Ektedir.	
10- Bilim Dalı: Fizikokimya Doçentlik B. Dalı Kodu: ISIC Kodu: Uzmanlık Alanı Kodu:	
11- Dağıtım (*): ☐ Sınırlı ☐ Sınırsız	
12- Raporun Gizlilik Durumu: ☐ Gizli ☐ Gizli Değil	

TBAG 1561 KAPSAMINDA YAPILAN BİLİMSEL YAYINLAR

1. Okay, O., "Phase Separation in Free-Radical Crosslinking Copolymerization: Formation of Heterogeneous Polymer Networks"
Polymer 40, 4117-2129 (**1999**)

2. Erbay, E. and Okay, O., "Pore-memory of Macroporous Styrene -Divinylbenzene Copolymer Beads"
J. Appl. Polym. Sci. 71, 1055-1062 (**1999**)

3. Erbay, E. and Okay, O., "Macroporous Styrene - Divinylbenzene Copolymers: Formation of Stable Porous Structures during the Copolymerization"
Polymer Bulletin 41, 379-385 (**1998**)

4. Okay, O., Sarıışık, S. B., Zor, D.S., "Swelling Behavior of Anionic Acrylamide-based Hydrogels in Aqueous Salt Solutions: Comparison of Experiment with Theory"
J. Appl. Polym. Sci. 70, 567-575 (**1998**)

5. Keskinel, M. and Okay, O., "Effects of Cyclization and Electrostatic Interactions on the Termination Rate of Macroradicals in Free-Radical Crosslinking Copolymerization"
Polymer Bulletin 40, 491- 498 (**1998**)

6. Okay, O. and Akkan, U., "Heterogeneities in polyacrylamide gels immersed in acetone- water mixtures"
Polymer Bulletin 41, 363-370 (**1998**)

7. Okay, O., and Sarıışık, S. B., "Swelling Behavior of Poly(acrylamide-co-sodium acrylate) Hydrogels in Aqueous Salt Solutions: Theory versus Experiments"
Eur. Polymer J. (**1999**)

8. Okay, O., "Formation of Heterogeneous Styrene - Divinylbenzene Copolymer Networks: Theory versus Experiments"
J. Appl. Polym. Sci. (1999)